SAND86-2275
TTC-0696
Unlimited Release
Printed May 1987

Distribution
Category UC-71

SAND--86-2275

DE87 010528

TARGET EFFECTS ON PACKAGE RESPONSE: AN EXPERIMENTAL AND ANALYTICAL EVALUATION*

Alex Gonzales
Transportation Systems Development and Testing Division
Sandia National Laboratories**
Albuquerque, NM 87185

ABSTRACT

Sandia National Laboratories has completed an experimental and analytical evaluation to compare the effects of a simple model transportation cask impacting on targets encompassing a range of stiffnesses. The cylindrical shaped unit was impacted into soil, concrete, and "unyielding" targets at velocities varying from 44 ft/s (30 mph) to 110 ft/s (75 mph). The 44 ft/s impact velocity correlates directly to a 30-ft drop height used in regulatory testing.

May 1987

*This work performed at Sandia National Laboratories, Albuquerque, New Mexico, supported by the United States Department of Energy under Contract DE-AC04-76DP00789

**A United States Department of Energy Facility

DISCLAIMER

TABLE OF CONTENTS

TABLE OF CONTENTS

DISCLAIMER

FIGURES

FIGURES

FIGURES

FIGURES

TABLES

ACKNOWLEDGMENTS

The author wishes to acknowledge Mike Neilsen of Division 1521, Sandia National Laboratories for performing the soil finite element analyses, Dan Swensen of Kansas State University for performing the concrete analyses and Duane Stenberg of Southwest Engineering Associates for instrumentation and testing hardware preparation.

1.0 INTRODUCTION

Sandia National Laboratories conducted an evaluation including experimental testing and analytical calculations to compare effects of a simple model transportation cask impacting onto various targets. A cylindrical-shaped unit was impacted into soil, concrete, and "unyielding" targets in a range of velocities. Cask responses at various impact velocities onto soil and concrete targets were compared with a 30-foot drop onto an essentially unyielding surface. The model transportation cask used in this program was a 5200 lb steel cylinder without energy mitigating devices or impact limiters attached.

An analytical evaluation was also performed for impacts onto the unyielding, concrete, and soil targets. These calculations concentrated on trying to account for soil and concrete cracking as the cask unit penetrated into the respective yielding targets. Experimental and analytical results were then compared to better understand the response generated by impacting different targets.

1.1 Scope

An unyielding target is described as a flat, horizontal surface of such character that any increase in its resistance to displacement or deformation upon impact by a package would not significantly increase the damage to the package [1,2]. A specific example of an unyielding target is a steel plate on the upper surface of a concrete block of mass at least ten times that of any

specimen to be dropped onto it. The block should be set on firm soil and the steel plate at least 0.5 inches thick. The target should be as close to cubic or cylindrical in form as possible [2]. The purpose of the unyielding target is to have all of the kinetic energy available from a drop test be absorbed by the package. This total absorption by the package produces maximum decelerations resulting in larger forces. Impacting a concrete or soil target will likely result in energy partitioning where some of the available impact energy is absorbed by the target. Thus, this energy absorption by a yielding target results in less available energy that can be applied to the impacting package. In addition, the unyielding target provides a repeatable and consistent impact surface producing results that can be more easily verified by analytical calculations.

A testing and analytical evaluation was performed to better determine the relationship between an unyielding target and targets in which yielding does occur. Concrete and soil represent the materials chosen for the yielding targets. These materials are typical of hazards found in a transportation environment as opposed to an unyielding target which is highly unlikely to exist for actual accidents. Concrete and soil represent a more realistic impact surface that will absorb some of the available energy of an impacting cask.

A simple-geometry cylindrical unit was used as the projectile impacting the various targets. The unit roughly modeled a half-scale truck cask without any energy mitigating devices attached. This was done to allow concentration of target effects upon impact without having to compensate for any impact limiter response. The simple geometry of the unit provided ease in instrumentation, duplication of data, and analytical modeling.

Both physical testing and computer analyses were performed to help correlate the results and to better understand the phenomenon of target yielding and its effects upon the projectile. In addition, improvements in computer modeling techniques were explored to better represent the yielding targets in analytical calculations.

1.2 Testing and Analysis

Testing was a critical and important component of the evaluation activities. Eleven tests, on five different targets were conducted at impact velocities ranging from 44 ft/s (30 mph) to 110 ft/s (75 mph). The 44 ft/s impact velocity stems from a 30-ft drop height used in regulatory testing. All drops performed on the cylindrical unit were end-on. This produced consistent loads, stresses, and accelerations along the axial direction at any circumferential point. All tests included the use of photometrics to visually analyze and record each drop.

Computer analyses using finite element methods also evaluated cask responses. Because of the cask geometry and orientation of impact, each finite element evaluation simplified to a two-dimensional analysis. From an analytical point of view, modeling a package impact into a rigid surface is quite simple and tends to be conservative since a perfectly unyielding target does not exist for actual experiments. In analyzing an impact into an unyielding target, only the impact projectile has to be modeled. The computer code can produce an impenetrable surface that will not absorb any energy. Thus, in this type of analysis no target geometrical modeling, material properties, or boundary conditions are needed. However, when variables

associated with a yielding target enter into an analysis, the appropriate modeling and calculations can be very different and even misleading. Depending on the target, factors such as cracking, unit penetration, and target energy absorption in addition to geometry, material properties and boundary conditions come into effect. These additional variables increase the difficulty of the analysis plus producing results that may not be duplicated by testing. With respect to the concrete and soil targets, these factors plus other phenomenon particular to each yielding surface were evaluated.

2.0 TARGETS

In comparing a rigid target to various yielding surfaces, targets common to everyday life were emphasized. This evaluation employed four types of targets in addition to the unyielding:

- concrete airport runway
- concrete highway
- undisturbed desert soil
- uncompacted soil

These yielding targets provided a range of impact stiffnesses and included environments a cask could realistically strike while transporting radioactive materials. Considerable effort was made to provide yielding surfaces representative of an environment which exists in real life. In addition, these targets needed to be reproducible either in construction or

characterization. Each of the targets, all located at Coyote Test Site in Albuquerque, are discussed in detail in the following sections.

2.1 Unyielding Target

The 340-ton steel-faced concrete target used in the test series to represent an unyielding surface is shown in Figure 1. This target, which was constructed in 1975, features a 22-ft diameter, 12-ft deep concrete mass. Integrally fastened to the concrete mass is a 10 x 10 x 0.42 ft steel plate. To aid in fastening the steel plate to the concrete is a network of steel tubes welded to the bottom of the plate (Figure 2). Theses tubes effectively spread any applied load to the concrete. Since 1975 this target has been used extensively for regulatory 30-ft (9 meter) drops, 1 meter puncture tests and higher velocity impacts for a variety of packages and scale models. This target satisfies the requirements set forth by the International Atomic Energy Agency (IAEA) as an unyielding target for the purpose of this evaluation program.

2.2 Concrete Targets

Special consideration was made to characterize yielding targets familiar in real life. Common concrete structures having specific quality assurance standards that must be met at the time of construction are highways and airport runways. These standards are common throughout the United States.

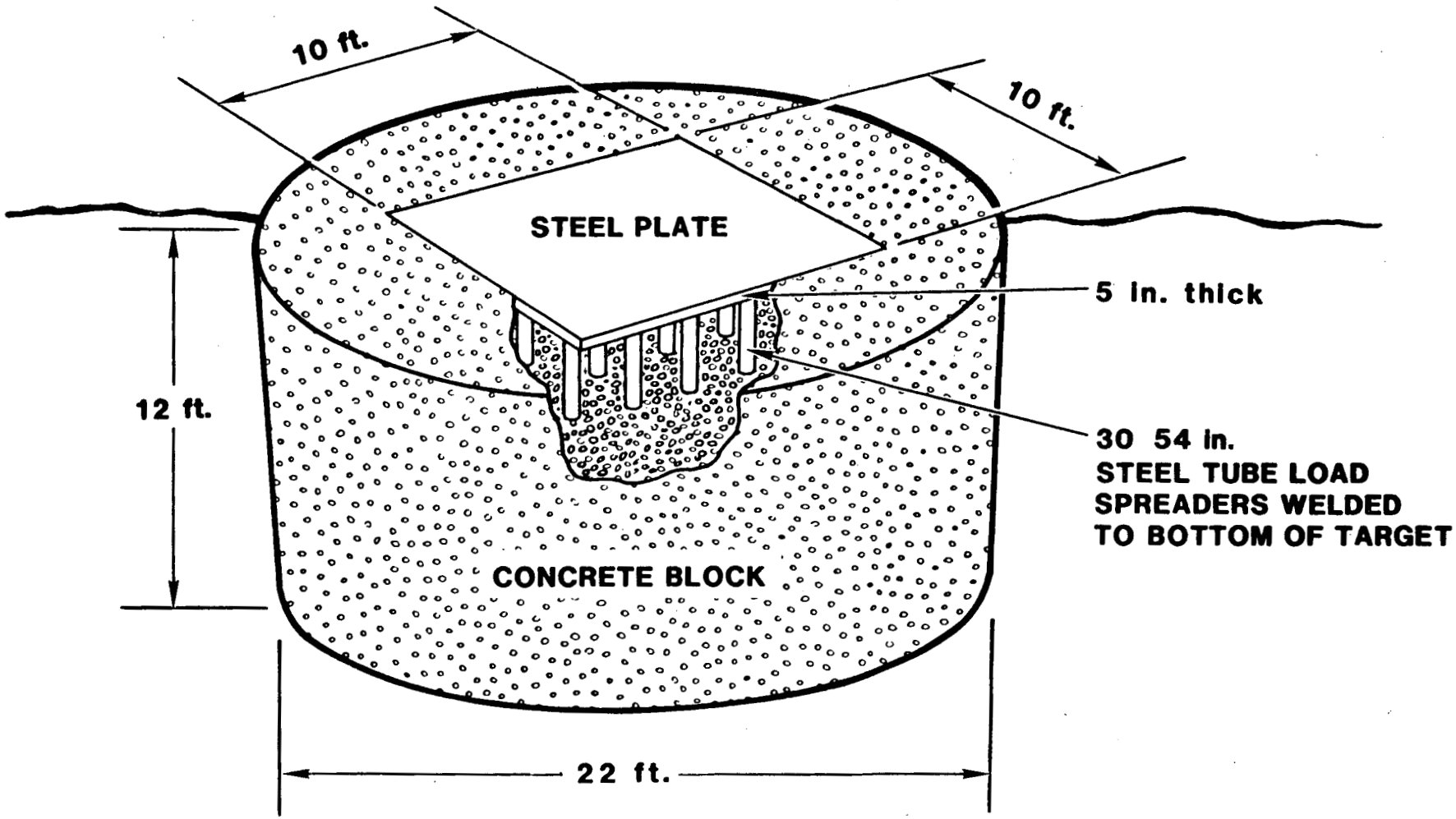

Figure 1 Unyielding Target at Sandia National Laboratories' Coyote Canyon Test Site

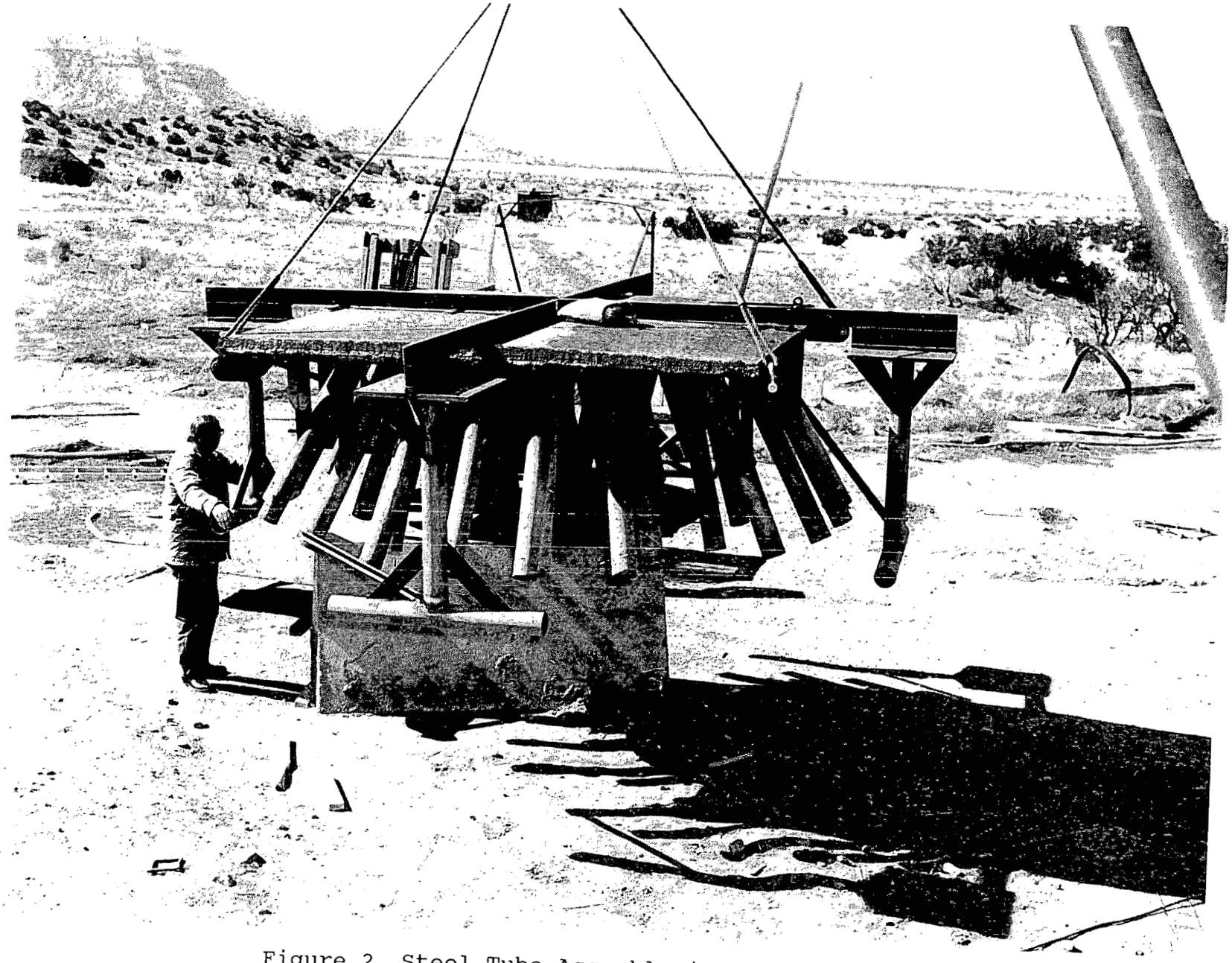

Figure 2 Steel Tube Assembly in Unyielding Target

2.2.1 Runway Concrete Targets

Three 20 x 20 ft concrete slabs shown in Figure 3 were used to represent the runway targets. These slabs were constructed for another program in 1976 (Figure 4) according to U. S. Federal Aviation Agency (FAA) design criteria [3] but they had not been used for testing. The 18 inch deep slab includes a 5 x 5 inch mesh steel reinforcement to provide strength in tension and shear. The compacted soil beneath the concrete underwent a series of plate bearing tests to assure proper soil strength and compaction (Figure 5). The value obtained from the test, k, is in units of pressure over length. The k value can be envisioned as the pressure required to produce a unit deformation of a bearing plate into the pavement foundation. The k value found for this particular soil was within the 500 psi/in. allowed in Reference 3.

Concrete cylinders and cores were also laboratory tested to obtain compressive and flexural strengths. For the concrete cylinder, the standard twenty-eight day compressive strength test resulted in a value of 5060 psi and a flexural stress of 670 psi was also obtained. The drilled cores yielded a compressive strength of 4800 psi. These values are within the FAA allowable limits for a 18-inch thick concrete slab designed to carry a 747 aircraft.

2.2.2 Highway Concrete Targets

Using applicable U. S. Federal Highway design criteria [4], three 10 x 10 ft concrete slabs (Figure 6) were constructed to represent the highway targets. A typical concrete highway cross section does not actually exist.

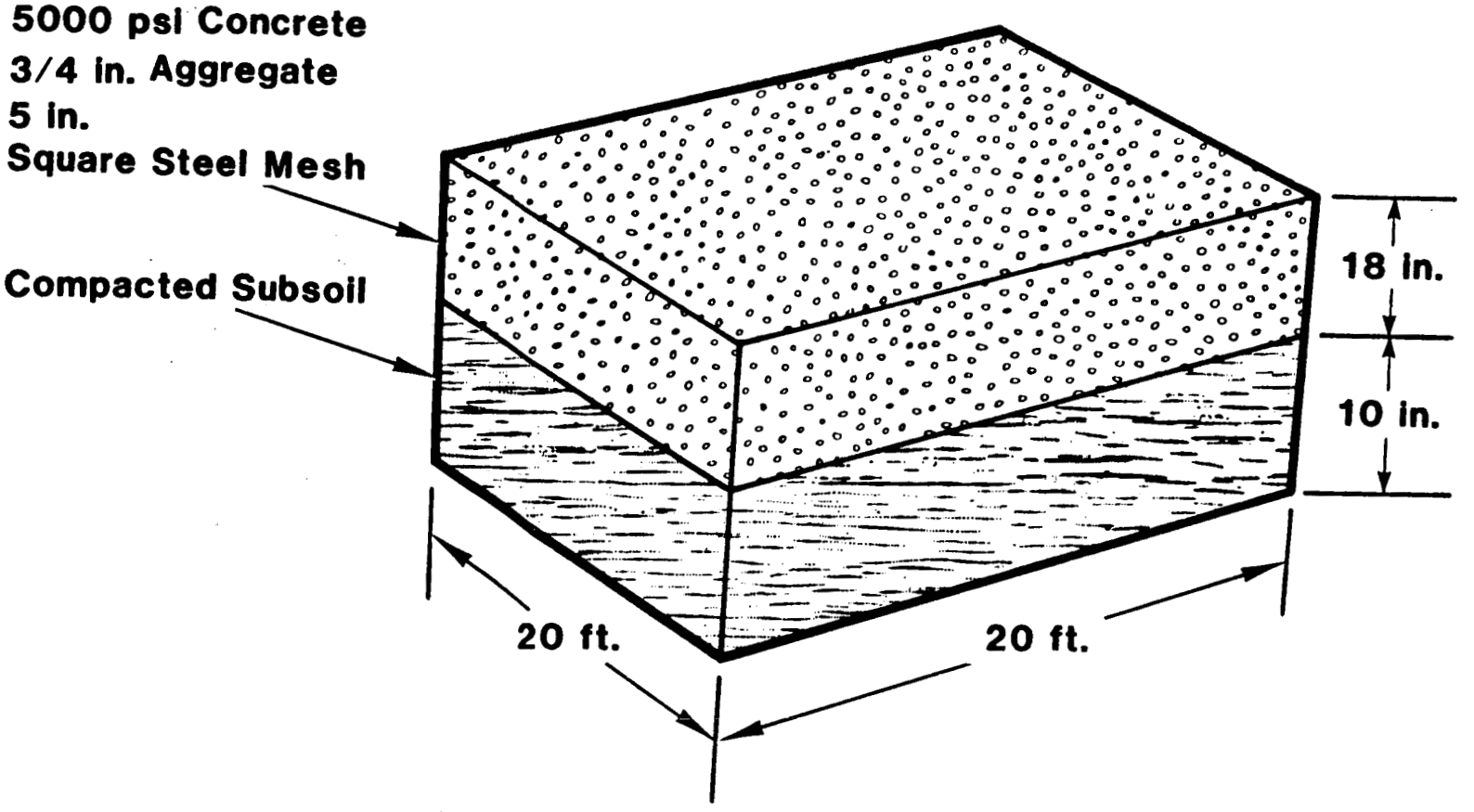

Figure 3 Federal Aviation Agency Runway Cross Section

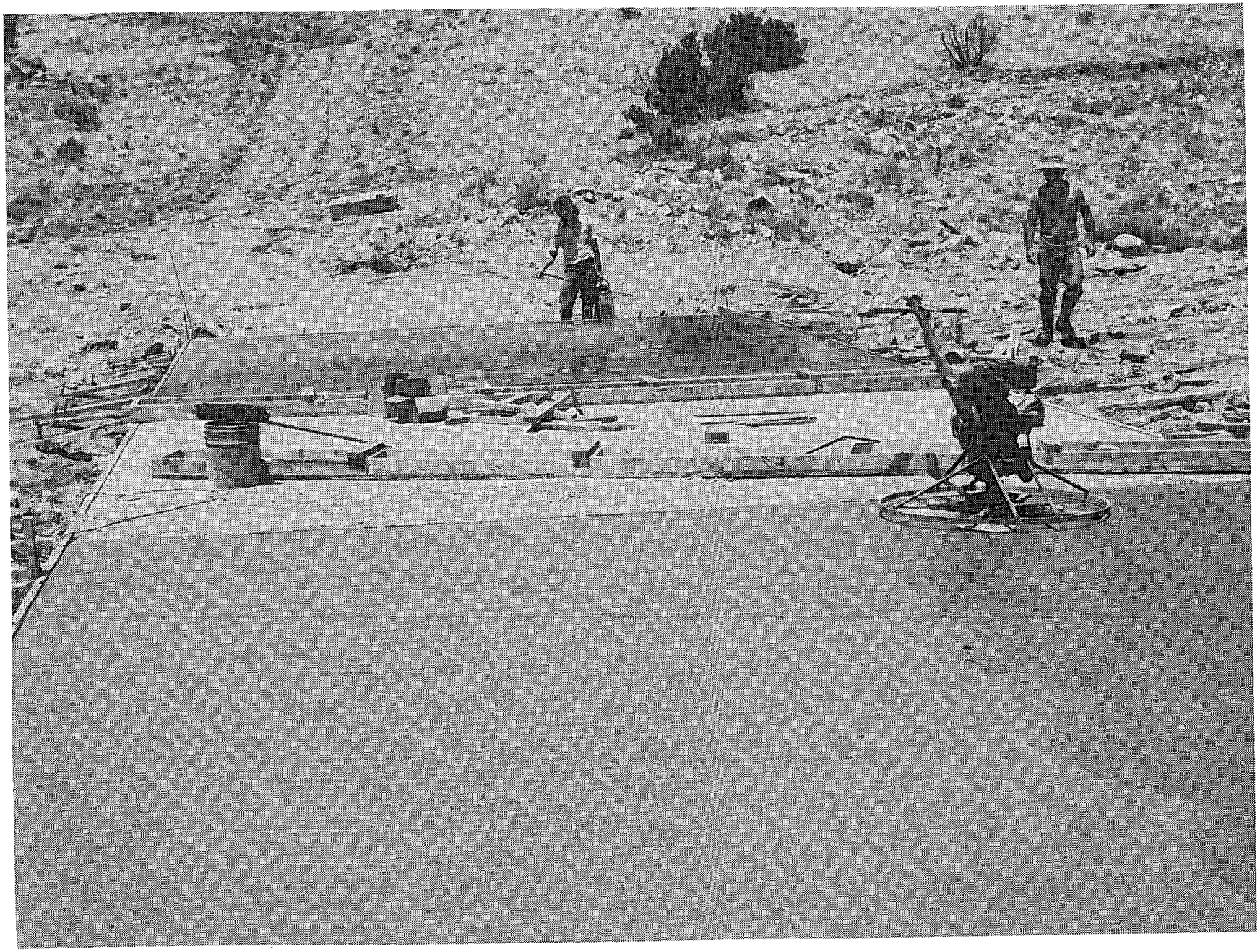

Figure 4 Construction of Concrete Runway Slabs

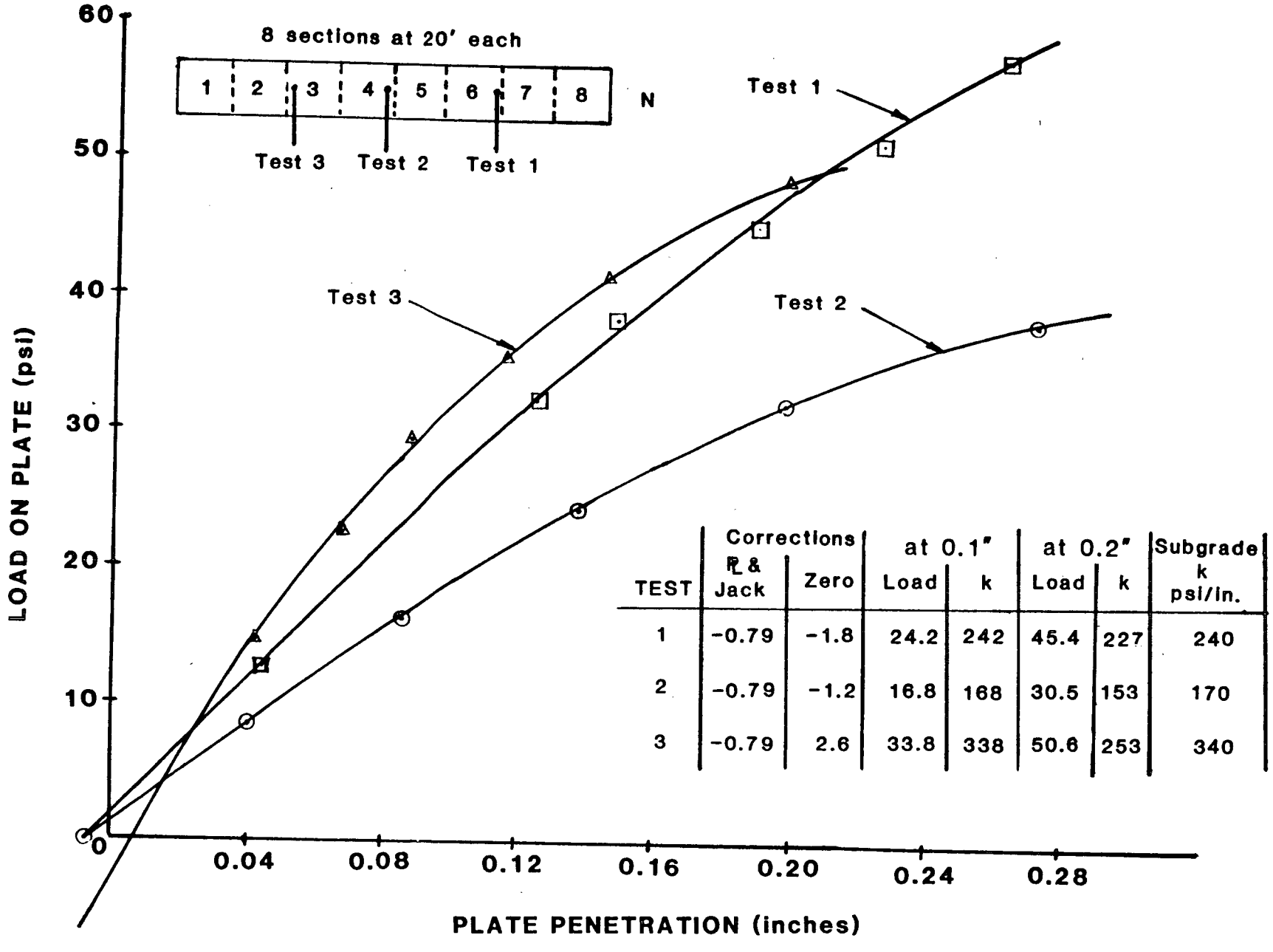

TEST	Corrections PL & Jack	Corrections Zero	at 0.1" Load	at 0.1" k	at 0.2" Load	at 0.2" k	Subgrade k psi/in.
1	-0.79	-1.8	24.2	242	45.4	227	240
2	-0.79	-1.2	16.8	168	30.5	153	170
3	-0.79	2.6	33.8	338	50.6	253	340

Figure 5 Results of Plate Bearing Tests for Concrete Runway

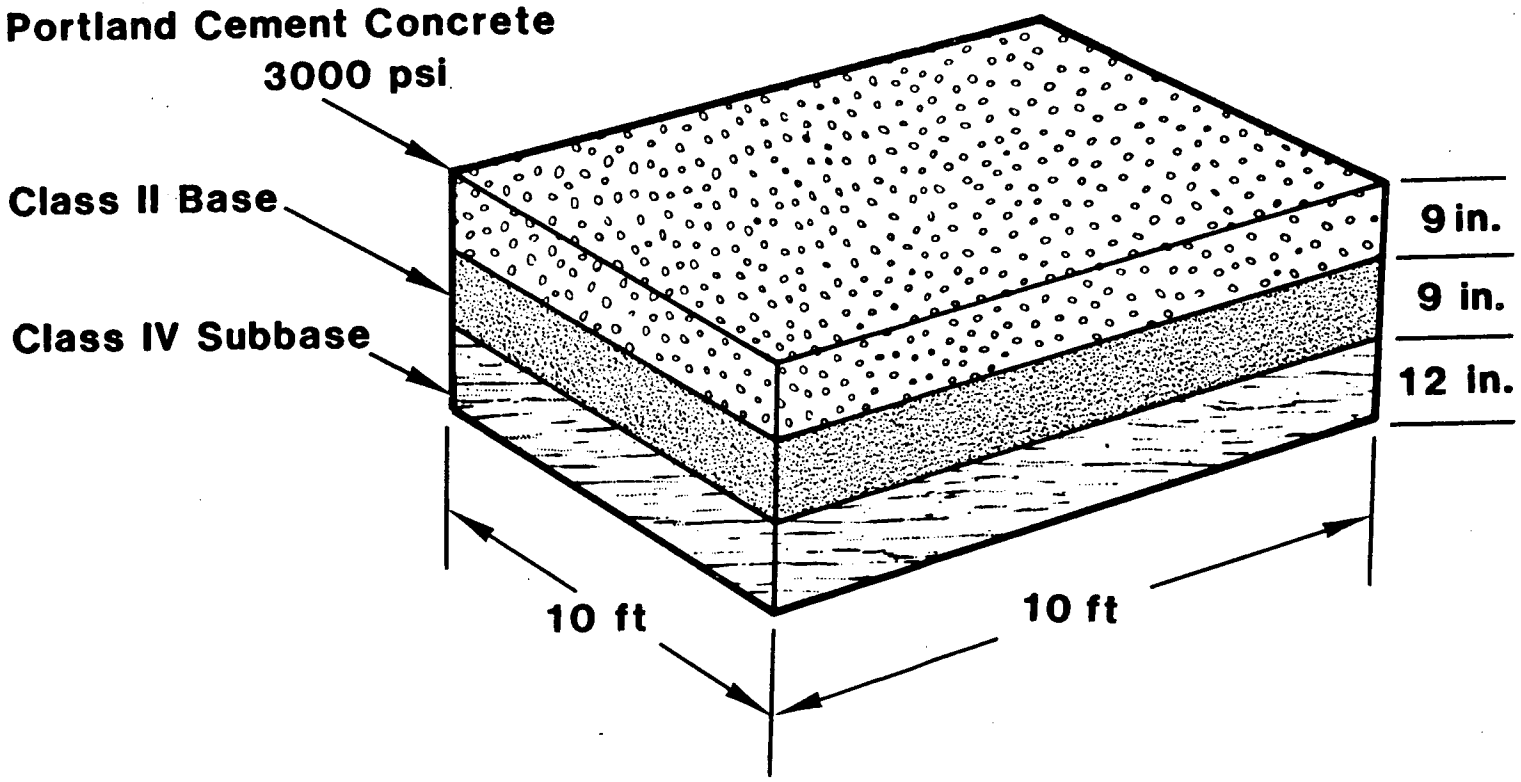

Figure 6 Concrete Highway Cross Section

However given the types of materials and cross sections used in highway design and construction, the selected configuration represents a roadway that is stiffer and more resistant to applied loads than the average interstate highway. This target cross section presents a more severe environment than a concrete bridge abutment which typically is less than 4 inches thick.

Native soil compacted to 95% of its optimum density [5] constituted the Class IV Subbase. Crushed quarry stone also compacted to 95% of its optimum density and satisfying highway [4] specifications represented the Class II base. A 3700 psi minimum compressive strength concrete slab, which is 9 inches thick, made up the roadway surface.

Reinforcing bar was not included in the roadway test sections constructed in 1985 for two reasons. First, recent highway rehabilitation projects in the United States have discovered steel reinforcing bars greatly increase the difficulty in replacing roadway sections. Thus, most highway designs are now omitting reinforcing bars to facilitate roadway maintenance and rehabilitation efforts. The second reason stems from an analytical perspective. Since analytical computer codes do not fully duplicate the response of concrete under large impact loading, the addition of reinforcing bars would further complicate any analyses. Thus, it was decided to avoid a variable that would increase the difficulty of the problem without providing any additional benefits.

2.3 Soil Targets

Determining a suitable soil target presented several problems. Since soil properties and characteristics can change drastically with location,

establishing a section that is universally typical proved to be impractical. Densities for common soils such as sand can range from 75 to 140 pcf [5]. Other variables used to define soils such as specific gravity, moisture content, plasticity index, and compression strength can also vary considerably. In addition, the composition within a given cross section usually varies not only in percentages of different types of soil constituents, but also in location. Since a universal soil definition does not exist, the native soil at the test facility was used for the targets. It is representative of a target category called soil but in reality there are potentially significant differences in the response of packages hitting soils.

The soil target was not altered in any way, instead considerable effort was made to fully characterize all of its properties. A series of laboratory and on-site tests performed by the University of New Mexico Civil Engineering Research Facility (NMERI-CERF) defined the soil properties [6]. The tests include compaction, density, moisture content, sieve analysis, triaxial, unconfined compression, confined compression and consolidation. Table 1 gives a description of the soil properties. Of the tests performed, the triaxial test (Figure 7) was the most valuable for obtaining pertinent material properties. In particular the triaxial test provides the relationship between the principal and shear stresses plus the friction angle which is required to perform the analytical calculations. The information obtained from one triaxial test is shown in Figure 8.

Through the depth of the soil, differences in properties were exhibited, particularly in the first two feet. These differences in properties were characterized in the finite element analysis as six separate layers of

SOIL PROPERTIES AND CHARACTERISTICS[+]								
Depth cm (inches)	Natural Moisture %	Natural Dry Density g/cm^3 (PcF)	Specific Gravity	ATTERBERG LIMITS		Unconfined Compressive Strength MPa (psi)	Consolidation 0.2MPa Loading %	SOIL TYPE
				Liquid Limit %	Plasticity Index %			
0-30 (0-12)	15.47	-	-	21.0	-	-	-	SM Gravely Silty Sand
30-61 (12-24)	17.1	1.43 (89.0)	2.63	33.0	14.4	-	24.8	CL-Lean Clay-Some Gravel
61-91 (24-36)	15.1 12.5	1.57 1.64 (97.8) (102.2)	2.65	32.0	14.0	0.119 (17.2)	16.4	SC-Silty Sandy Clay
91-122 (36-48)	14.9 13.3	1.72 1.59 (107.4) (98.6)	2.65	36.0	19.0	0.097 (14.0)	28.3	SC-Silty Sandy Clay
122-152 (48-60)	12.6 11.2	1.67 1.62 (104.0) (101.0)	2.63	29.0	10.0	0.093 (13.5)	17.5	SC-Silty Sandy Clay
152-183 (60-72)	16.9 8.5	1.59 1.62 (99.1) (104)	2.64	30.0	10.0	- -	11.7 -	SC-Silty Sandy Clay SM-Silty Sand

[+] more than one value indicates the property had a given range for the stated depth

Table 1

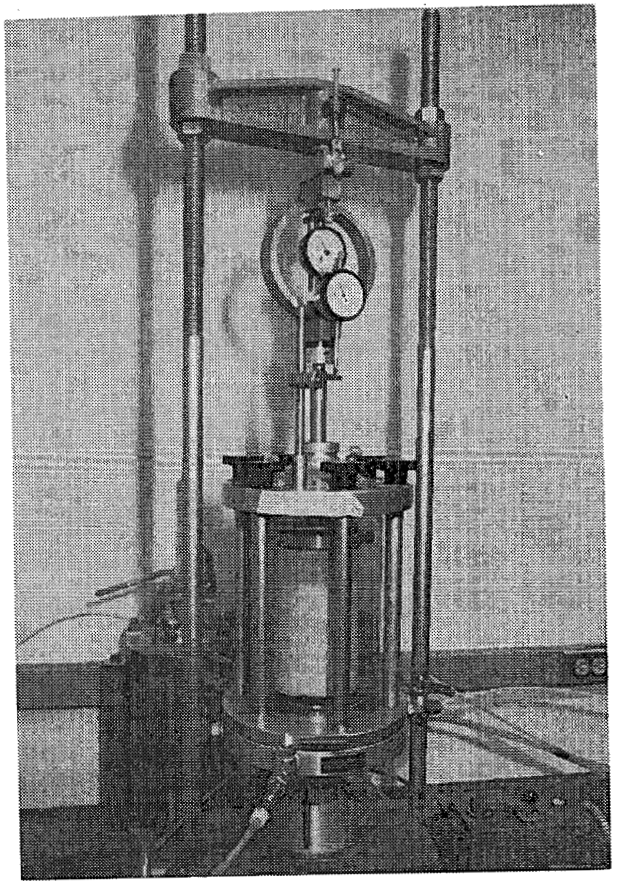

Figure 7 Triaxial Test

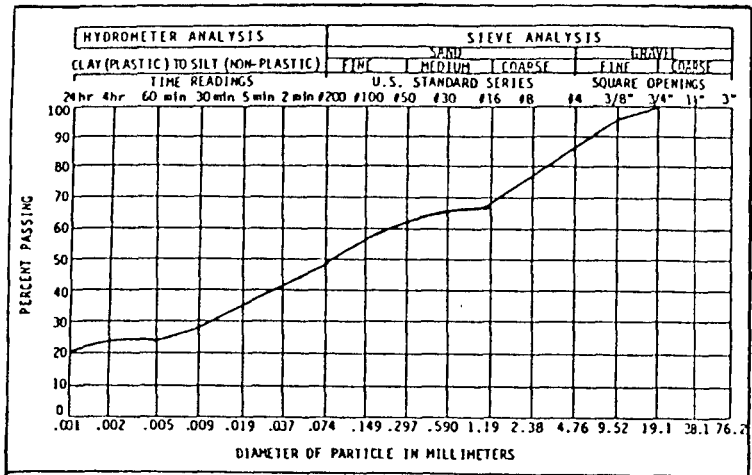

SOIL CLASSIFICATION CL-SC

LL= 32 % PI 14 % SPECIFIC GRAVITY 2.65

	TEST NO.	B-1	A-1	A-2		
INITIAL	WATER CONTENT, W_o %	12.5	15.1	15.1		
	DRY DENSITY pcf	102.2	97.8	97.8		
	VOID RATIO, e_o	.561	.691	.691		
	SATURATION, S_o %	.52	.89	.89		
BEFORE TEST	W.C. AFTER SATURATION, W_s %	-	-	-		
	SATURATION, S %	-	-	-		
	CONSOL. PRESSURE psi	0	5.0	7.5		
	W.C. AFTER CONSOL, W_c %	-	-	-		
	VOID RATIO AFTER CONSOL, e_c	-	-	-		
AT FAILURE	MAJ. PRIN. STRESS, psi	17.2	33.4	41.3		
	MIN. PRIN. STRESS, psi	0	5.0	7.5		
	PORE PRESSURE, u psi	-	-	-		
	WATER CONTENT, W_F %	-	-	-		
	VOID RATIO, e_F	-	-	-		
SPECIMEN DIAMETER inches		2.85	2.85	2.85		
INITIAL HEIGHT inches		6.25	6.0	6.0		
TEST TIME TO FAILURE minutes		8.3	10.0	16.0		

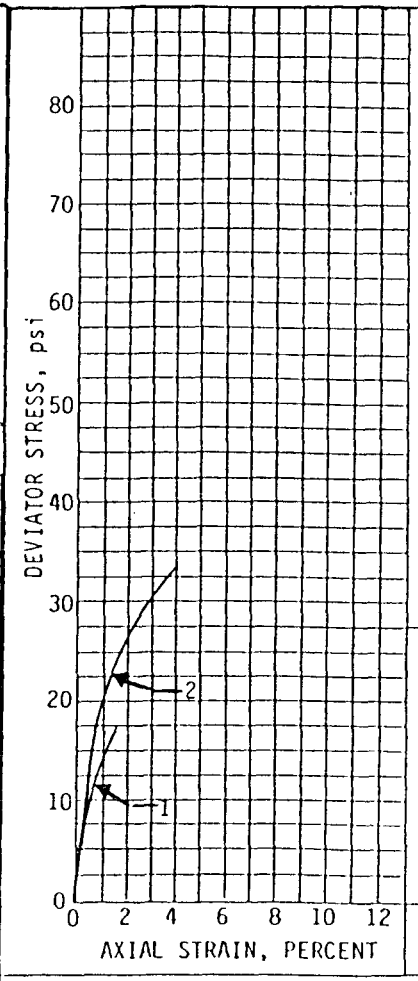

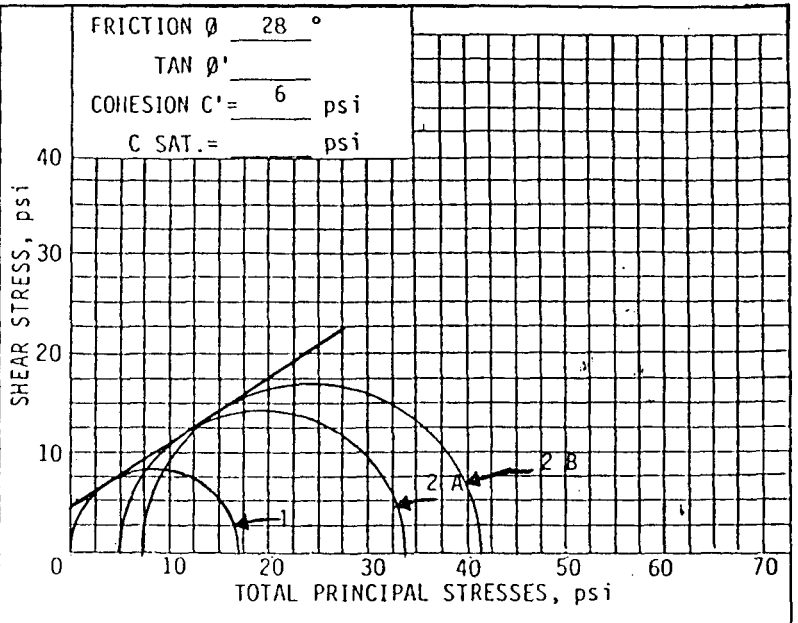

REMARKS : B-1 UU TEST

A-1, A-2 CU TEST

SAMPLE FROM TEST HOLE 1A,1B AT DEPTH 24"-36"

COMPOSITE

TYPE OF TEST

- [X] UNCONSOLIDATED UNDRAINED
- [X] CONSOLIDATED UNDRAINED
- [ ] CONSOLIDATED DRAINED
- [X] CONSTANT RATE OF STRAIN 0.015 inches/minute
- [ ] CONSTANT RATE OF STRESS _____ psi/minute

TYPE OF SPECIMEN

- [X] NATURAL
- [ ] REMOLDED

_____ % Gs _____

OPTIMUM MOISTURE _____ %

SAMPLE TYPE: SHELBY TUBE

Job No. 56201-0
Prepared by: V. Cassino
Date: 1-31-86

TRIAXIAL SHEAR TEST RESULTS
TOTAL STRESS TEST

Figure 8 Data Obtained from Triaxial Test

material. This radical variation of properties illustrates the complexity of characterizing soil both experimentally and analytically.

A second soil target was also tested to obtain a comparison between soils having different compaction. The native soil has a compaction that is relatively high thus providing a stiff soil target. To produce a softer soil target, a seven foot hole was excavated and replaced with uniform imported borrow. The soil was placed using a hand held tapper with water added to help the material settle. No heavy compaction equipment was used to bring the relative density to that found in the native desert soil. A dynamic core penetrometer test was performed on both the new soil target and native desert soil for comparisons (Figure 9). This test measures the soil resistance to an applied dynamic load. For the soft soil target, it took an average of 10 to 12 blows by a 12-pound weight falling 12 inches to force a coned-faced rod to penetrate one foot into the soil. By contrast over 80 blows were required to obtain the same one foot penetration into the native desert soil. A comparison of unit penetration into the respective targets are made in the experimental results section 3.2.3.

3.0 EXPERIMENTAL TESTING

The test program consisted of a series of drops onto the different targets to determine package response characteristics caused by the various relative stiffnesses of the impact surfaces. Table 2 is the test matrix showing the variety of impact velocities used for each respective target. The 44 ft/s (30 mph) impact velocity correlates directly to a 30-ft drop height used in regulatory testing. The other impact velocities of 66 ft/s (45 mph),

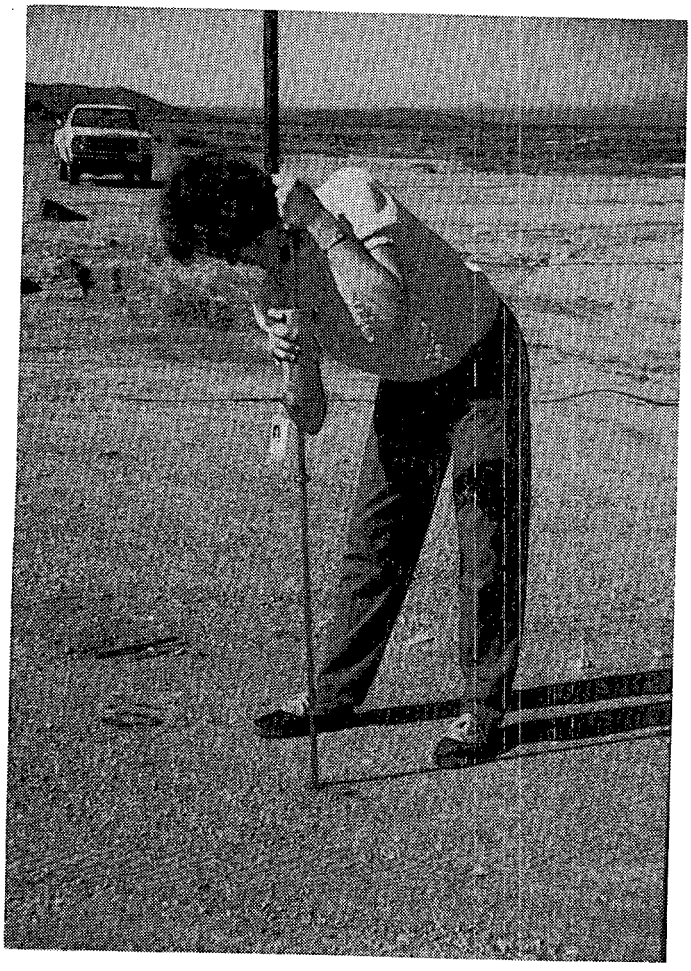

Figure 9 Dynamic Core Penetrometer Test

TEST MATRIX

TARGET	IMPACT VELOCITY (ft/s)			
	44	66	88	110
IN-SITU DESERT SOIL	X	X	X	
UNCOMPACTED IMPORTED BORROW				X
CONCRETE RUNWAY	X	X	X	
CONCRETE HIGHWAY	X	X•	X	
UNYIELDING TARGET	X			

• Actual impact velocity 44 ft/s because of test malfunction, no data at this velocity

Table 2

88 ft/s (60 mph) and 110 ft/s (75 mph) correspond to free fall drop heights of 68 ft, 120 ft, and 188 ft, respectively. The uncompacted soil target represented the softest environment while the rigid unyielding surface constituted the most severe.

3.1 Test Unit

The test unit was a simple cylindrical-shaped projectile. The unit, constructed out of Grade A36 mild steel, was tested without impact limiters or energy mitigating devices. This was done to better differentiate between the responses obtained from impacting the various targets without having to compensate for any effects provided by the impact limiters. At 6 ft long and 20 inches in diameter, the unit represents a simplified half-scale truck transportation cask (Figure 10). The unit consists of two hollow cylinder sections fastened together with a double set of radial pins. The two cylinders represent an outer cask body and an inner shielding liner respectively. The bottom cap is welded around the unit perimeter to the outer cylinder. Twelve 0.5-inch diameter bolts secure the lid to the test unit. To model cask contents, a stack of steel plates fill the unit bringing the total weight to 5200 lb. These plates are held together by a rod/bolt connection keeping them from moving independently inside the cavity and in turn making the contents act as a solid mass. A total of six test units were used in this program.

Instrumentation on each test unit included eight strain gages and at least four accelerometers, depending on the target (Figure 10). Strain gages, every 90° around the unit, were situated in two levels, 2.75 and 12 inches

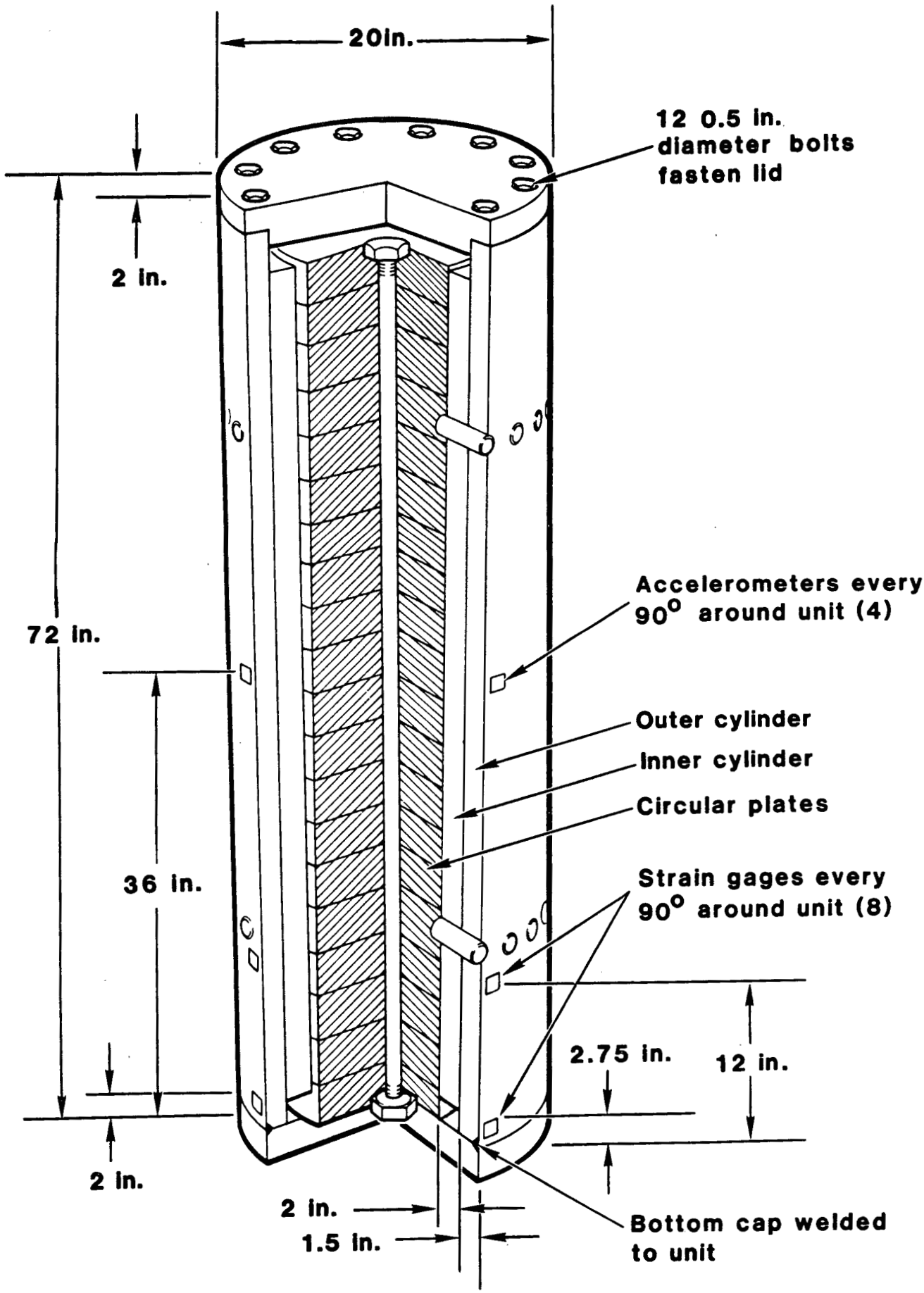

Figure 10 Test Unit Used for Experimental Program

from the bottom. The lower level of strain gages coincides with the gap between the outer cylinder and circular plates. This is where the maximum strains and package deformation was expected. For tests where small or micro-deformation was expected, Micro Measurements CEA-06-125UW-350 [7] strain gages were used. These gages are functional up to 15% strain levels. Micro Measurement EP-08-125AC-350 gages, which can adequately account for strains up to 50% instrumented the test unit for impacts expected to generate large deformations. These gages were installed using techniques recommended by the manufacturer [7]. The strain gage specifications are listed in Appendix A.

A primary set of accelerometers were also placed every 90° around the unit at the midplane. Any additional accelerometers were situated at the 45° point between the primary accelerometers. Every accelerometer was located to measure the same axial acceleration in the direction of impact. Thus, duplication of magnitude was sought by all accelerometers and strain gages.

Two types of accelerometers with different applicable ranges were used to instrument the test unit. Entran Devices EGAXT-23-F-5000 and EGAXT-48-F-10000 [8] are capable of measuring accelerations in the 5000 g and 10,000 g range, respectively. Both types of Entran accelerometers are damped to help avoid the effects of any resonating the system may have during impact that could reduce the validity of the accelerometer response. Endevco 2262 (damped) and 2264 (undamped) [9] are capable of measuring 25,000 g and 50,000 g acceleration levels, respectively. The acceleration specifications are given in Appendix A.

Each projectile unit underwent geometric inspection for length, diameter and circumference before and after each test to monitor deformations. Also, photometrics, ranging in camera speed from real time to 2000 frames/second,

were employed for velocity measurements and event recording. A plan view of the camera setup is shown in Figure 11. Recorded data included test unit strain, acceleration, deformation, impact velocity and penetration into the target. Comparison of this information was made between experimental results and analytical calculations.

The test apparatus consisted of a 75-ft long I-beam attached vertically to a frame (Figure 12). The I-beam helped guide the unit via a sled in addition to keeping the projectile perpendicular as it fell toward the target. The test unit was fastened to the sled by three 0.5-inch diameter explosive bolts (Figure 13). The use of rockets enabled the unit to obtain higher velocities without having to increase the drop height (Figure 14). Upon reaching the lower section of the I-beam, the test unit separated from the guide sled and impacted unrestrained into the target.

3.2 Results

The results obtained from the test series included information ranging from anticipated to unexpected. The unyielding target, as expected, produced the most severe strains, accelerations and deformations. However, the drop tests onto the yielding targets provided some unusual strain gage and accelerometer data. Of the eleven tests performed, five resulted in permanent deformations to the test unit. Differences in radius and length were measured for each test unit. In the cases of permanent deformations, the maximum radial strains occurred between three to four inches from the impact end of the unit. This is because of the added stiffness provided by the bottom cap

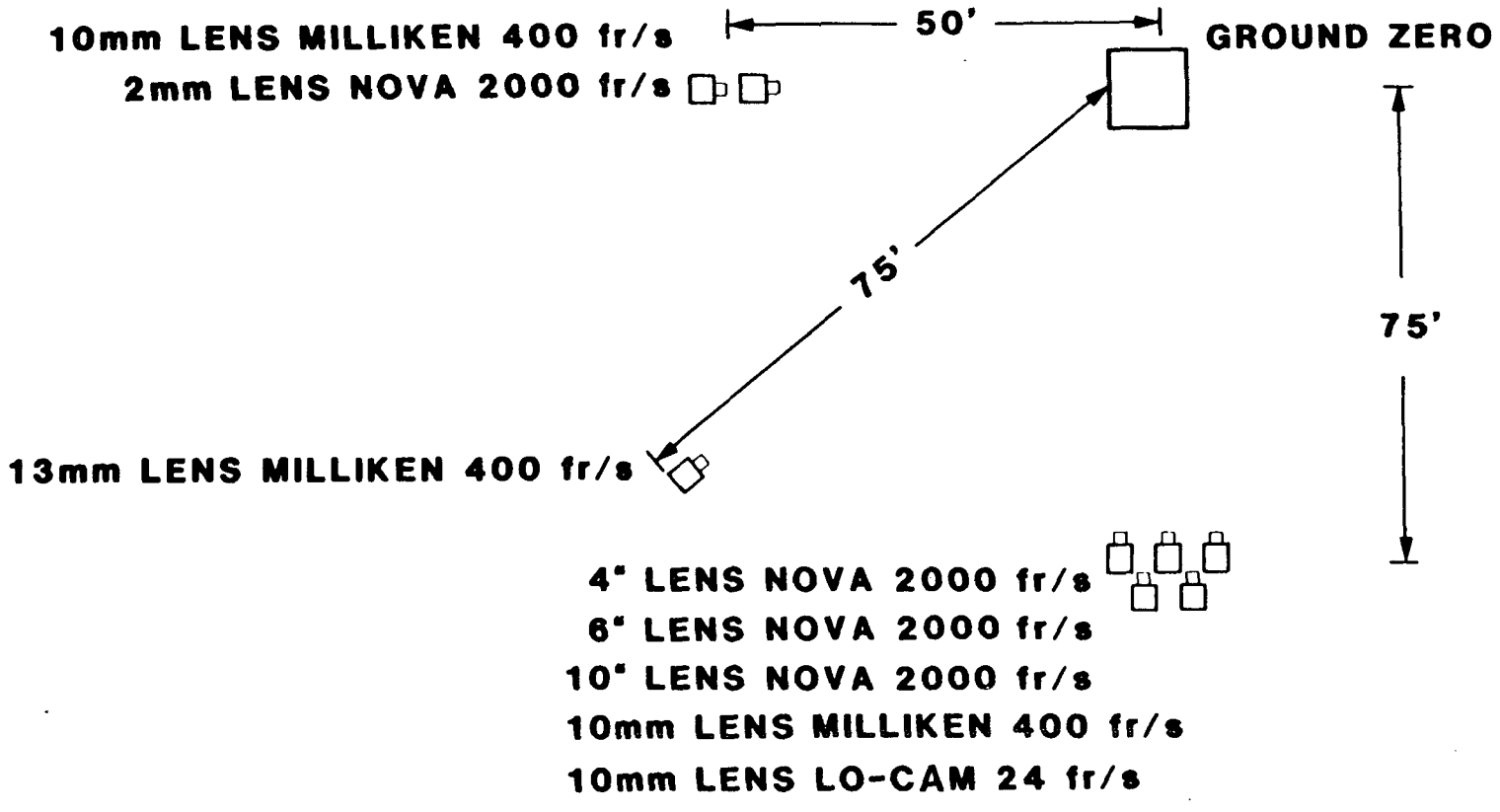

Figure 11 Camera Setup Used for Photometric Coverage

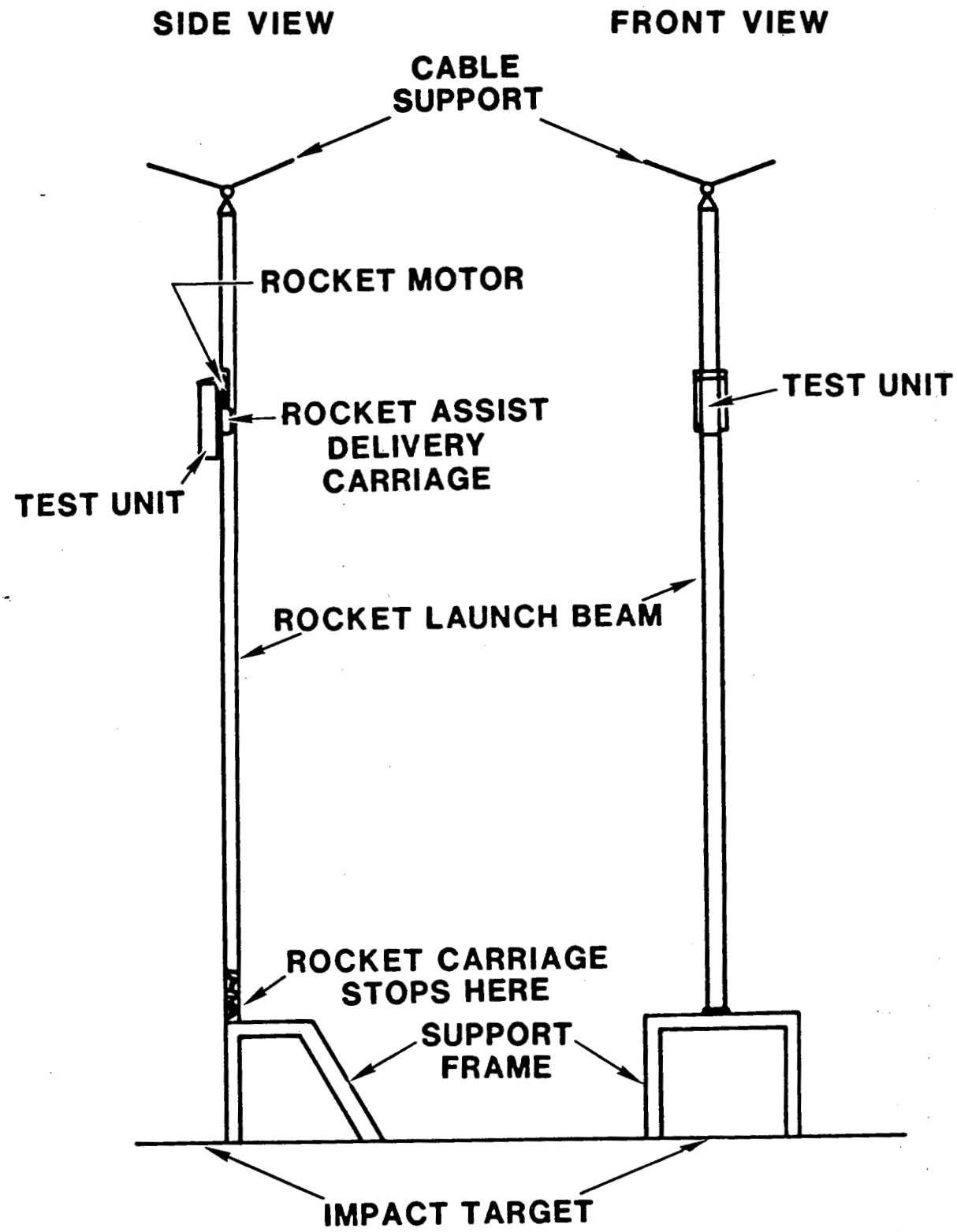

Figure 12 Test Apparatus

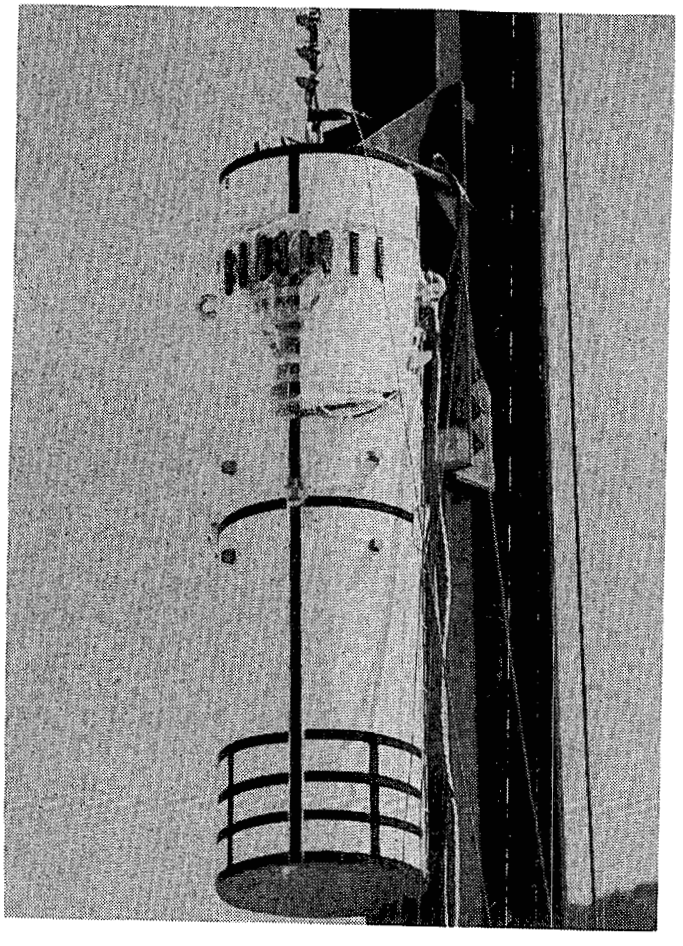

Figure 13 Test Unit Fastened to Sled

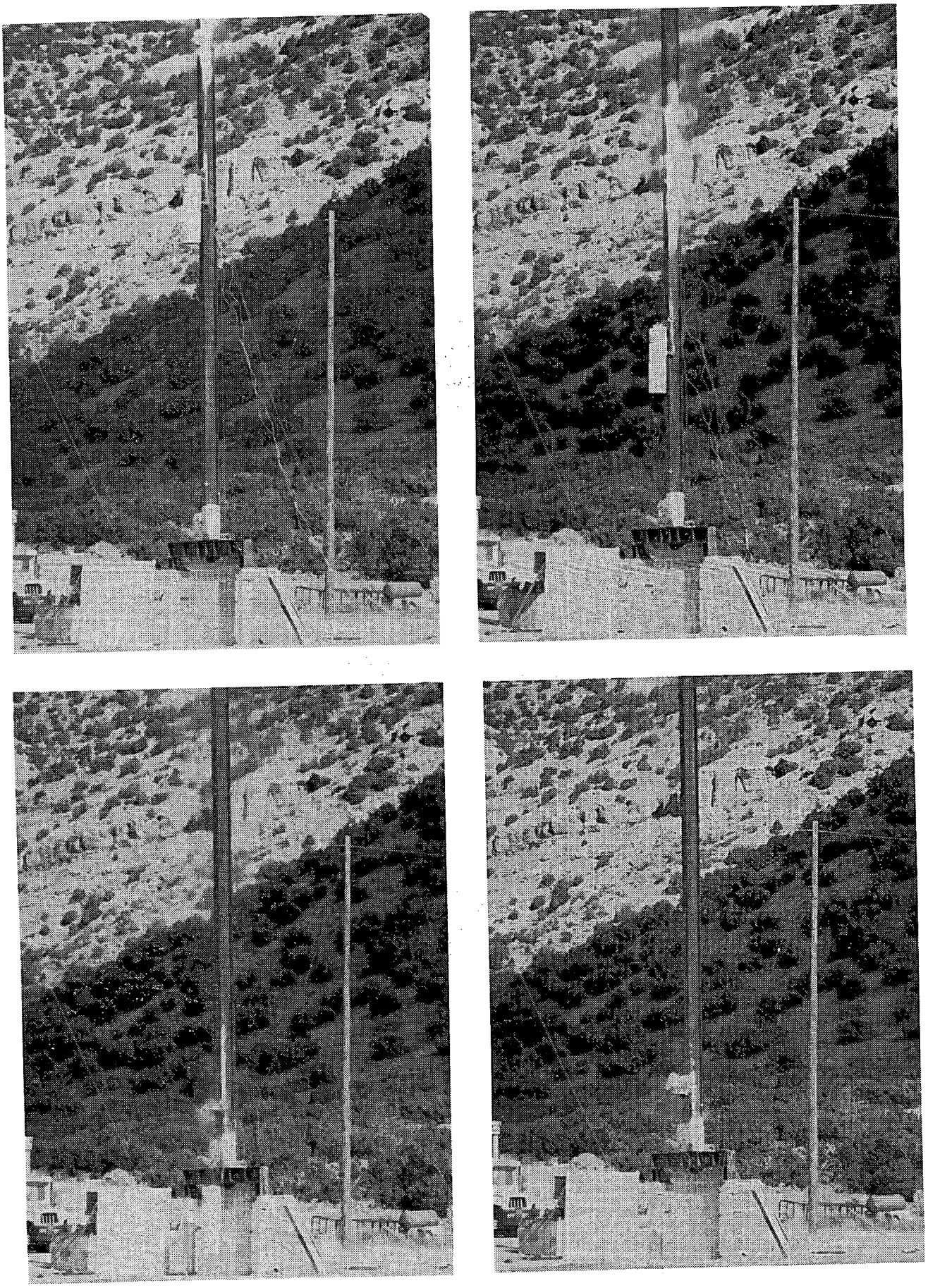

Figure 14 Test Unit Propelled by Rockets Impacting Target

being welded to the unit perimeter. Discussion of these results are detailed in the following sections.

3.2.1 Unyielding Target

The test unit was subjected to a 30-ft drop onto an unyielding target (Figure 15). After striking the target, the unit rebounded approximately six feet. The largest cask deformation experienced during the testing program occurred from this impact into the rigid target. At four inches above the point of impact, the maximum circumferential expansion occurred. The distance from the cask center-of-axis to the outer wall (radial length) increased 0.09 inches from its original 10 inches and the overall 6 ft length was shortened by 0.1 inches. The damage could not be detected visually so mechanical inspection had to be employed to measure the deformations on the order of one-hundredth of an inch. Thus, the maximum plastic deformations of the test units were on the order of 1% or less of its overall dimension.

Of the two types of instrumentation used to monitor cask responses, strain gage measurement provided much more reliable and consistent data. Accelerometer readings are inherently sensitive to the natural frequency of the test unit [10]. The possibility of exciting the natural frequencies of the test unit was increased since impact limiters were not present. This frequency which is activated from impact could cause the instrumentation to resonate ("ring") producing accelerometer readings that could be misleading. In addition, accelerometer response is highly susceptible to frequency playback that may be used during data reduction processes [11]. Every accelerometer was calibrated before and after each test to ensure validity in

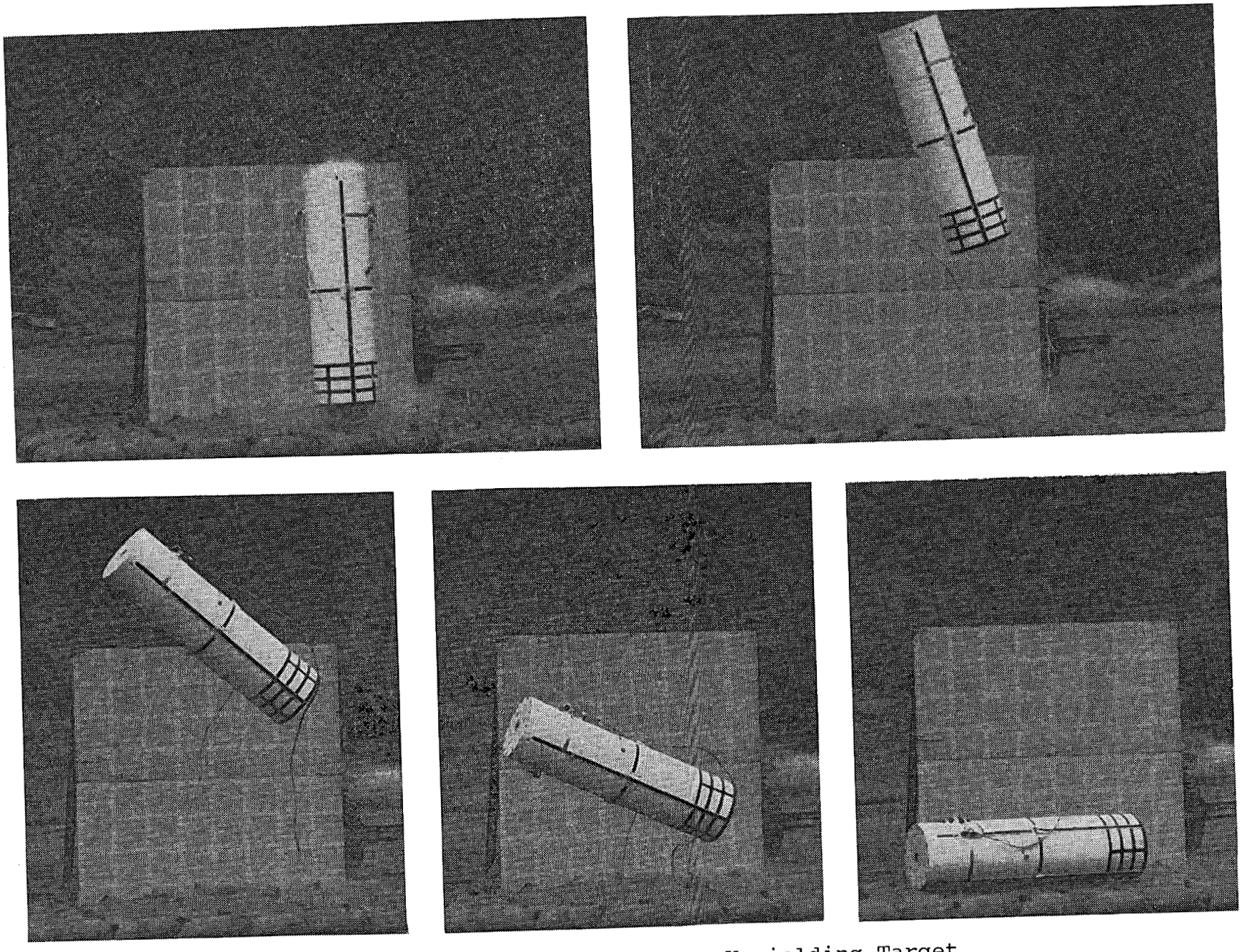

Figure 15 44 ft/s Impact into the Unyielding Target

test data and instrumentation integrity. The calibration tests performed to validate the accelerometers were the drop ball and 1000-g centrifuge. These tests were done in accordance with Sandia National Laboratories' procedures [12].

Figure 16 presents accelerometer data obtained from the 44 ft/s impact onto the rigid target. The response shows a maximum acceleration of approximately 1300 g's. The strain gage data (Figure 17) shows how the cask outer wall first compressed then proceeded to bow outward producing tension in the material. Regarding the mechanics behind this deformation mode, the impact forces the test unit into compression but because the load rate is so high the outer wall begins to buckle. This buckling stretches the outer wall thus producing a tensile reading in the strain gages. This particular strain gage was located 12 inches from the bottom of the test unit. A final permanent strain of 3000 μ in./in. (which is greater than the elastic strain limit of approximately 1200 μ in./in.) indicates plastic deformation did occur. This deformation translates to approximately 37,000 to 40,000 psi uniaxial stress at this point. Comparing the acceleration and strain gage data at the time of impact shows as the unit begins to plastically deform, energy absorption is occurring. This absorption is decreasing the response from impact. In other words, as the unit undergoes plastic deformation the magnitude of deceleration decreases. Referring to Figure 17, note that between 1 and 2 milliseconds into the event the strain gage is recording the process of plastic deformation. During the same time frame acceleration levels are decreasing dramatically (Figure 16). This is the justification for the use of impact limiters. As large deformations to impact limiters occur,

DATA FILE: R5601A
CHARGE # R803144
FILTER 10 KHZ
IIR FILTER

SAMPLE RATE 100000.0
START 0.000 MSEC
STOP 40.000 MSEC
CUTOFF= 2000.0 HZ

DIGITIZED: 20 MAR., 1986
ZERO TIME 20:36:32.309000
STATIC RUN LEVEL 0.000
LOWPASS

SYS ID: A3 CEN,AD3
HIGH CAL 5000.0000
LOW CAL 0.0000

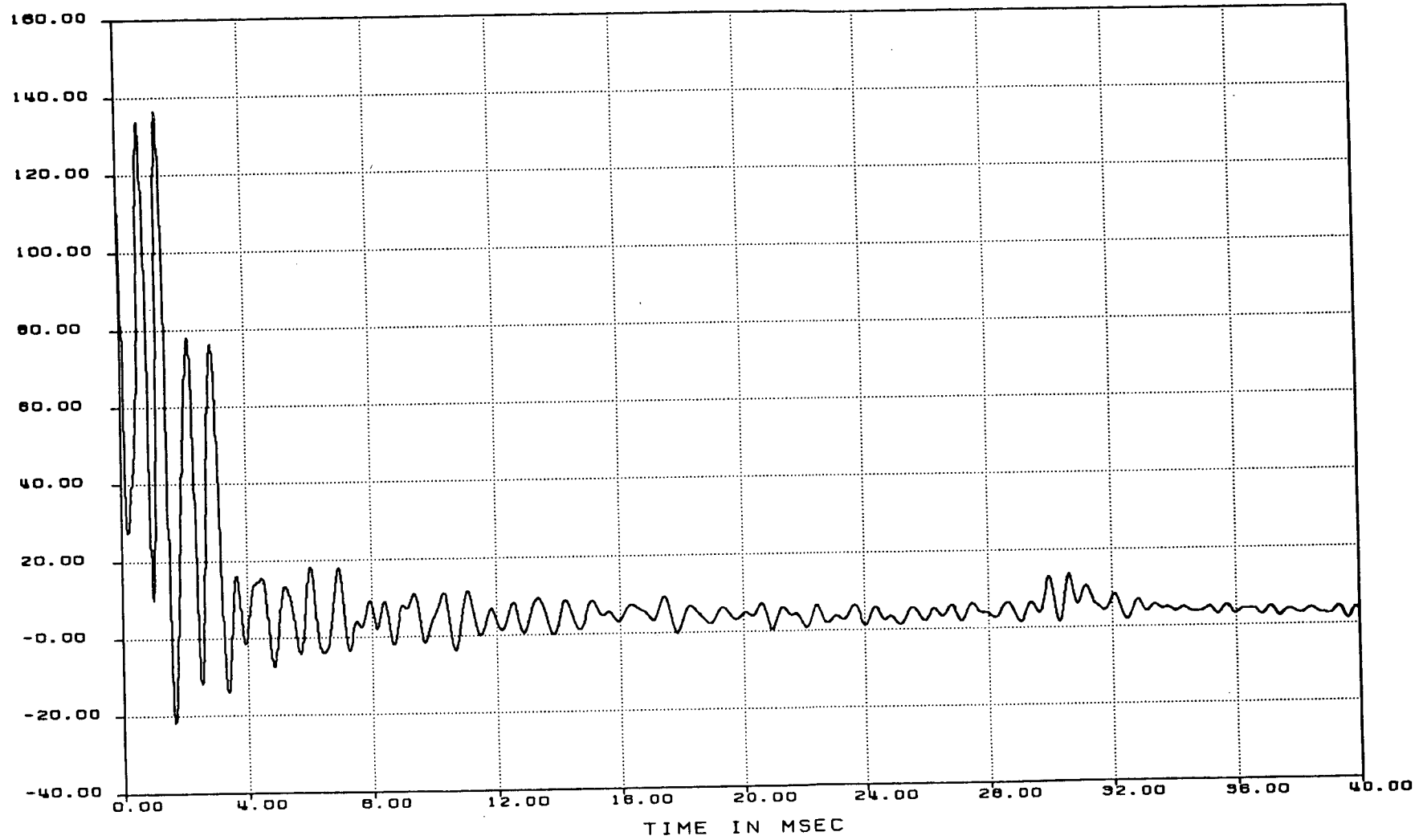

CHANNEL ID: A-1 TRACK # 9

TEST ID: TARGET HARDNESS TEST DATE: 3/14/86

Figure 16 Acceleration Data for 44 ft/s Impact Velocity into Unyielding Target

DATA FILE: R5601A	SAMPLE RATE 100000.0	DIGITIZED: 20 MAR., 1986	SYS ID: A3 CEN,AD4
CHARGE # R803144	START -5.000 MSEC	ZERO TIME 20:36:32.309000	HIGH CAL 3000.0000
FILTER 10 KHZ	STOP 20.000 MSEC	STATIC RUN LEVEL 0.000	LOW CAL 0.0000
IIR FILTER	CUTOFF= 1000.0 HZ	LOWPASS	

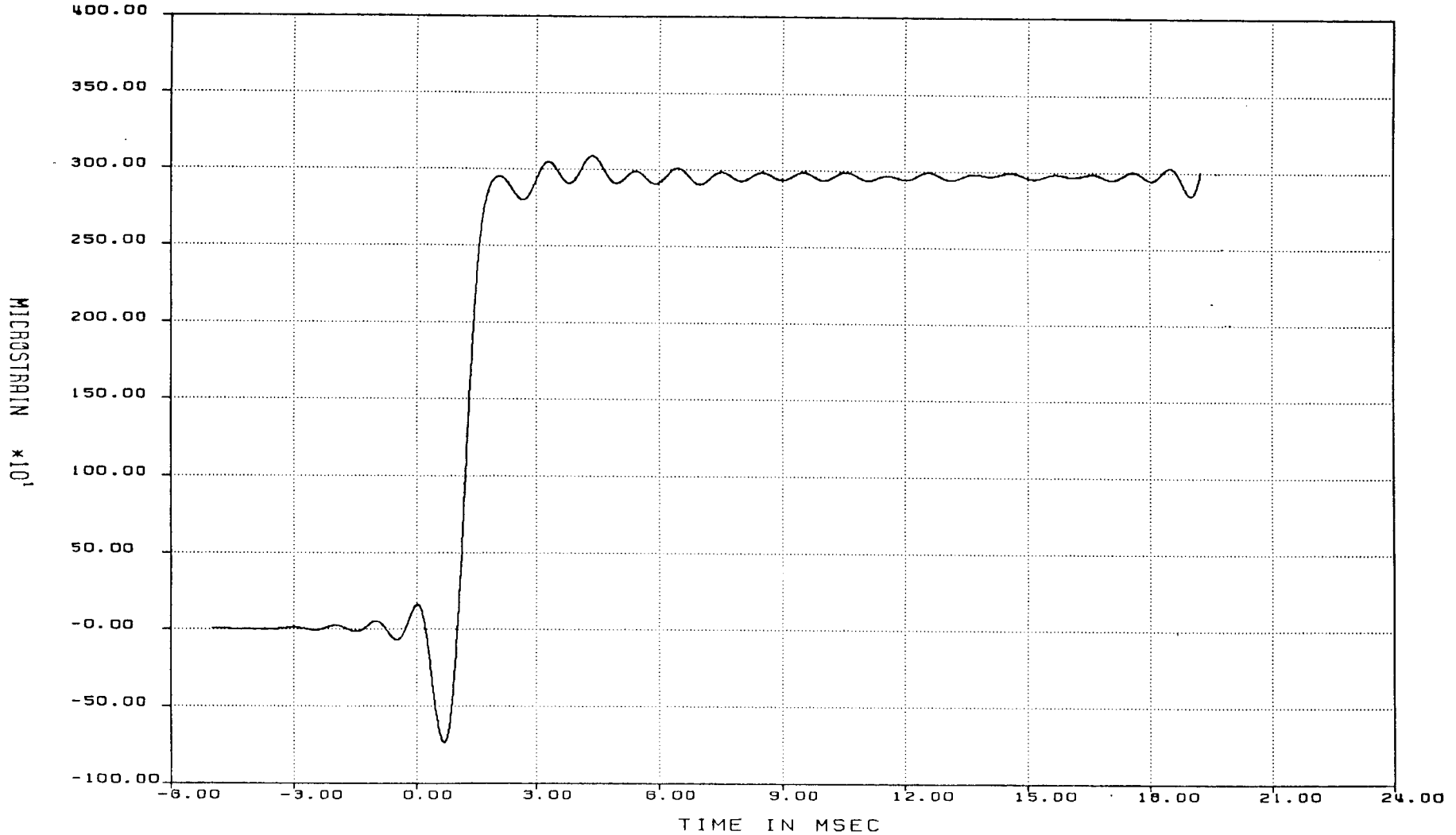

CHANNEL ID: S-4 TRACK # 4

TEST ID: TARGET HARDNESS TEST DATE: 3/14/86

Figure 17 Strain Gage Data for 44 ft/s Impact Velocity into Unyielding Target

energy is being absorbed thus reducing the magnitude of accelerations experienced by the impacting package.

3.2.2 Concrete Targets

Impacting the blunt-end object into concrete targets provided a variety of results. In every case where a concrete plug was formed, the shape of the plug was conical in geometry (Figure 18). The 45° shear plane formed from impact matches the failure theory of concrete when subjected to axial compressive loads. This failure is evident when a concrete test cylinder is subjected to an axial compressive load to the point of total fracture. At ultimate strength, or when total fracture occurs, a 45° shear plane will form. This failure mechanism was apparent in every impact test into a concrete target that resulted in a shear plug.

In every concrete target test, accelerometer data produced results disapportionately higher than expected. This was in direct contrast to the strain gage readings which recorded values well within the expected range. An explanation of the unexpected accelerometer readings relates to the rigidity and the abrupt method of failure of the concrete targets. The lack of energy mitigating devices (impact limiters) on the test unit results in an increased susceptibility to resonance as a result of high natural frequency excitations in the package. In other words, the accelerometers react to the high frequency resonance generated at impact rather than the actual deceleration rate of the package. If no soft impact limiters are present to reduce the amount of high frequency oscillations produced during impact, the accelerometers naturally record a higher frequency. If a test unit

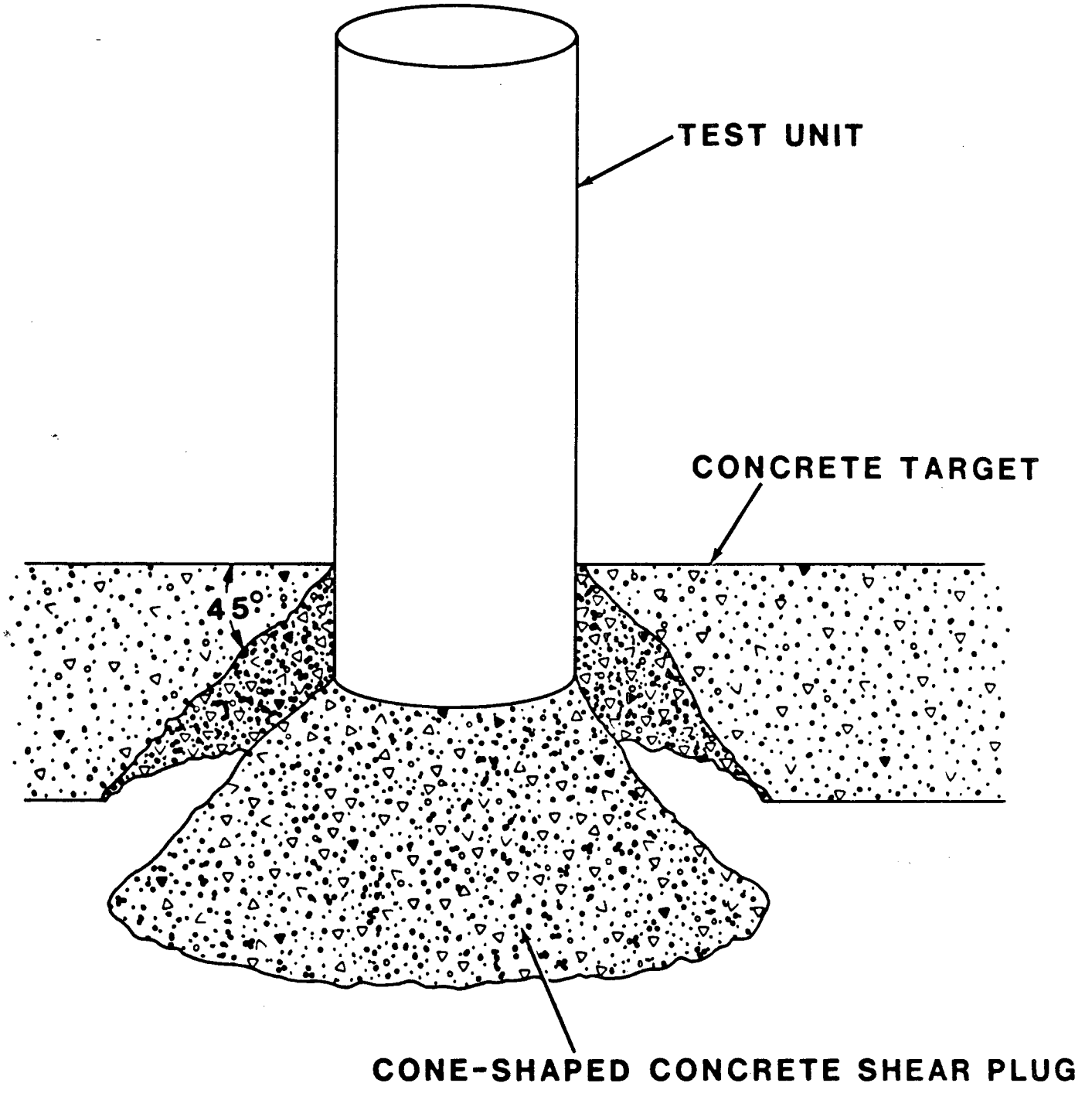

Figure 18 Shear Plug Formed in Concrete Targets

experiences a high frequency that approaches its natural frequency, resonance or "ringing" may result. If the test unit begins to resonate, it will directly effect the accelerometers and produce higher recorded g-loadings. For the test units used in this program, this susceptibility to ringing is increased by impacting onto a concrete target. An acceleration spike occurs at the point of impact producing a stress wave throughout the test unit. Once the concrete shear plug is formed, the resistance to cask motion decreases markedly. At this point the concrete material is providing very little resistance to cask travel. The soil underneath the plug then provides the stiffness needed to stop the test unit motion. With the decrease in resistance to cask travel, there is relatively little consistent support under the test unit to absorb the stress wave. A resonating effect becomes apparent producing a response in the accelerometers. In other words, the large and consistent force against the projectile as it impacted the unyielding target appears to have damped the ringing response of the test unit. Whereas with the concrete targets, the high initial force was quickly relaxed and there was no significant immediate damping of the natural frequency excitation of the test unit.

The following sections summarize the results of each concrete target test.

3.2.2.1 44 ft/s Impact into the Concrete Runway

The 44 ft/s impact into the concrete runway target penetrated approximately 0.25 inches (Figure 19). The impact produced radial cracking in the concrete target from the point of impact. This radial cracking was

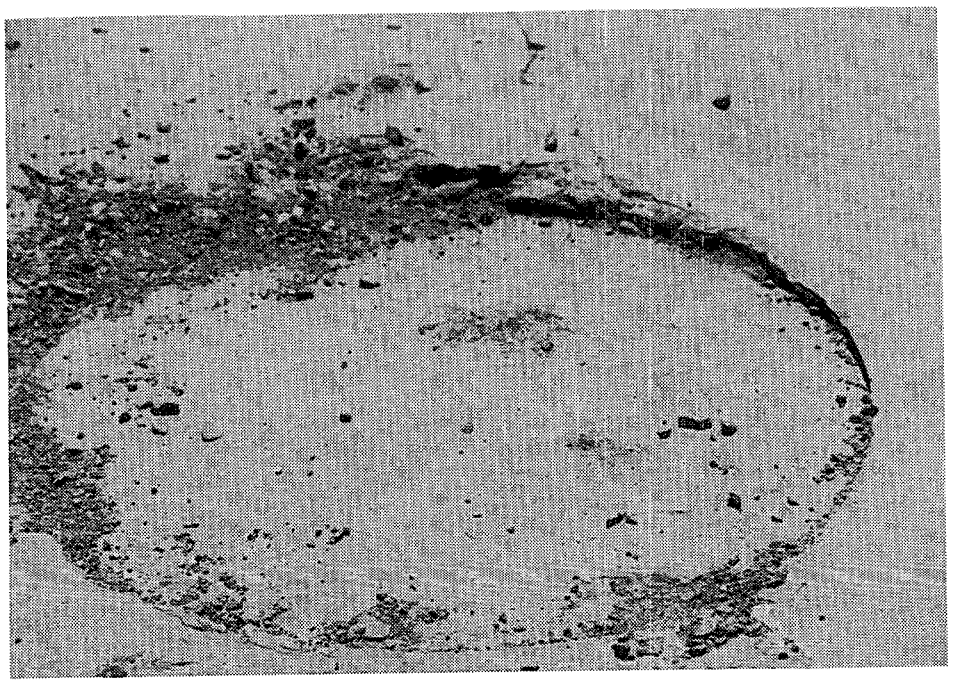

Figure 19 Concrete Runway Surface After an Impact at a Velocity of 44 ft/s

slight, but presented a phenomenon becoming more pronounced in higher velocity impacts. A very slight measurable cask deformation was determined from mechanical inspection. The test unit radial length expanded a maximum of 0.01 inches at 3.0 inches from the cask bottom.

Figures 20 and 21 present the recorded accelerations and strains measured from the drop test. A maximum acceleration of 480 g's resulted in strain levels of approximately 900 μ in./in. in compression. This strain gage, located twelve inches from the bottom, showed residual strain of 400 μ in./in. in tension which indicates a very slight permanent deformation. This correlates with the findings obtained from mechanical inspection.

3.2.2.2 66 ft/s Impact into the Concrete Runway

Impacting the 18-inch thick concrete runway at 66 ft/s resulted in a cask penetration of 4 inches (Figure 22). The radial length increased 0.03 inches, at the point 3.0 inches from the cask bottom. A shear plug (Figure 23) was formed with the top face a perfect imprint of the bottom of the test unit.

The peak recorded acceleration of 900 g's (Figure 24) and peak strains of 2,300 μ in./in. (Figure 25) are a definite increase in magnitude from the values obtained from the 44 ft/s impact. As with the impact into the unyielding target, the phenomenon of the outer wall compressing upon impact then bowing outward occurred. The material in the outer cylinder reached strains in compression in the order of 1000 μ in./in., then bowed outward producing strains in tension. A residual strain of approximately 500 μ in./in. shows the unit suffered permanent deformation. This strain reading

DATA FILE: R5542A	SAMPLE RATE 100000.0	DIGITIZED: 16 AUG., 1985	SYS ID: A3 CEN,AD6
CHARGE # 8950433	START -5.000 MSEC	ZERO TIME 19:28:19.270000	HIGH CAL 5000.0000
FILTER 10 KHZ	STOP 20.000 MSEC	STATIC RUN LEVEL 0.000	LOW CAL 0.0000
IIR FILTER	CUTOFF= 1000.0 HZ	LOWPASS	

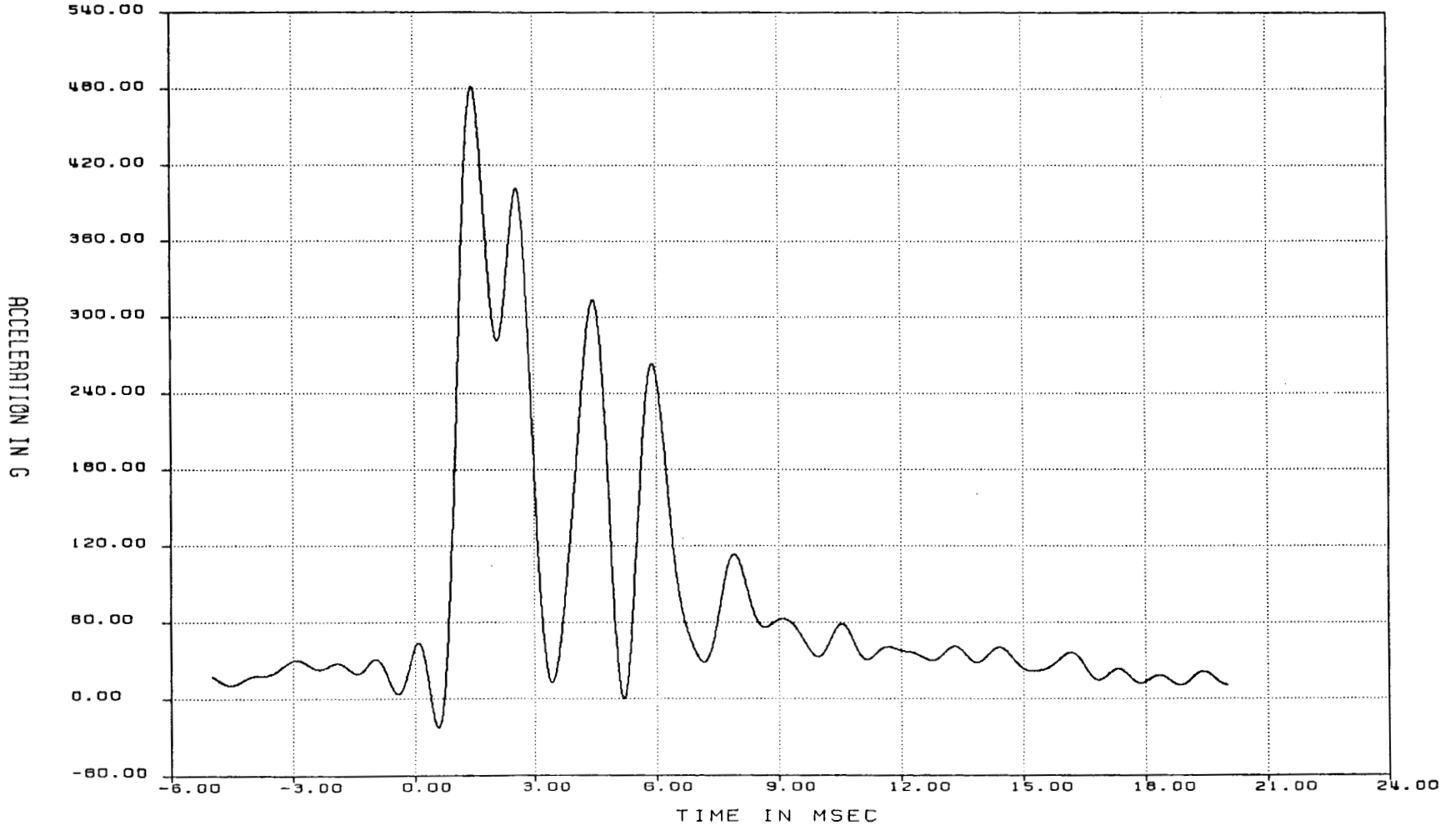

Figure 20 Acceleration Data for 44 ft/s Impact Velocity into Concrete Runway Target

DATA FILE: R5542A	SAMPLE RATE 100000.0	DIGITIZED: 16 AUG., 1985	SYS ID: A3 CEN,AD5
CHARGE # 8950433	START -5.000 MSEC	ZERO TIME 19:28:19.270000	HIGH CAL 1000.0000
FILTER 10 KHZ	STOP 20.000 MSEC	STATIC RUN LEVEL 0.000	LOW CAL 0.0000
IIR FILTER	CUTOFF= 1000.0 HZ	LOWPASS	

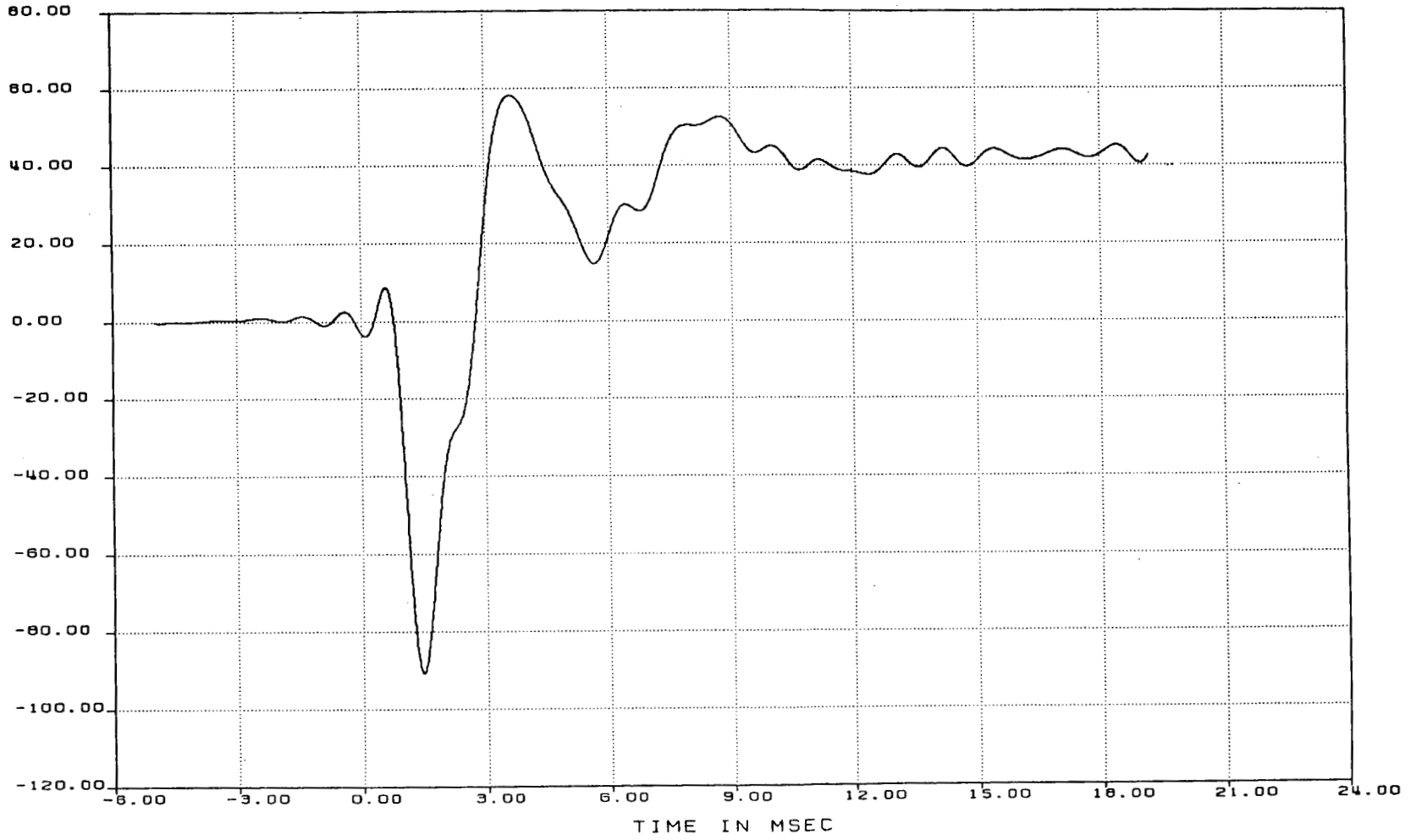

CHANNEL ID: S-8 TRACK #12

TEST ID: TARGET HARDNESS # 4 TEST DATE: 8/15/85

Figure 21 Strain Gage Data for 44 ft/s Impact Velocity into Concrete Runway Target

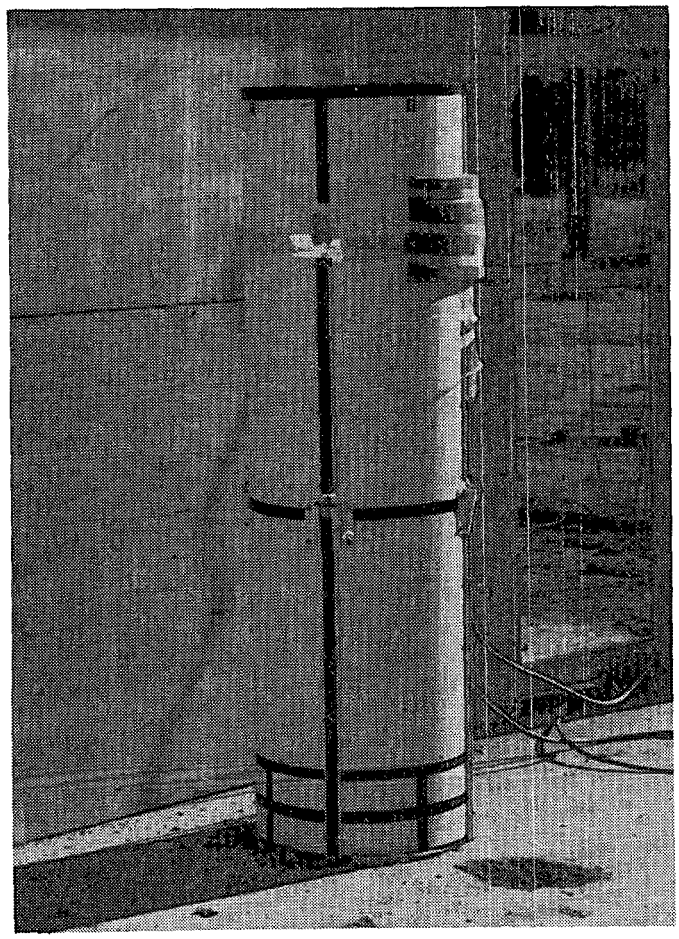

Figure 22 Test Unit's 4-inch Penetration into the Concrete Runway After Impacting at a Velocity of 66 ft/s

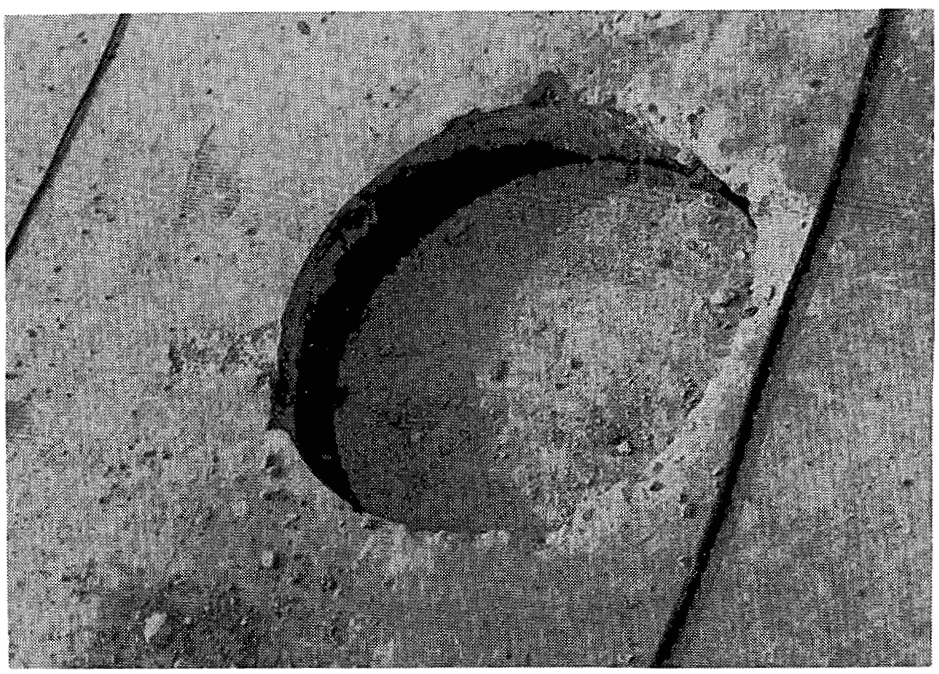

Figure 23 Shear Plug Formed in Concrete Runway After Impacting at a Velocity of 66 ft/s

DATA FILE: R5570A | SAMPLE RATE 100000.0 | DIGITIZED: 7 NOV., 1985 | SYS ID: A3 CEN,AD1
CHARGE # 8950.433 | START -5.000 MSEC | ZERO TIME 21:35:28.192000 | HIGH CAL 5000.0000
FILTER 10 KHZ | STOP 15.000 MSEC | STATIC RUN LEVEL 0.000 | LOW CAL 0.0000
IIR FILTER | CUTOFF= 500.0 HZ | LOWPASS

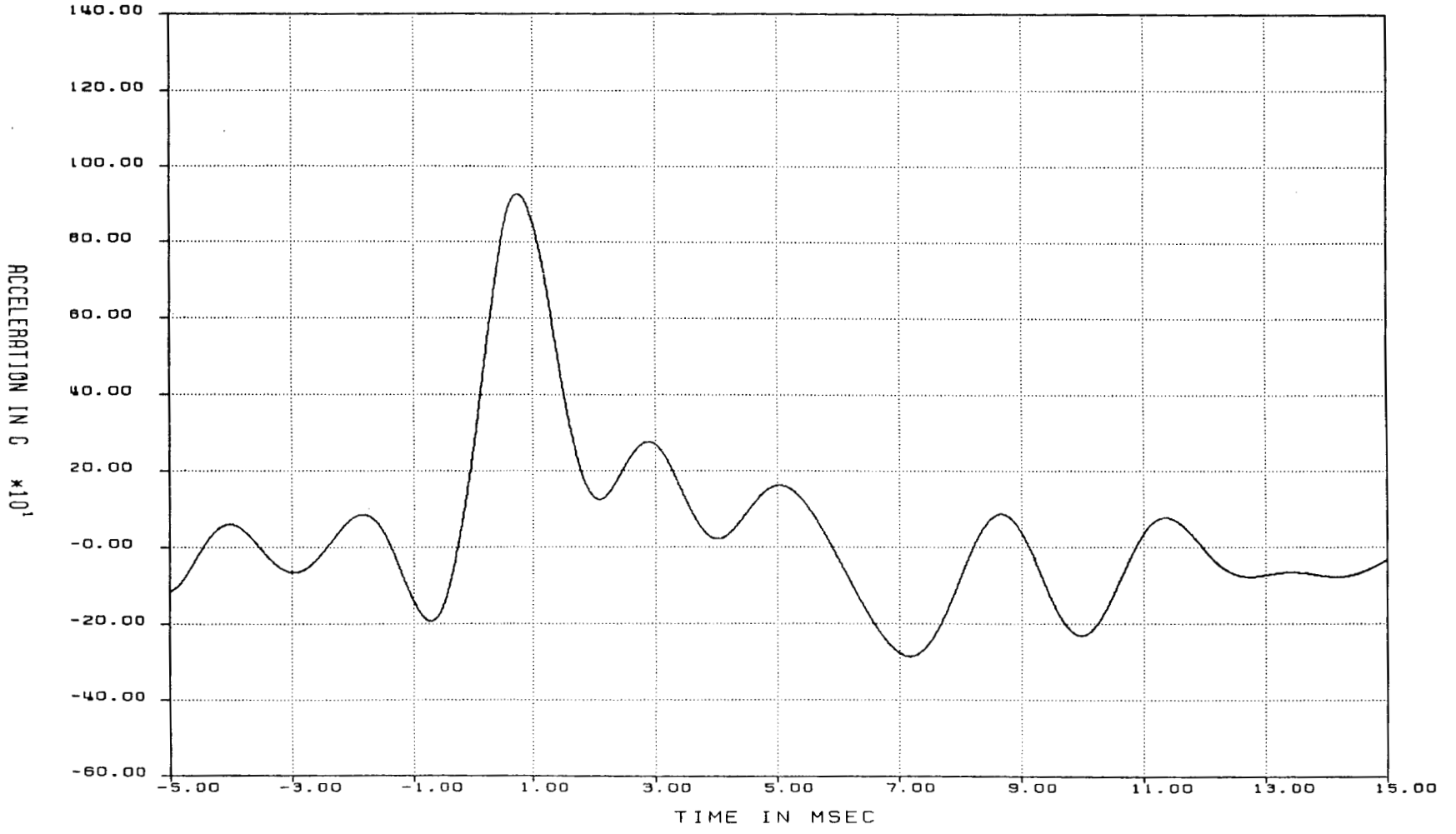

CHANNEL ID: A-1 TRACK # 1

TEST ID: TARGET HARDNESS #6 TEST DATE: 11/ 1/85

Figure 24 Acceleration Data for 66 ft/s Impact Velocity into Concrete Runway Target

DATA FILE: R5570A	SAMPLE RATE 100000.0	DIGITIZED: 7 NOV., 1985	SYS ID: A3 CEN,AD7
CHARGE # 8950.433	START -5.000 MSEC	ZERO TIME 21:35:28.192000	HIGH CAL 2000.0000
FILTER 10 KHZ	STOP 50.000 MSEC	STATIC RUN LEVEL 0.000	LOW CAL 0.0000
IIR FILTER	CUTOFF= 1000.0 HZ	LOWPASS	

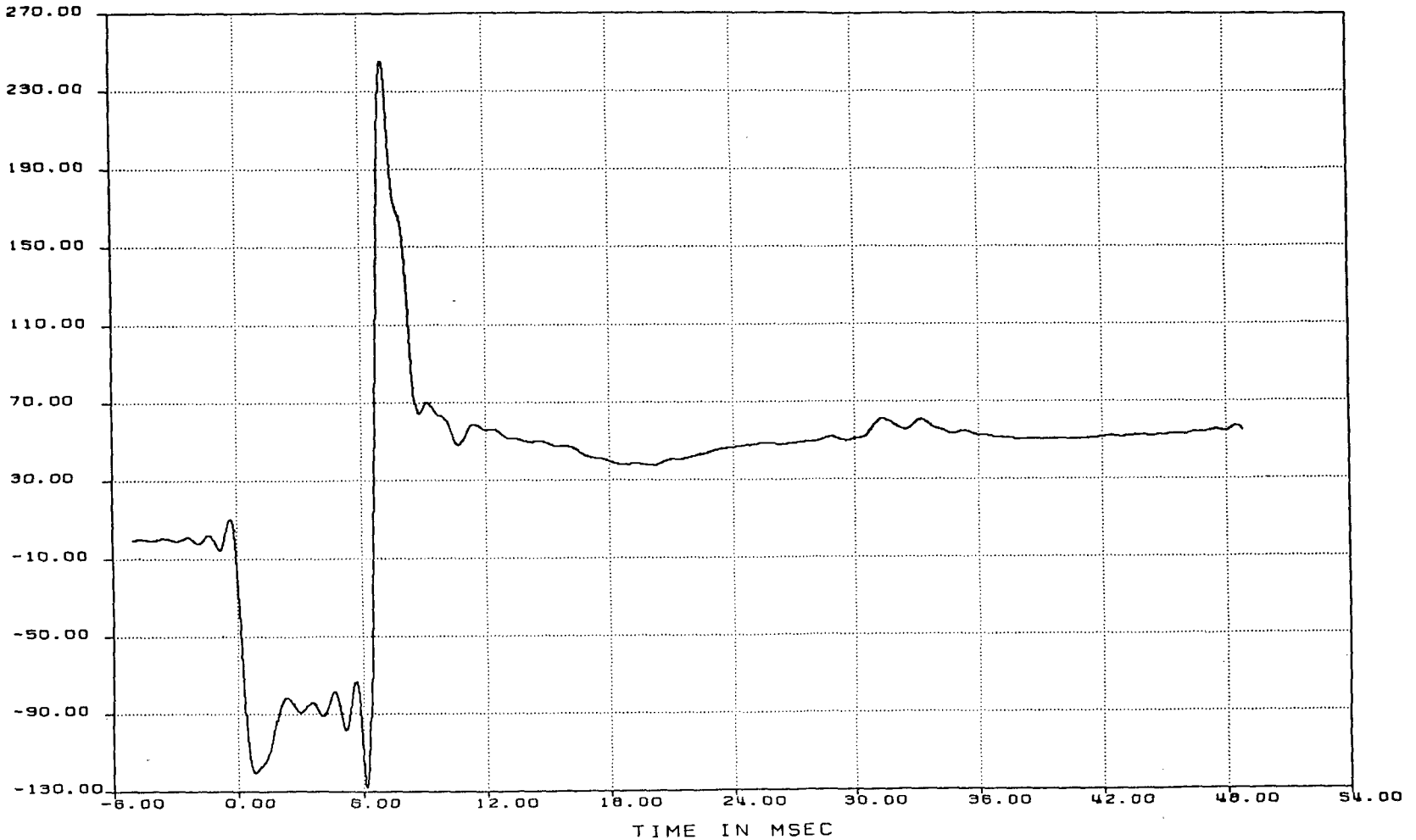

CHANNEL ID: S-3 TRACK # 7

TEST ID: TARGET HARDNESS #6 TEST DATE: 11/ 1/85

Figure 25 Strain Gage Data for 66 ft/s Impact Velocity into Concrete Runway Target

again coincides with the permanent deformation found from posttest measurements.

3.2.2.3 88 ft/s Impact into the Concrete Runway

The highest impact velocity of 88 ft/s into the concrete runway target produced a cask penetration of 8 inches (Figures 26 and 27). The unit suffered an increase in radial length of 0.08 inches at 3.5 inches from the cask bottom. The unit's overall axial length shortened 0.08 inches.

Recorded accelerations were in the range of 1000 g's. Figure 28 shows a positive acceleration pulse of 1000 g's and a negative pulse of approximately 900 g's. This negative pulse of such a large magnitude is an anomaly in the data which is not typical of the type of accelerometer readings expected. The negative pulse occurs at approximately six milliseconds into the impact event. A possible explanation of this pulse relates to Figures 29 and 30 where the strain gage levels change drastically at the six milliseconds mark. As discussed previously, this change in magnitude directly effects the measured acceleration levels. A large drop in strain levels correlates to a decreased magnitude in accelerations which in this case have been over compensated by the instrumentation.

Figures 29 and 30 present strain gage data at two different points on the test unit. Figure 29 shows data from a strain gage 2.75 inches from the cask bottom. Data from a strain gage located 90° around the unit and 12 inches from the bottom is shown in Figure 30. Figure 29 shows at the location close to the point of impact the material was strained to 5500 μ in./in. in compression and finally ended up with 4800 μ in./in. in residual compressive

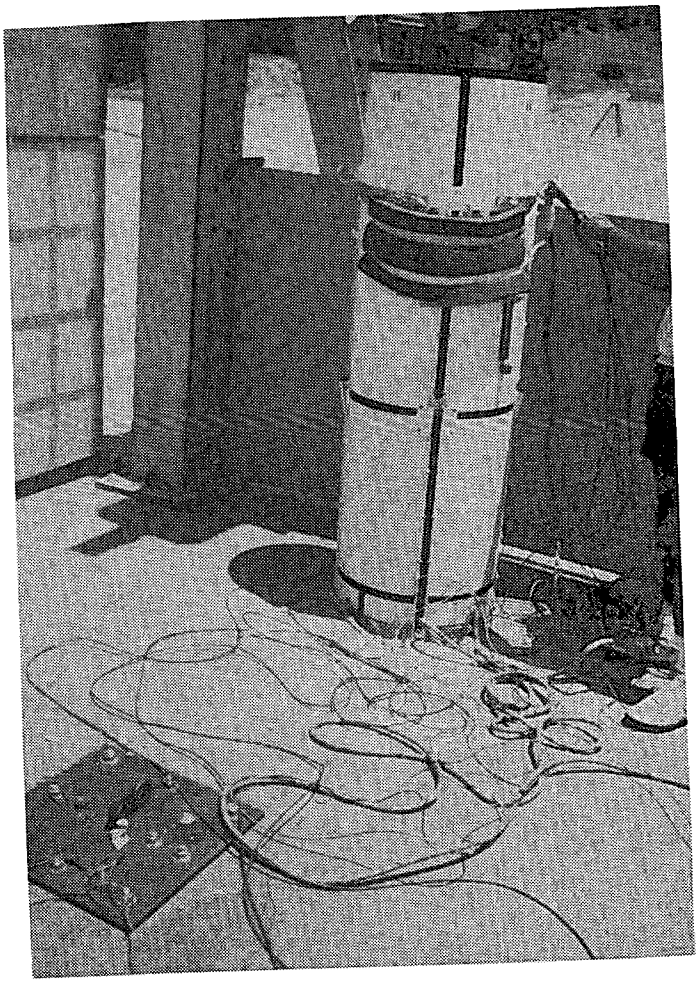

Figure 26 Test Unit's 8-inch Penetration into the Concrete Runway After Impacting at a Velocity of 88 ft/s

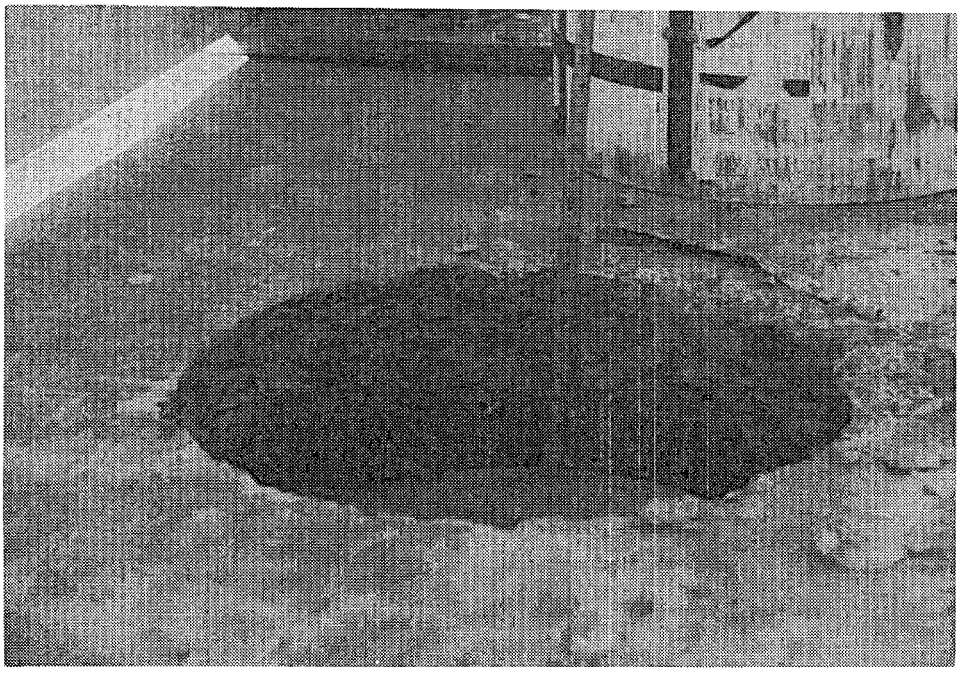

Figure 27 Shear Plug Formed in Concrete Runway After Impacting at a Velocity of 88 ft/s

DATA FILE: R5640A | SAMPLE RATE 100000.0 | DIGITIZED: 24 JUNE, 1986 | SYS ID: A3 CEN,AD1
CHARGE # R803144 | START -5.000 MSEC | ZERO TIME 19:19:29.080580 | HIGH CAL 10000.000
FILTER 10 KHZ | STOP 50.000 MSEC | STATIC RUN LEVEL 0.000 | LOW CAL 0.0000
IIR FILTER | CUTOFF= 500.0 HZ | LOWPASS

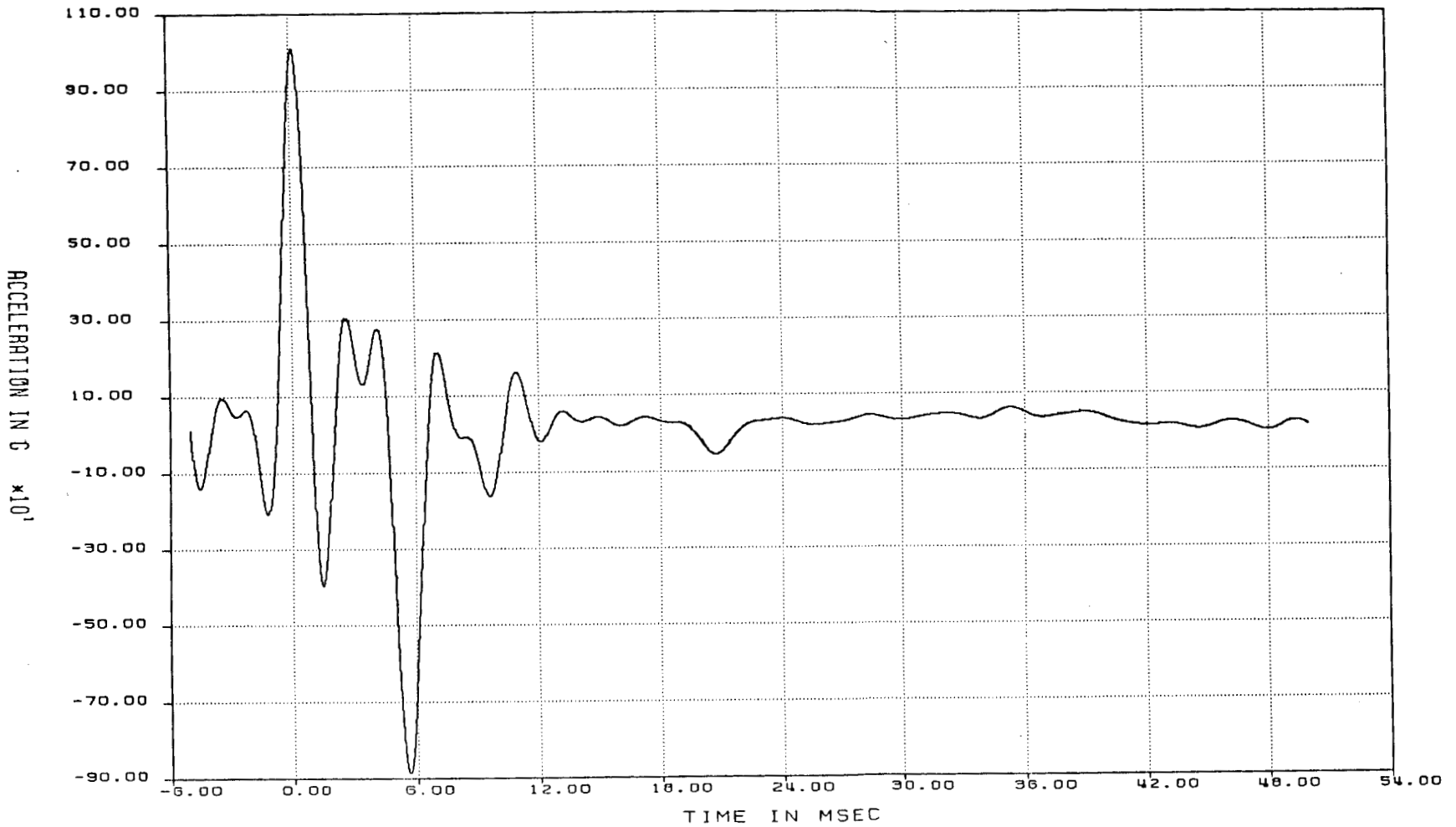

CHANNEL ID: A-1 TRACK # 1

TEST ID: TARGET HARDNESS # 11 TEST DATE: 6/17/86

Figure 28 Acceleration Data for 88 ft/s Impact Velocity into Concrete Runway Target

DATA FILE: R5640A
CHARGE # R803144
FILTER 10 KHZ
IIR FILTER

SAMPLE RATE 100000.0
START -5.000 MSEC
STOP 50.000 MSEC
CUTOFF= 1000.0 HZ

DIGITIZED: 24 JUNE, 1986
ZERO TIME 19:19:29.080580
STATIC RUN LEVEL 0.000
LOWPASS

SYS ID: A3 CEN,AD3
HIGH CAL 3000.0000
LOW CAL 0.0000

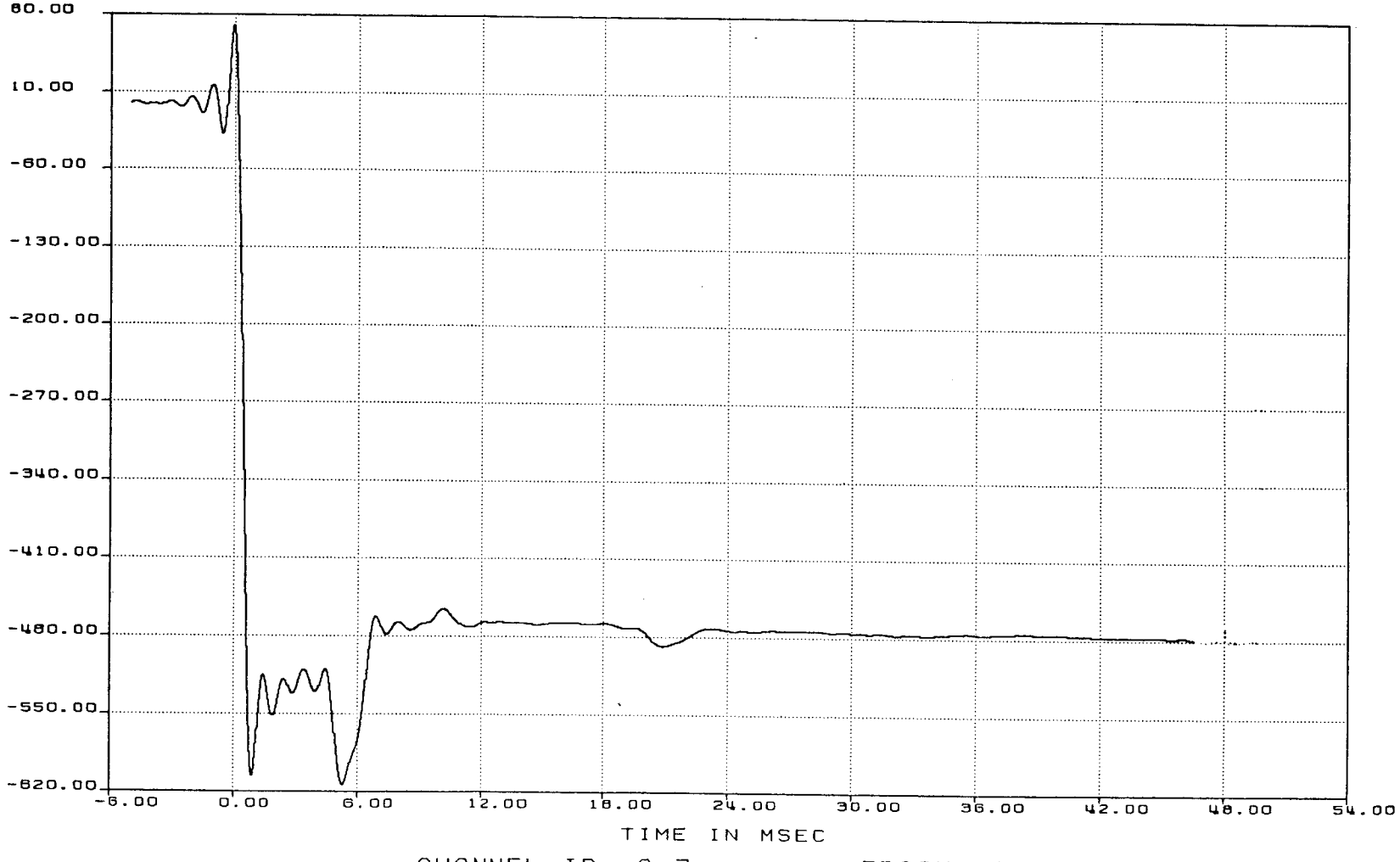

CHANNEL ID: S-7 TRACK #11

TEST ID: TARGET HARDNESS # 11 TEST DATE: 6/17/86

Figure 29 Strain Gage Data for 88 ft/s Impact Velocity into Concrete Runway Target

DATA FILE: R5640A	SAMPLE RATE 100000.0	DIGITIZED: 24 JUNE, 1986	SYS ID: A3 CEN,AD6
CHARGE # R803144	START -5.000 MSEC	ZERO TIME 19:19:29.080580	HIGH CAL 3000.0000
FILTER 10 KHZ	STOP 50.000 MSEC	STATIC RUN LEVEL 0.000	LOW CAL 0.0000
IIR FILTER	CUTOFF= 500.0 HZ	LOWPASS	

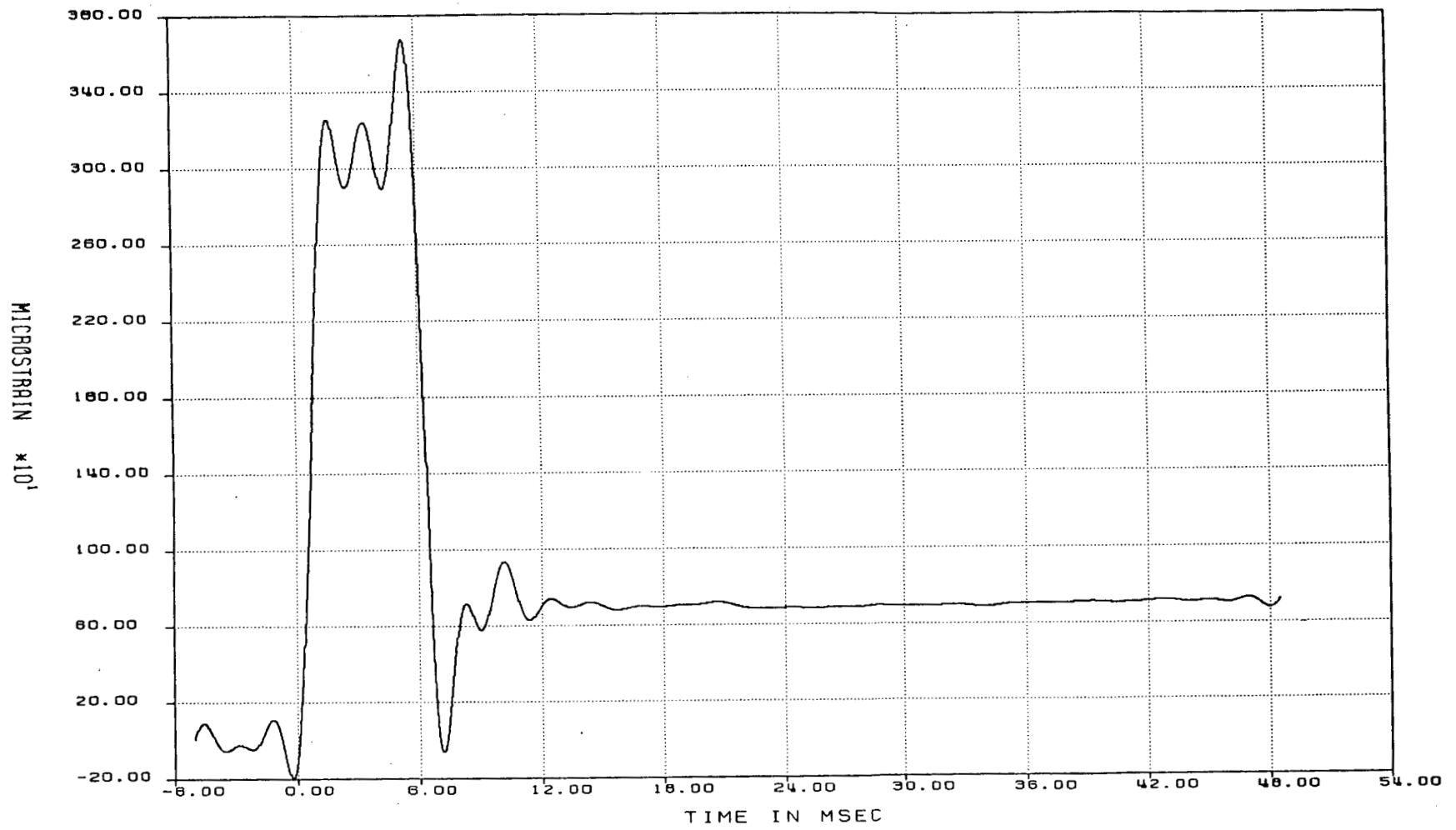

CHANNEL ID: S-2 TRACK # 6

TEST ID: TARGET HARDNESS # 11 TEST DATE: 6/17/86

Figure 30 Strain Gage Data for 88 ft/s Impact Velocity into Concrete Runway Target

strain. Here, the material did not bow outward but compressed axially. About 9 inches above this point on the unit the material did expand outward as indicated by the maximum 3400 μ in./in. with a residual strain of approximately 600 μ in./in. in tension. These two figures are representative of the phenomenon that exists when a hollow-shaped cylinder, whose head end is highly constrained, is impacted into a target to produce plastic deformation.

3.2.2.4 44 ft/s Impact into Concrete Highway

Impacting into the 9-inch thick concrete highway targets produced extensive radial and concentric cracking (Figure 31) on the impact surface with the formation of a shear plug. As the impact speed increased so did the magnitude of target damage. The target cracking and deflection became more pronounced such that the final deformed shape was concave in appearance. At 44 ft/s impact velocity, the test unit penetrated 4 inches into the target (Figure 32). No permanent cask deformation resulted from the drop test.

A measured acceleration of 350 g's was recorded (Figure 33). The maximum strain of 900 μ in./in. in compression produced no residual strain (Figure 34) thus correlating with the mechanical inspection findings of no permanent deformation.

3.2.2.5 66 ft/s Impact into Concrete Highway

This particular test was marred with technical difficulties with respect to the test rockets and instrumentation. The rockets misfired resulting in an impact velocity of approximately 44 ft/s. Inoperable instrumentation produced

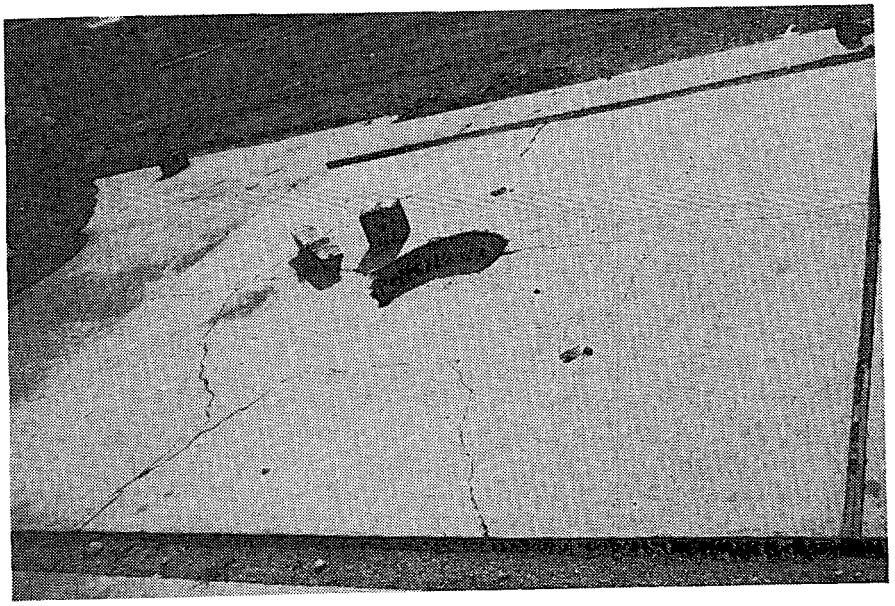

Figure 31 Concrete Highway Damage After Impacting at a Velocity of 44 ft/s

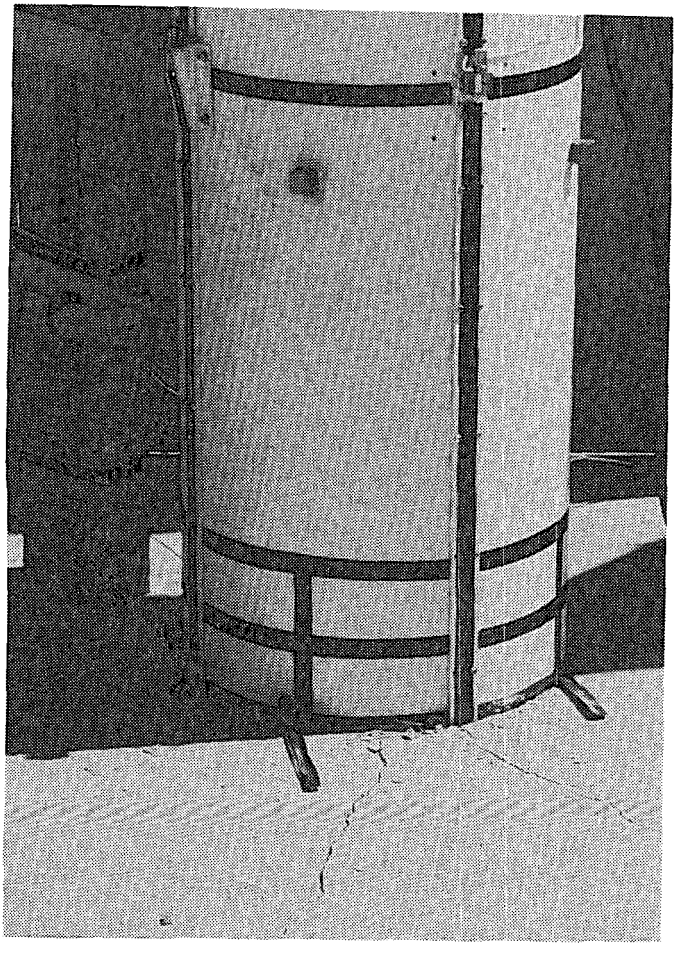

Figure 32 Test Unit's 4-inch Penetration into the Concrete Runway After Impacting at a Velocity of 44 ft/s

DATA FILE: R5554A	SAMPLE RATE 100000.0	DIGITIZED: 13 SEPT, 1985	SYS ID: A3 CEN,AD5
CHARGE # 8950.433	START -5.000 MSEC	ZERO TIME 19:50:41.956000	HIGH CAL 500.0000
FILTER 10 KHZ	STOP 20.000 MSEC	STATIC RUN LEVEL 0.000	LOW CAL 0.0000
IIR FILTER	CUTOFF= 500.0 HZ	LOWPASS	

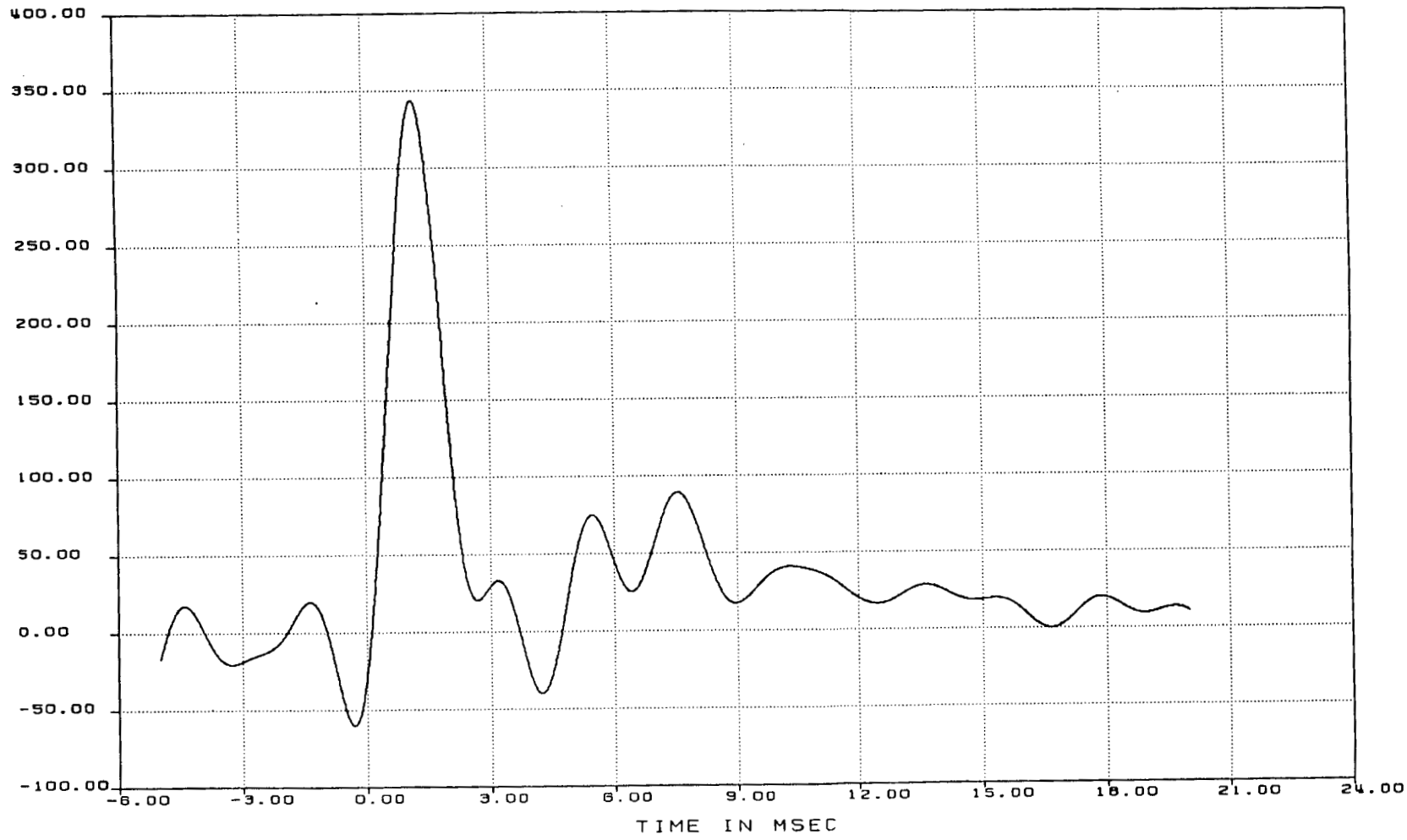

CHANNEL ID: A-5 TRACK # 5

TEST ID: TARGET HARDNESS EVENT #5 TEST DATE: 9/12/85

Figure 33 Acceleration Data for 44 ft/s Impact Velocity into Concrete Highway

DATA FILE: R5554A	SAMPLE RATE 100000.0	DIGITIZED: 13 SEPT, 1985	SYS ID: A3 CEN,AD6
CHARGE # 8950.433	START -5.000 MSEC	ZERO TIME 19:50:41.956000	HIGH CAL 1000.0000
FILTER 10 KHZ	STOP 50.000 MSEC	STATIC RUN LEVEL 0.000	LOW CAL 0.0000
IIR FILTER	CUTOFF= 1000.0 HZ	LOWPASS	

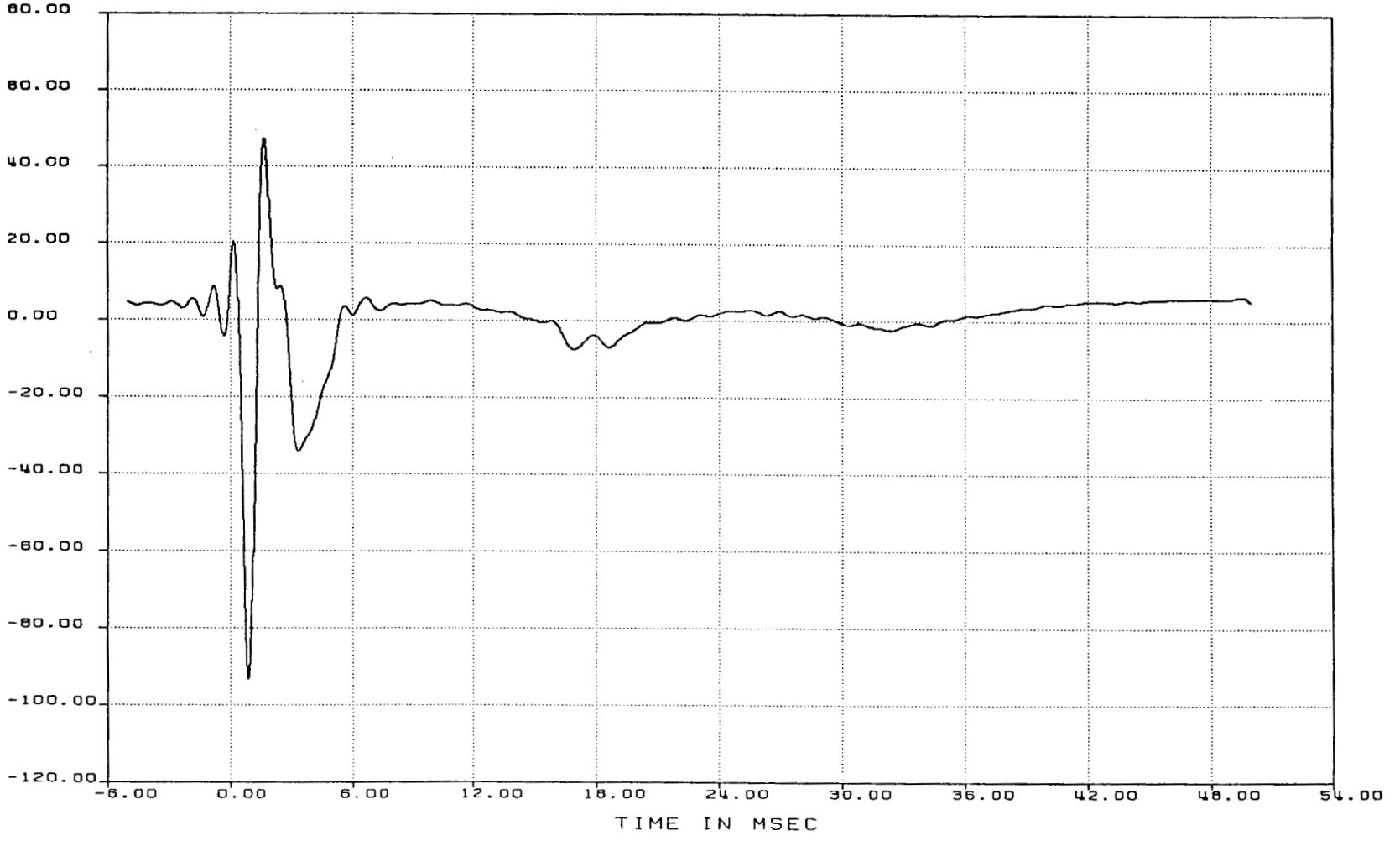

CHANNEL ID: S-7 TRACK #13

TEST ID: TARGET HARDNESS EVENT #5 TEST DATE: 9/12/85

Figure 34 Strain Gage Data for 44 ft/s Impact Velocity into Concrete Highway Target

no acceleration or strain gage data. However, the cask penetration into the target of 4 inches matched that obtained from the earlier 44 ft/s drop. The target damage between the two tests was identical (Figure 35). Thus, with respect to unit penetration and target damage, reproducible results were obtained impacting a concrete highway target twice at a velocity of 44 ft/s.

3.2.2.6 88 ft/s Impact into Concrete Highway

A penetration of 19 inches resulted from the 88 ft/s impact into the concrete highway (Figure 36). Taking into account a high impact velocity and large unit penetration, the target damage and cracking was identical in geometrical appearance to that found in the two previous concrete highway tests. At 3.5 inches above the bottom of the test unit, the maximum increase in radial length was 0.02 inches.

As with the 88 ft/s impact into the concrete runway, acceleration readings were disapportionately higher than expected (Figure 37), however the magnitude of the highway impact was much greater. At impact the accelerometers recorded 4500 g's. This is the cask response at the point the test unit strikes the target and energy is absorbed into forming the shear plug. Approximately 6 milliseconds later another acceleration load of 7500 g's is recorded. This represents the test unit stopping after the soil underneath locks up. These acceleration magnitudes do not coincide with expected values and in fact are contradictory with respect to measured deformations and recorded strains. Note that the 18-inch thick concrete runway recorded lower acceleration magnitudes (1000 g's) than this 9-inch thick highway slab. This is an anomaly since the stiffer runway should

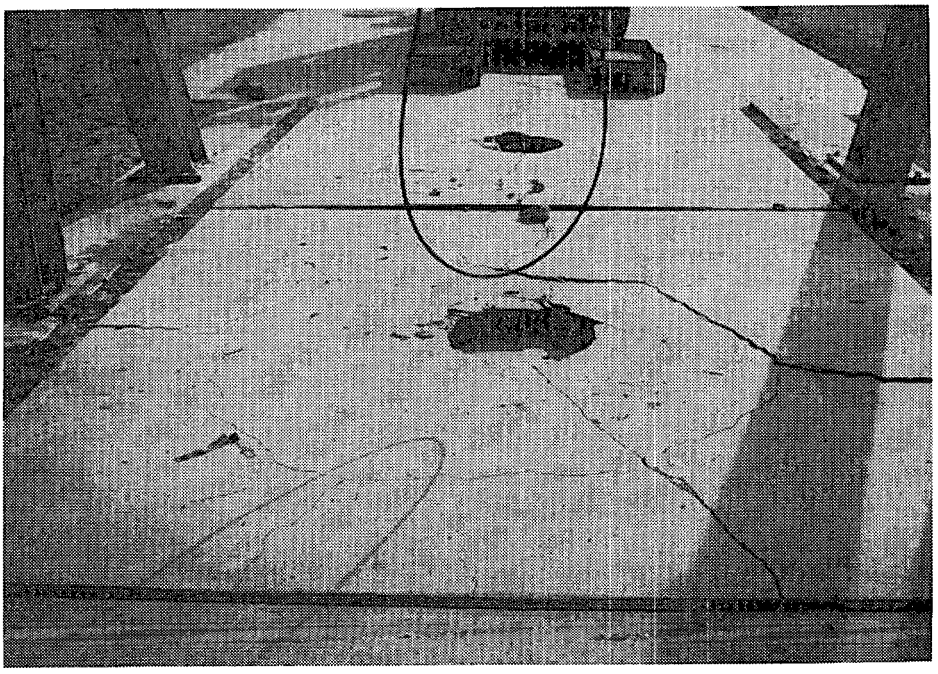

Figure 35 Concrete Highway Damage from Impacting at a Velocity of 44 ft/s

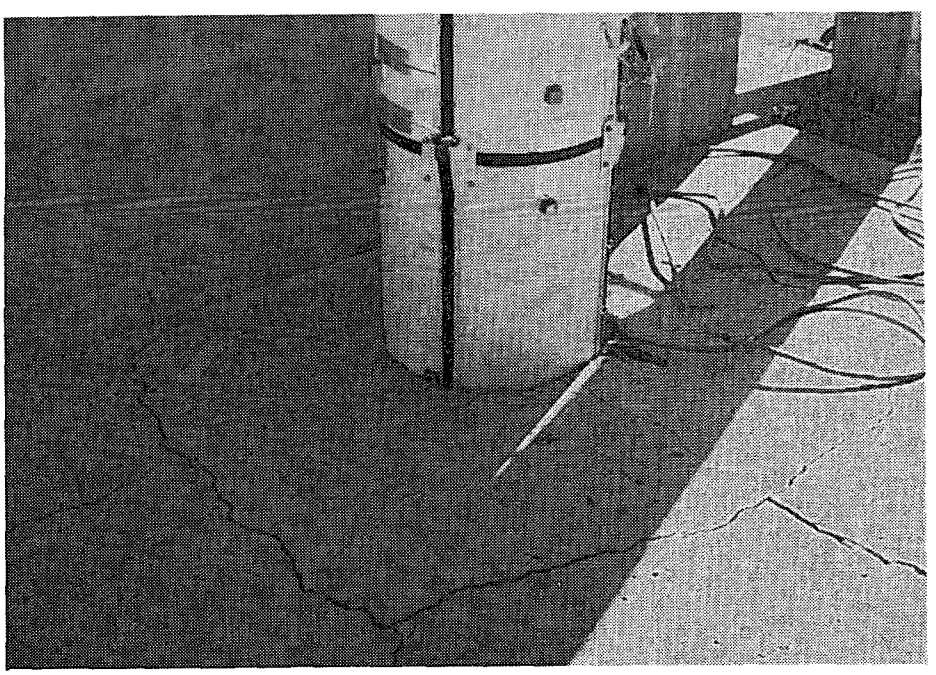

Figure 36 Test Unit's 19-inch Penetration into the Concrete Highway After Impacting at a Velocity of 88 ft/s

DATA FILE: R5592A
CHARGE # 8950.433
FILTER 10 KHZ
IIR FILTER

SAMPLE RATE 100000.0
START -5.000 MSEC
STOP 40.000 MSEC
CUTOFF= 500.0 HZ

DIGITIZED: 27 JAN., 1986
ZERO TIME 19:51:21.931000
STATIC RUN LEVEL 0.000
LOWPASS

SYS ID: A3 CEN,AD5
HIGH CAL 10000.000
LOW CAL 0.0000

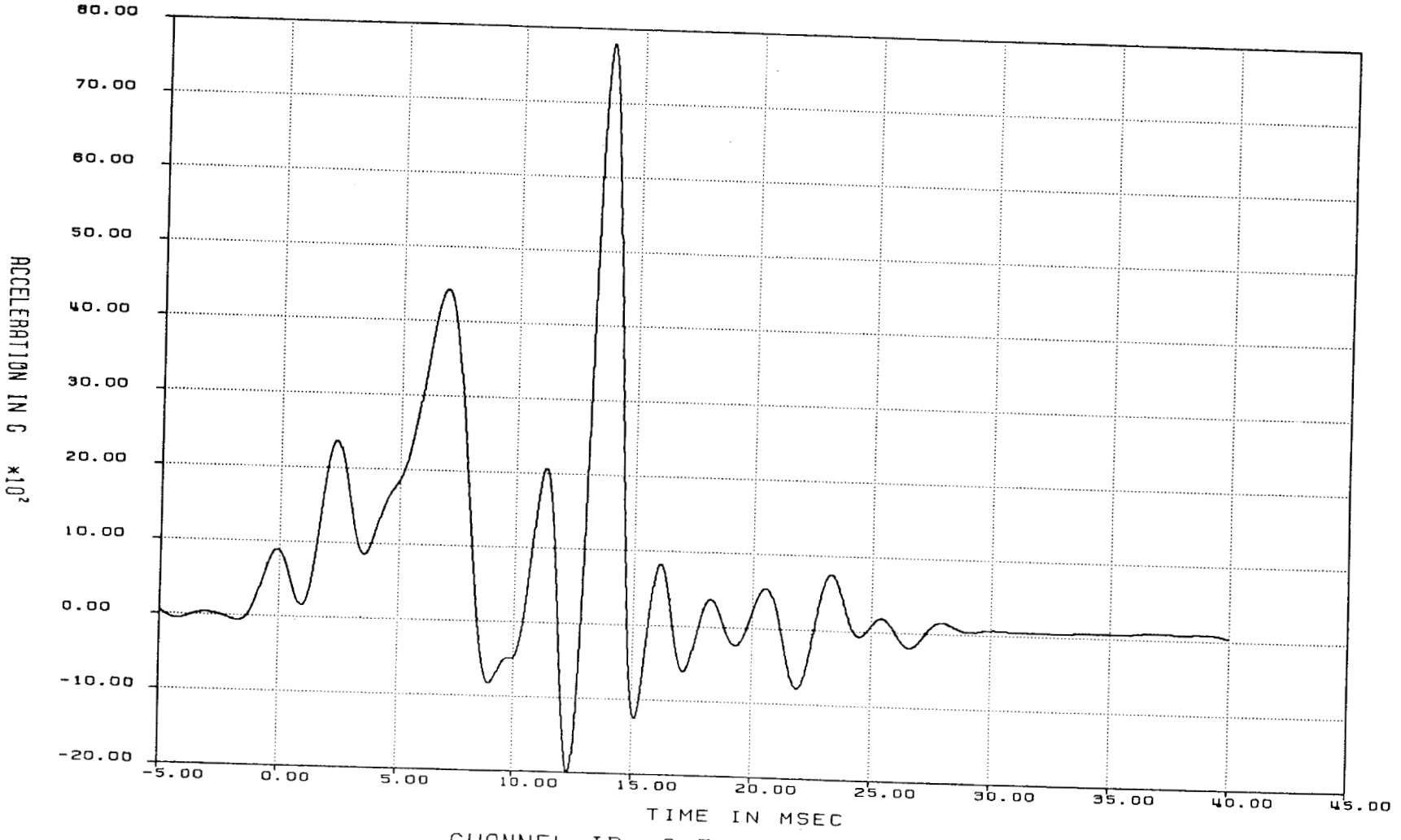

CHANNEL ID: A-5 TRACK #19

TEST ID: TARGET HARDNESS #7 TEST DATE: 1/24/86

Figure 37 Acceleration Data for 88 ft/s Impact Velocity into Concrete Highway Target

produce higher decelerations. The maximum strain in compression of 1800 μ in./in. produced a residual strain of 1300 μ in./in. (Figure 38) which correlates well with the 0.02 in. measured axial deformation. This strain gage was located 12 inches from the bottom. Figure 39 shows the recorded data of a strain gage 2.75 inches from the cask's bottom. The unit suffered a maximum compressive strain of 800 μ in./in. then experienced 2400 μ in./in. in tension. A 600 μ in./in. residual strain correlates with the elongation of the cask circumference. Thus, the recorded accelerations are assumed to be directly affected by the frequencies generated by impacting a brittle target. The natural frequencies of the test unit are excited and produce artificially high readings in the accelerometers.

3.2.3 Soil Targets

Four drops ranging in velocity from 44 ft/s (30 mph) to 110 ft/s (75 mph) into soil generated results of impacting a relatively soft target. Two types of soil were used as targets. For the velocities of 44 ft/s, 66 ft/s, and 88 ft/s an in-situ undisturbed native desert soil represented the target. Imported borrow, uncompacted for a depth of 7 ft, constituted the target for the 110 ft/s impact. The 7 ft depth was based on analytical calculations to determine final penetration depth of the test unit impacting at a velocity of 110 ft/s. The phenomenon of a dual acceleration spike that occurred in the 88 ft/s concrete highway test becomes more pronounced in the soil tests. The following sections summarizes the series of soil impact tests.

DATA FILE: R5592A	SAMPLE RATE 100000.0	DIGITIZED: 27 JAN., 1986	SYS ID: A3 CEN,AD1
CHARGE # 8950.433	START -5.000 MSEC	ZERO TIME 19:51:21.931000	HIGH CAL 2000.0000
FILTER 10 KHZ	STOP 40.000 MSEC	STATIC RUN LEVEL 0.000	LOW CAL 0.0000
IIR FILTER	CUTOFF= 500.0 HZ	LOWPASS	

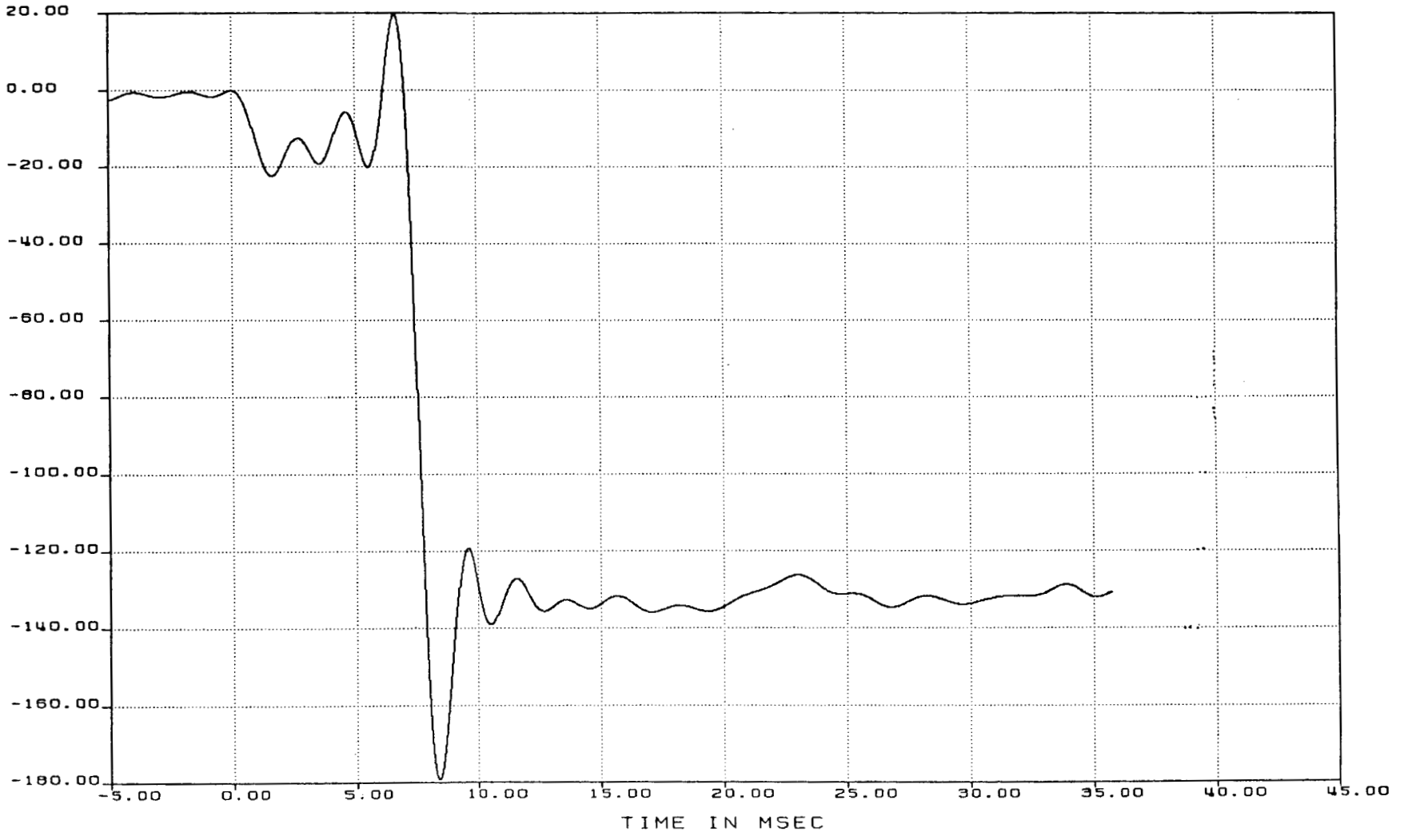

CHANNEL ID: S-2 TRACK # 8

TEST ID: TARGET HARDNESS #7 TEST DATE: 1/24/86

Figure 38 Strain Gage Data for 88 ft/s Impact Velocity into Concrete Highway Target

DATA FILE: R5592A
CHARGE # 8950.433
FILTER 10 KHZ
IIR FILTER

SAMPLE RATE 100000.0
START -5.000 MSEC
STOP 40.000 MSEC
CUTOFF= 1000.0 HZ

DIGITIZED: 27 JAN., 1986
ZERO TIME 19:51:21.931000
STATIC RUN LEVEL 0.000
LOWPASS

SYS ID: A3 CEN,AD6
HIGH CAL 2000.0000
LOW CAL 0.0000

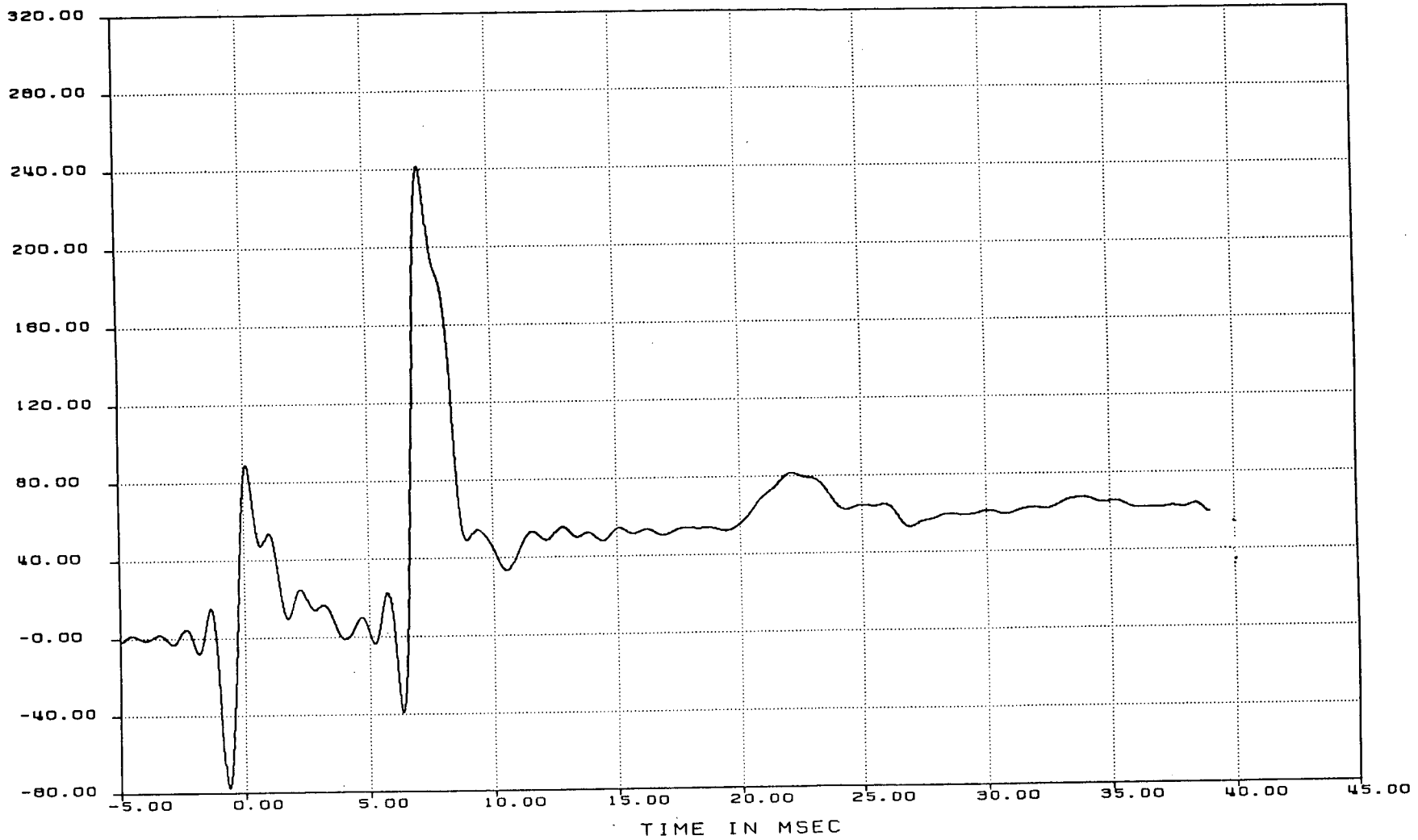

CHANNEL ID: S-7 TRACK #13

TEST ID: TARGET HARDNESS #7. TEST DATE: 1/24/86

Figure 39 Strain Gage Data for 88 ft/s Impact Velocity into Concrete Highway Target

3.2.3.1 44 ft/s Impact into Desert Soil

The test unit penetrated 19 inches into the soil after impacting the target at 44 ft/s (Figure 40). Maximum acceleration levels reached 100 g's (Figure 41). No permanent deformations on the test unit resulted from the maximum recorded strain level of 180 μ in./ in. which correlates to zero residual strain (Figure 42).

3.2.3.2 66 ft/s Impact into Desert Soil

An impact velocity of 66 ft/s resulted in a 25 inch penetration into the soil (Figure 43). Figure 44 shows the two acceleration spikes approximately 15 milliseconds apart. The strain gage readings also show two spikes 15 milliseconds apart (Figure 45). The first spike represents the time of impact while the second spike signifies the unit coming to rest. Note that between the two spikes the signal basically approaches zero for both strain and accelerometer gages. The second spike represents the cask stopping due to soil lock-up then rebounding. Film studies show that after initial impact, the test unit velocity is relatively constant until the cask stops. Maximum accelerations reached 120 g's while maximum strains on the test unit were approximately 500 μ in./in. with no permanent deformations.

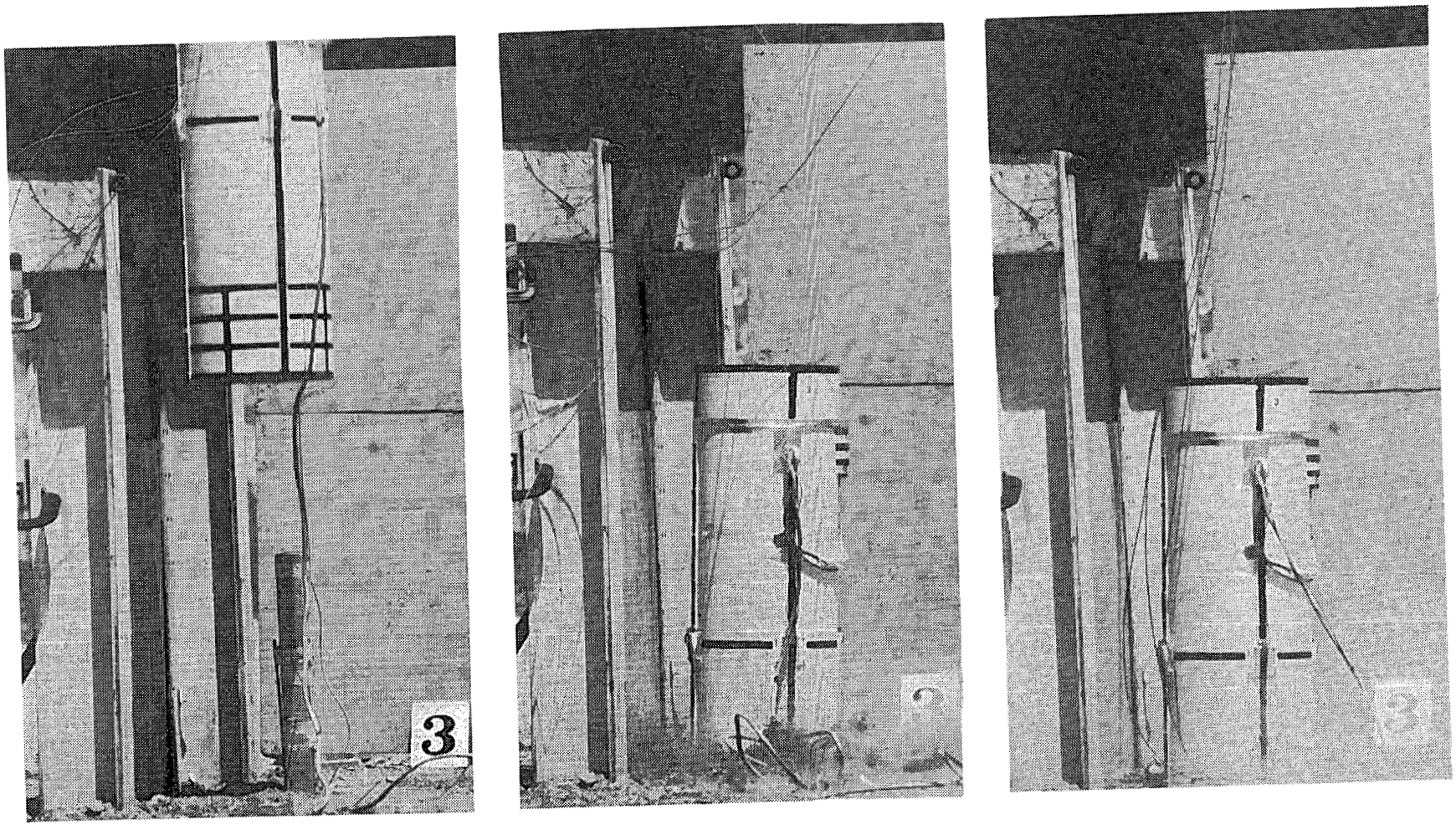

Figure 40 Impacting at a Velocity of 44 ft/s into the Soil Producing a 19-inch Cask Penetration

DATA FILE: R5539A	SAMPLE RATE 100000.0	DIGITIZED: 7 AUG., 1985	SYS ID: A3 CEN,AD1
CHARGE # 8950.433	START -20.000 MSEC	ZERO TIME 19:15:51.897000	HIGH CAL 500.0000
FILTER 10 KHZ	STOP 100.000 MSEC	STATIC RUN LEVEL 0.000	LOW CAL 0.0000
IIR FILTER	CUTOFF= 500.0 HZ	LOWPASS	

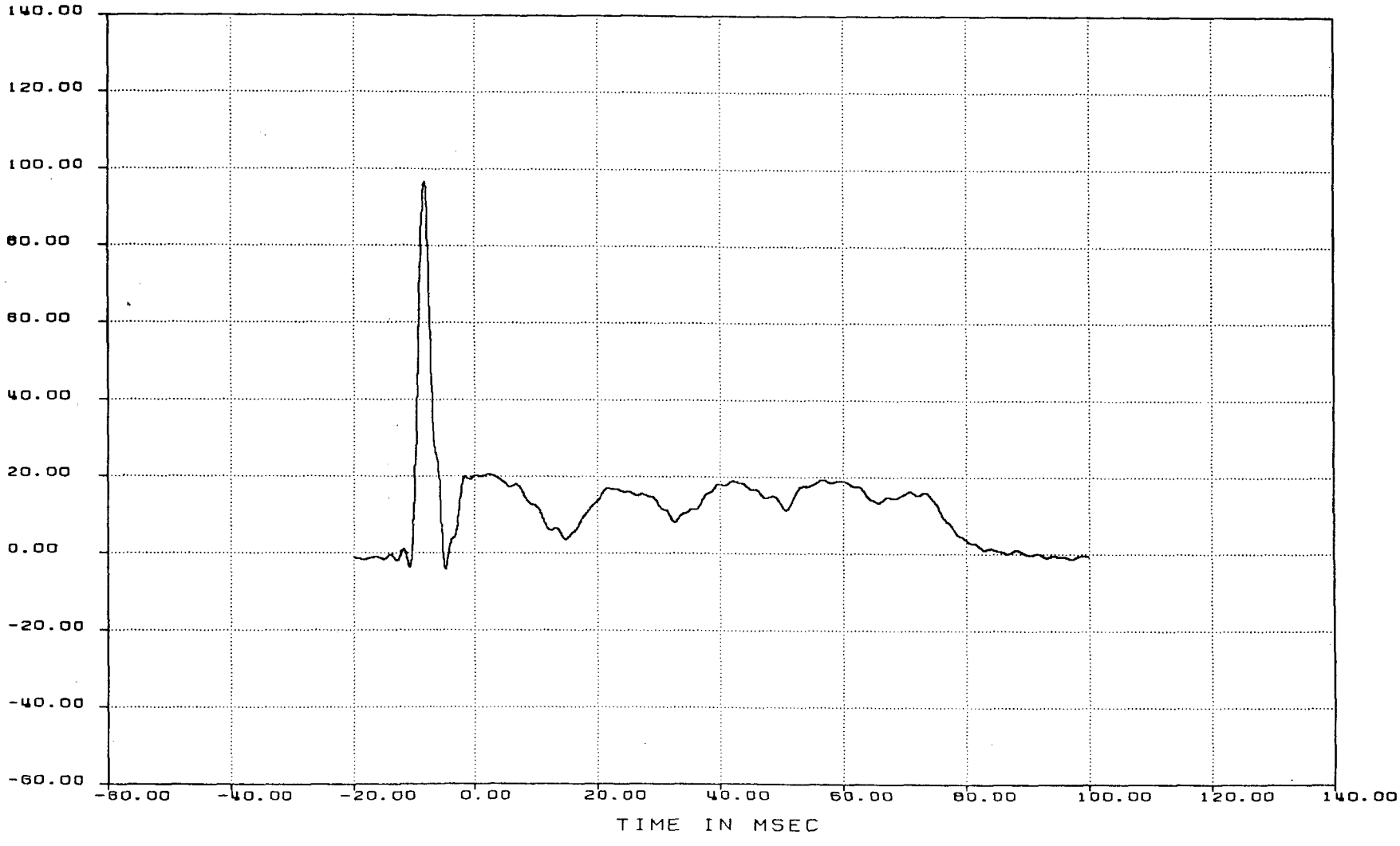

CHANNEL ID: A-1 TRACK # 1

TEST ID: TARGET HARDNESS EVENT #3 TEST DATE: 8/ 6/85

Figure 41 Acceleration Data for 44 ft/s Impact Velocity into Soil Target

DATA FILE: R5539A
CHARGE # 8950.433
FILTER 10 KHZ
IIR FILTER

SAMPLE RATE 100000.0
START -20.000 MSEC
STOP 100.000 MSEC
CUTOFF= 500.0 HZ

DIGITIZED: 7 AUG., 1985
ZERO TIME 19:15:51.897000
STATIC RUN LEVEL 0.000
LOWPASS

SYS ID: A3 CEN,AD5
HIGH CAL 1000.0000
LOW CAL 0.0000

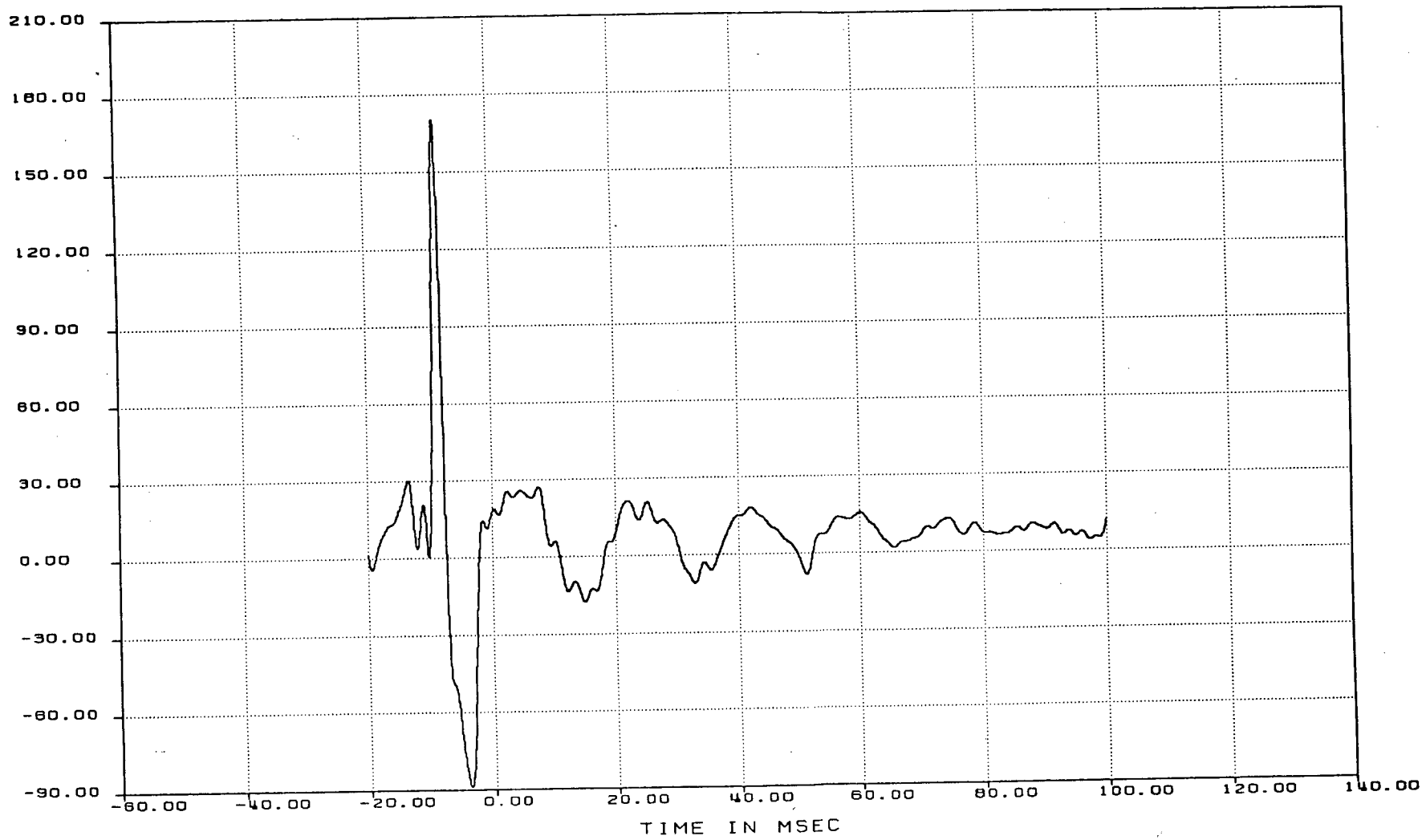

CHANNEL ID: S-1 TRACK # 5

TEST ID: TARGET HARDNESS EVENT #3 TEST DATE: 8/ 6/85

Figure 42 Strain Gage Data for 44 ft/s Impact Velocity into Soil Target

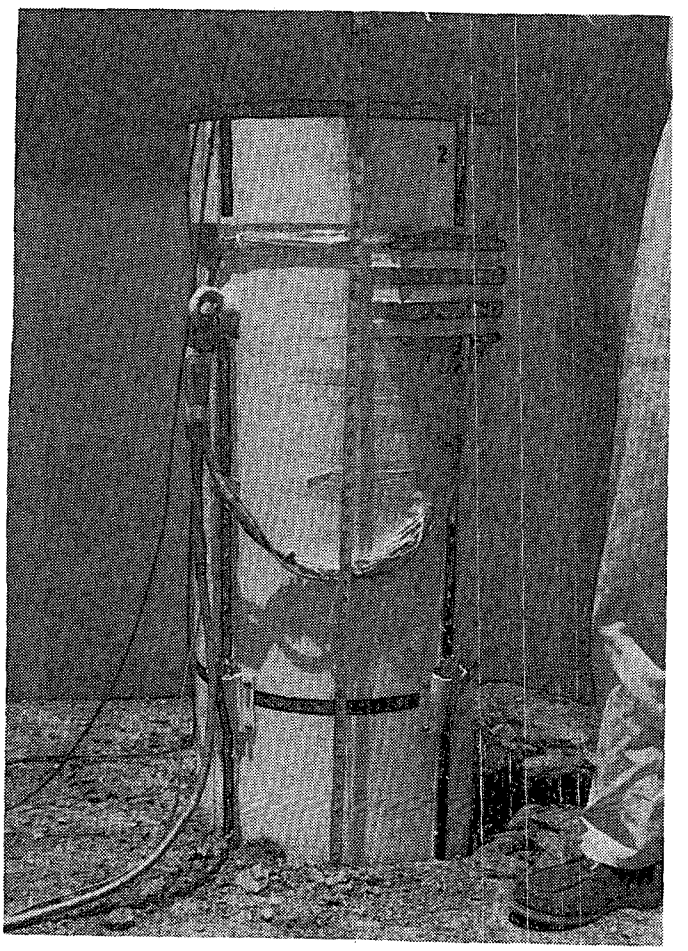

Figure 43 Test Unit's 25-inch Penetration into the Soil After Impacting at a Velocity of 66 ft/s

DATA FILE: R5533B	SAMPLE RATE 100000.0	DIGITIZED: 26 JULY, 1985	SYS ID: A3 CEN,AD1
CHARGE # 8950433	START -5.000 MSEC	ZERO TIME 18:58:43.141000	HIGH CAL 500.0000
FILTER 10 KHZ	STOP 50.000 MSEC	STATIC RUN LEVEL 0.000	LOW CAL 0.0000
IIR FILTER	CUTOFF= 500.0 HZ	LOWPASS	

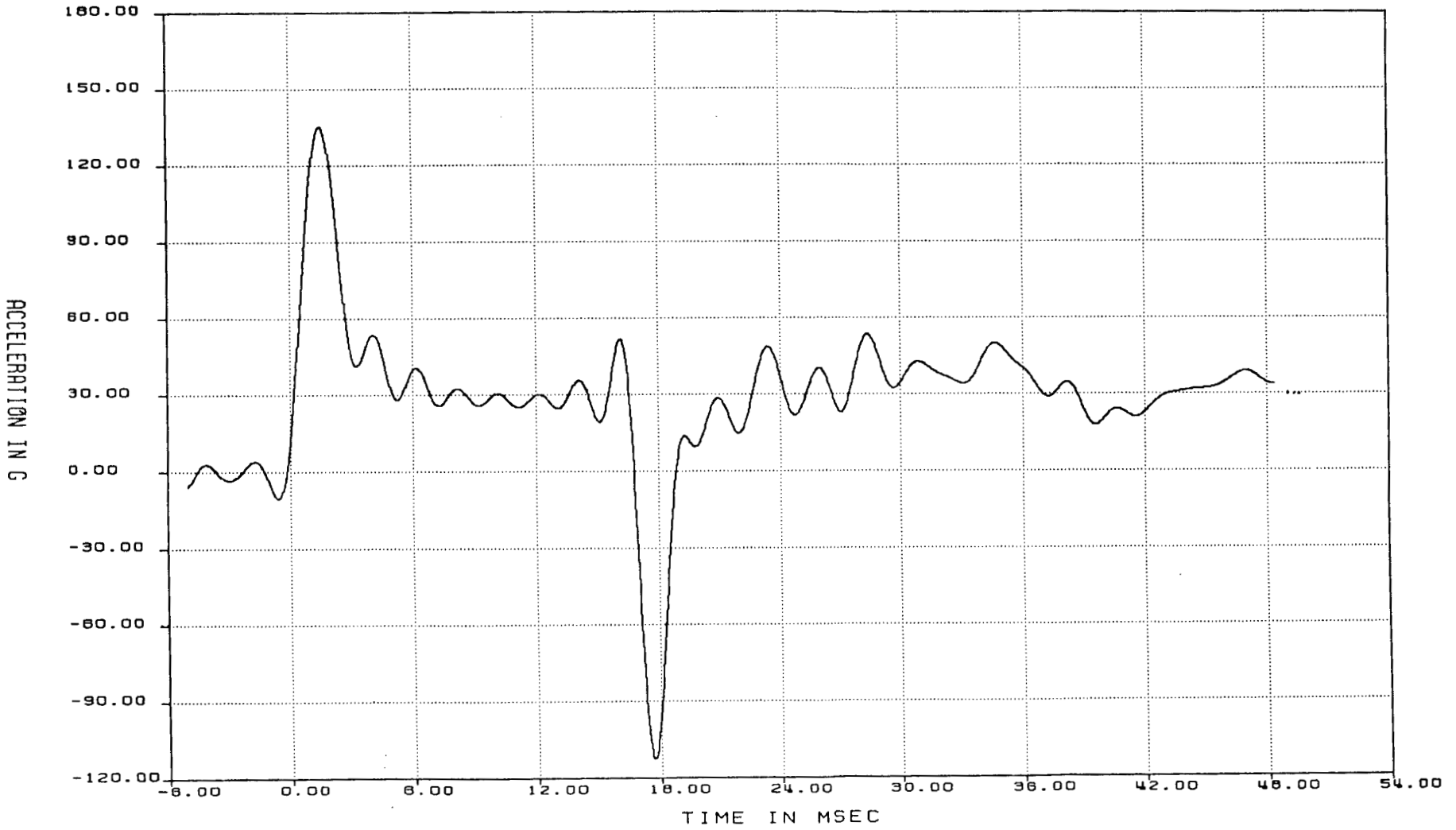

CHANNEL ID: A-1 TRACK # 1

TEST ID: TARGET HARDNESS # 2 TEST DATE: 7/26/85

Figure 44 Acceleration Data for 66 ft/s Impact Velocity into Soil Target

DATA FILE: R5533B | SAMPLE RATE 100000.0 | DIGITIZED: 26 JULY, 1985 | SYS ID: A3 CEN,AD5
CHARGE # 8950433 | START -5.000 MSEC | ZERO TIME 18:58:43.141000 | HIGH CAL 1000.0000
FILTER 10 KHZ | STOP 25.000 MSEC | STATIC RUN LEVEL 0.000 | LOW CAL 0.0000
IIR FILTER | CUTOFF= 1000.0 HZ | LOWPASS

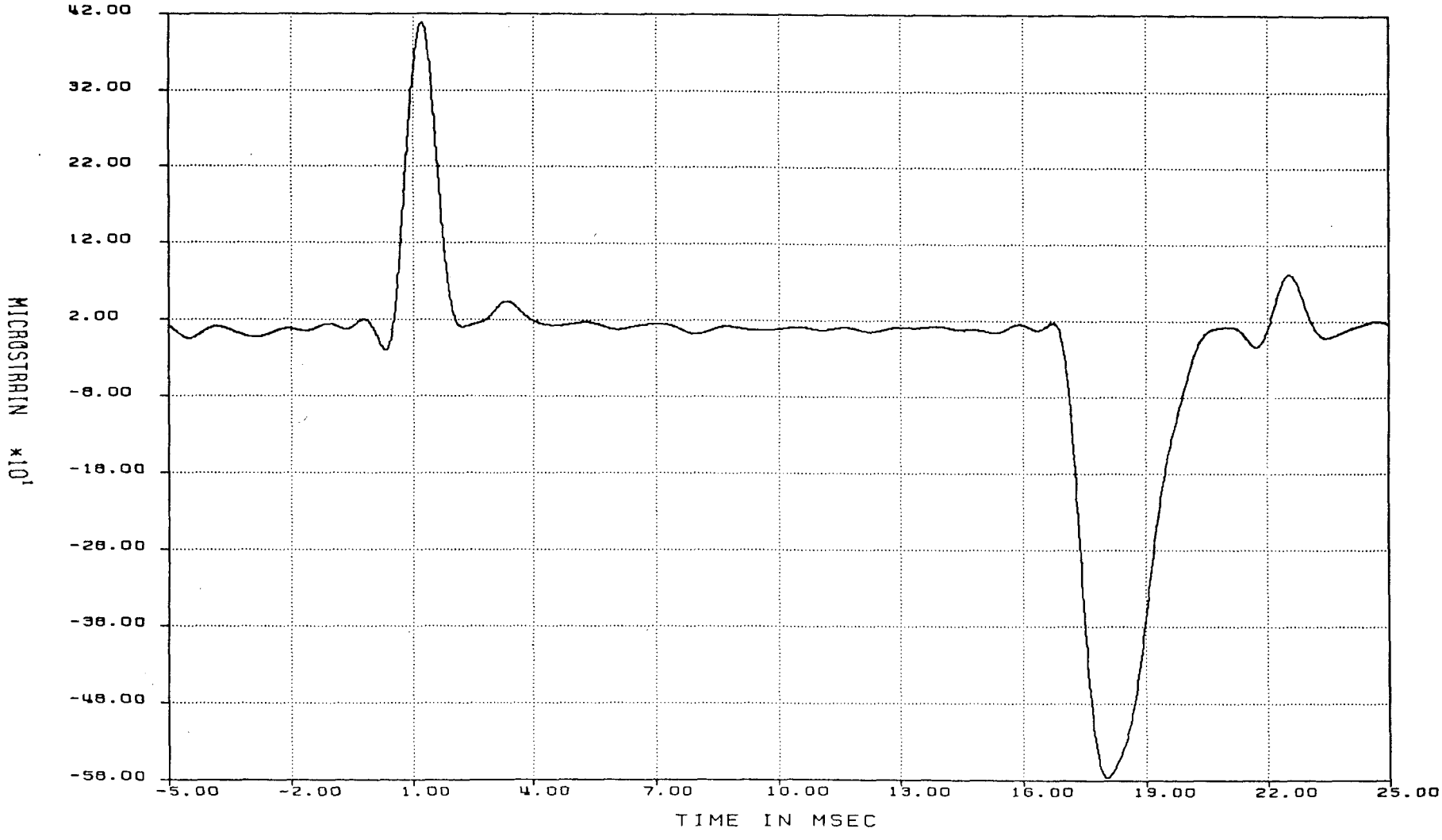

CHANNEL ID: S-1 TRACK # 5

TEST ID: TARGET HARDNESS # 2 TEST DATE: 7/26/85

Figure 45 Strain Gage Data for 66 ft/s Impact Velocity into Soil Target

3.2.3.3 88 ft/s Impact into Desert Soil

At 88 ft/s impact velocity, the cask came to rest 36 inches into the soil (Figure 46). The impact produced a maximum acceleration of 250 g's (Figure 47). The strain gage on the test unit recorded a double spike with a maximum strain of 900 μ in./in. in compression (Figure 48). No permanent deformations resulted from the impact.

3.2.3.4 110 ft/s Impact into Uncompacted Soil

This particular test was performed to determine the penetration depth sensitivity to soil compaction. Impacting at 110 ft/s into uncompacted soil resulted with a final penetration of 92 inches and completely burying the 72-inch long test unit. This was much farther than the 46-inch penetration calculated analytically prior to the test. As the test unit entered the soil, past the instrumentation cables, the signal to the data collection system was completely severed. Thus, no data was recorded. However, the test unit was inspected for posttest damage and no permanent deformation was found.

3.3 Comparison of Test Results

A comparison of the eleven drop tests is made evaluating the cask responses, deformations, and penetrations. A summary of the test results described in the previous sections are given in Table 3. Of the various

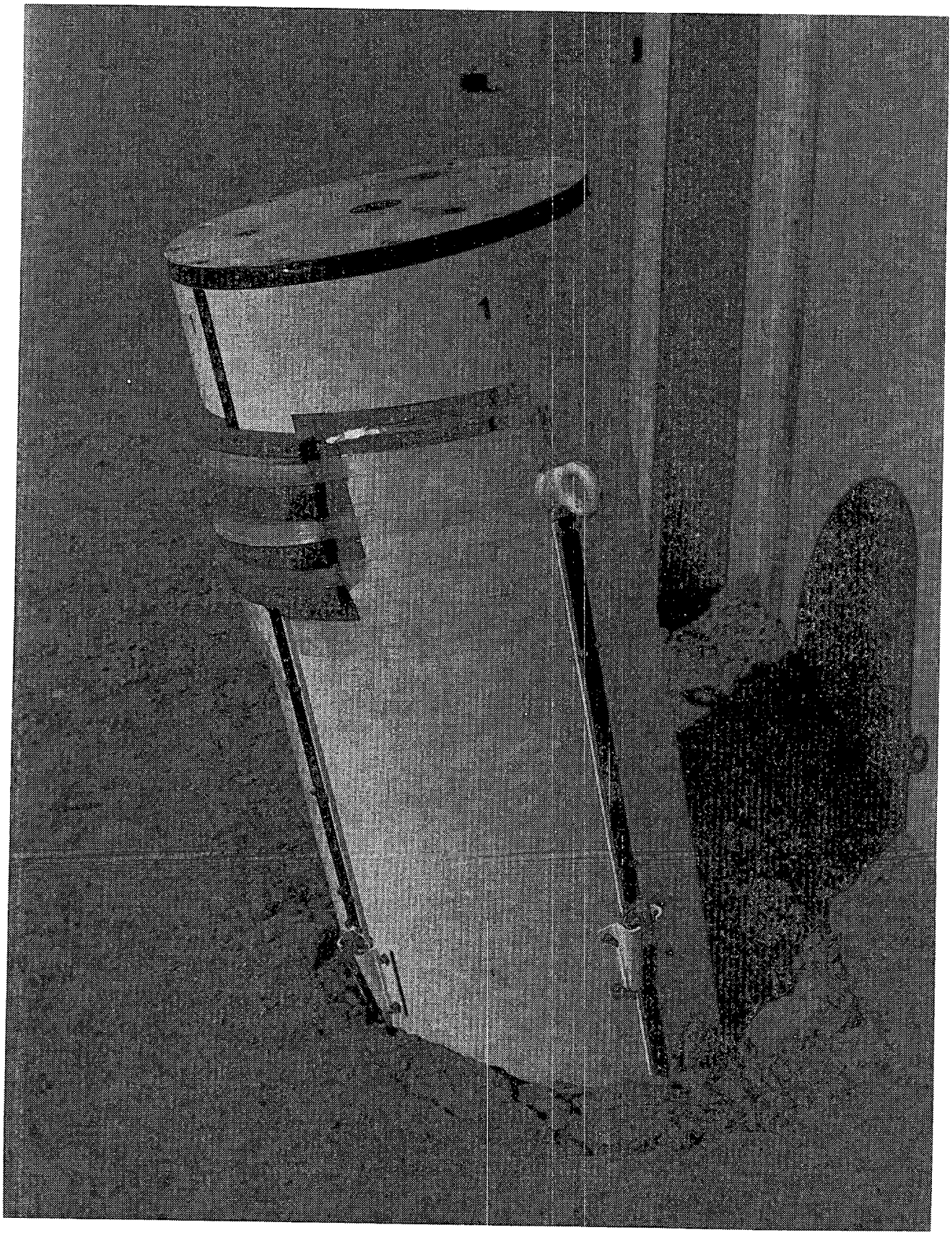

Figure 46 Test Unit's 36-inch Penetration into the Soil After Impacting at a Velocity of 88 ft/s

DATA FILE: R5532A	SAMPLE RATE 100000.0	DIGITIZED: 18 JULY, 1985	SYS ID: A3 CEN,AD1
CHARGE # 8950433	START -5.000 MSEC	ZERO TIME 21: 8:39.928000	HIGH CAL 200.0000
FILTER 10 KHZ	STOP 50.000 MSEC	STATIC RUN LEVEL 0.000	LOW CAL 0.0000
IIR FILTER	CUTOFF= 500.0 HZ	LOWPASS	

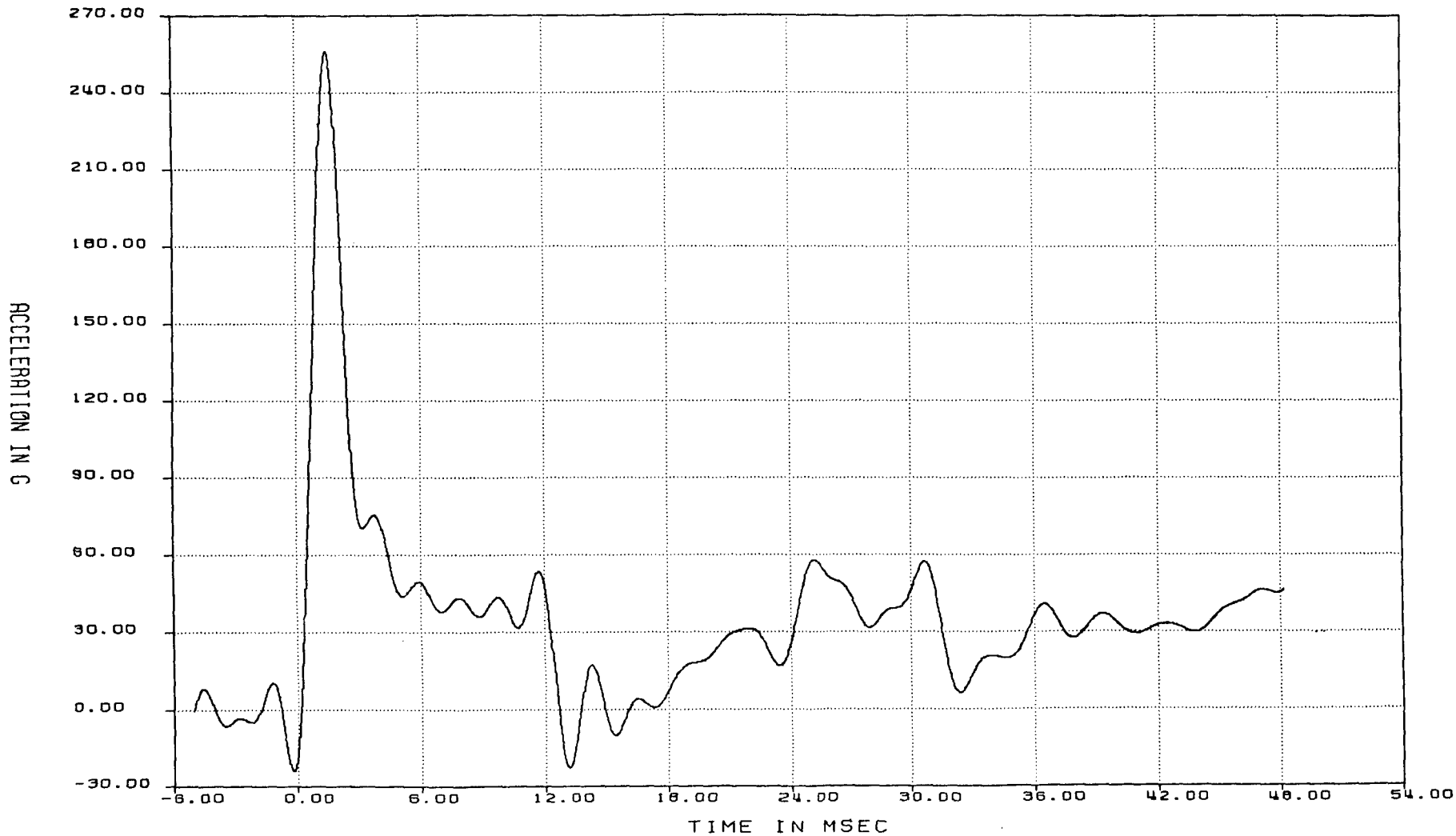

CHANNEL ID: A-1 TRACK # 1

TEST ID: TARGET HARDNESS EVENT #1 TEST DATE: 7/17/85

Figure 47 Acceleration Data for 88 ft/s Impact Velocity into Soil Target

DATA FILE: R5532A
CHARGE # 8950433
FILTER 10 KHZ
IIR FILTER

SAMPLE RATE 100000.0
START -5.000 MSEC
STOP 50.000 MSEC
CUTOFF= 1000.0 HZ

DIGITIZED: 18 JULY, 1985
ZERO TIME 21: 8:39.928000
STATIC RUN LEVEL 0.000
LOWPASS

SYS ID: A3 CEN,AD4
HIGH CAL 1000.0000
LOW CAL 0.0000

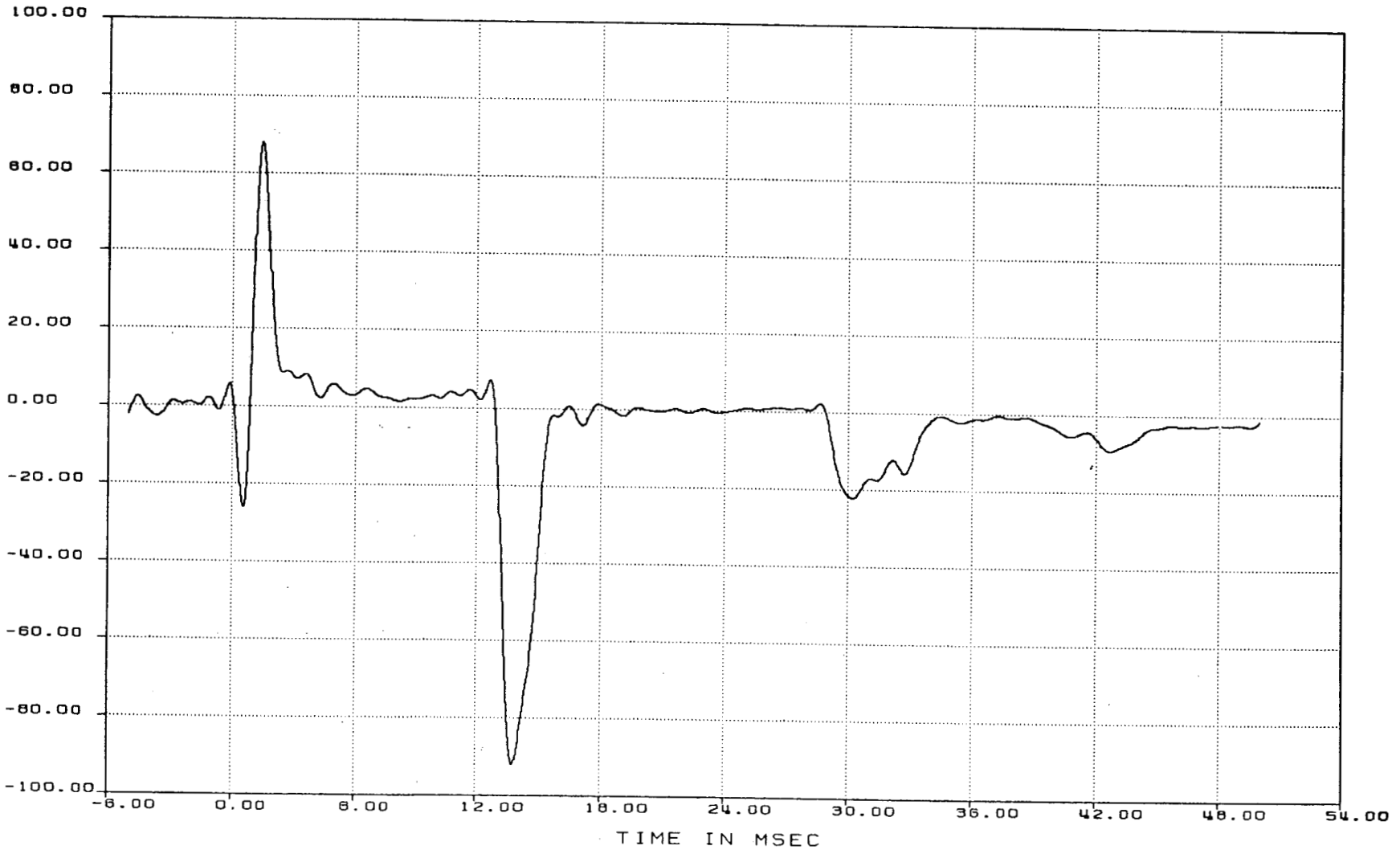

CHANNEL ID: S-7 TRACK #11

TEST ID: TARGET HARDNESS EVENT #1 TEST DATE: 7/17/85

Figure 48 Strain Gage Data for 88 ft/s Impact Velocity into Soil Target

TARGET HARDNESS TEST RESULTS

TEST		MAXIMUM RECORDED ACCELERATION (g's)	MAXIMUM RECORDED STRAIN (u in/in)		RECORDED PERMANENT STRAIN (u in/in)		PENETRATION (in)	MAXIMUM INCREASE IN RADIAL LENGTH (in)
			axial (comp)	radial (tension)	axial (comp)	radial (tension)		
UNYIELDING TARGET	44 ft/s	1300	-750	3000	0	3000	0	0.09
CONCRETE RUNWAY	44 ft/s	480	-900	600	0	400	0.25	0.01
	66 ft/s	900	-1000	2300	0	500	4	0.03
	88 ft/s	1000	-5500	3000	-4800	600	8	0.08
CONCRETE HIGHWAY	44 ft/s	350	0	900	0	0	4	0
	* 44 ft/s	-	-	-	-	-	4	-
	88 ft/s	7500	-1800	2400	-1300	500	19	0.02
COMPACTED SOIL	44 ft/s	100	-90	170	0	0	19	0
	66 ft/s	130	-580	420	0	0	25	0
	88 ft/s	250	-900	600	0	0	36	0
UNCOMPACTED SOIL	+ 110 ft/s	-	-	-	-	-	92	0

* SCHEDULED FOR 66 ft/s HOWEVER ROCKETS DID NOT FIRE AND INSTRUMENTATION WAS NOT OPERATING

+ INSTRUMENTATION WAS LOST FROM EXCESS PENETRATION INTO SOIL

Table 3

columns of information presented, only the acceleration magnitudes deviate from the values expected.

3.3.1 Accelerations

The recorded accelerations are directly related to the frequency generated on impact. Since the test unit has no impact limiters, high frequencies are generated upon impact lasting only a short duration. The test unit can be thought of as a cylindrical bar that is struck on one end. In the case of impacting the unyielding target, most of the energy is absorbed by the projectile with very little taken by the target itself. The frequency response is large, however the test unit is fully supported by the unyielding target until rebound. At this point the acceleration from rebound is slight compared to impact and any resonance of the test unit that may effect the accelerometers is easily determined and can be filtered out.

Impacting into the soil targets produced acceleration histories that were proportional to those obtained in the unyielding target drop. The typical acceleration response consisted of a spike at the point of impact, another spike in the negative direction when the test unit comes to rest and relatively small response in between. The mechanics behind the soil impacts lies in its ability to resist movement of the traveling projectile. At the point the unit impacts the soil, energy is absorbed in producing a shear plane underneath the impact area of the test unit. Once this is accomplished the unit travels into the target, compressing the soil. As the soil compresses, the resistance to load increases until lock-up occurs for a particular velocity and stops the unit. The unit rebounds to produce the second

acceleration and strain gage spike (Figures 44 and 45). The soil acts somewhat as an impact limiter while continually supporting the test unit as it penetrates. This continual support becomes important when comparing with the response for impacting the concrete targets.

The mechanics involved in striking the concrete targets is similar to that of the soil except for two important factors. The phenomenon of two separate responses at impact and at rest, with a minimal readings in between, is still evident. However, the magnitude of the acceleration from initial impact is very large compared to any other response. This is the point where the concrete shear plug is formed which absorbs a substantial amount of available energy. Along with the formation of the concrete shear plug, the soil underneath undergoes establishment of shear planes. This allows the test unit to travel into the target at a relatively small deceleration until the soil locks up to provide enough stiffness to stop the unit.

The response of the test unit at impact is such that the frequency is quite high. The unit absorbs this frequency and excites the accelerometers. After the concrete and soil form their respective shear planes the relative support upon the cask drops dramatically. Even though the unit is compressing the soil, the differential response between initial impact and subsequent travel is very large. The resulting environment is that of the cask suspended in air and being struck by a stiff brittle object at one end. Without any firm support to provide damping, the unit resonates at the produced frequency. Thus, the accelerometers are measuring both the frequency associated with deceleration forces, and frequencies related to the test unit resonating.

This phenomenon was recorded by two accelerometers manufactured by independent sources. The test unit was instrumented with 10,000 g EGAXT-24

Entran [8] and 50,000 g 2264 Endevco [9] units. The Entran units are damped accelerometers that resist impulses due to test hardware resonating. The Endevco are undamped, however, due to their large 50,000 g range are less susceptible to resonating excited by low frequencies. Both of these accelerometers produced data within 5% of each other during the course of testing on this program. The reaction of the accelerometers recording the resonating effect of the test unit suggest this phenomenon was a major portion of the response the unit experienced. Thus, even with the built in factor of the damped Entrans and high range Endevos used to avoid effects from cask resonating, the accelerometers could not compensate for the applied frequencies. The recorded response on the two types of accelerometers was real, however, the phenomena is directly dependent on the target impacted.

For this particular program, accelerometer data was a tool to be evaluated rather than to provide absolute empirical results. Confidence was generated in the acceleration values obtained in the soil and unyielding target tests. However, with the concrete targets, the accelerometer data is subject to interpretation. Consequently, for impacts into yielding targets, the validity of the acceleration data is dependent on the characteristics of the test unit and the penetration phenomena experienced by the target surface.

3.3.2 Strains and Deformations

Strains and deformations have a relationship in that any residual strains directly coincide with permanent deformations. Table 3 lists five tests in which residual strains were obtained from impacting the various targets. All three concrete runway impact tests along with the 88 ft/s impact into the

concrete highway produced permanent deformations. However, only the 88 ft/s impact into the runway exhibited strains and deformations on the order of that found from the drop onto the unyielding target. Reviewing the strain levels of the respective 88 ft/s into the runway and 44 ft/s into the unyielding target tests show a higher absolute magnitude from the concrete drop. Figure 29 presents the strain gage measurement at 2.75 inches from the cask bottom for the 88 ft/s impact into the runway. The large -5500 μ in./in. strain in compression can be attributed to the stiffness from the geometrical configuration. In this case, the bottom cap welded to the outer cylinder precludes the wall from buckling or deforming outward. This directs all of the applied axial load to be absorbed in compression.

Comparing the two strain gages located twelve inches from the cask bottom, Figures 17 and 30 respectively present data from the unyielding and the 88 ft/s runway impacts. At this cask location, the outer cylinder is allowed to buckle outward producing tensile stresses. These two gages are similar in response for the first six milliseconds. At this time the concrete shear plug has formed decreasing the resistance to cask motion. This is evident by the drop in tensile stress shown in Figure 30. Once the concrete shear plug has formed, cask stresses decrease allowing the material to recover from the applied loading. However, the unyielding target continues the applied load until the impacting system rebounds. Under these conditions, the cask material must deform in order to absorb energy.

The additional deformation with increased impact velocity is approximately equal in proportion to the change in amount of available kinetic energy. For example, from 44 ft/s to 66 ft/s results in 2.25 times the additional amount of kinetic energy. This produces an increase in radial

deformation in the unit from 0.01 inch to 0.03 inch. The resulting factor of 3 is comparatively close to the factor of 2.25 increase in kinetic energy. From 66 ft/s to 88 ft/s the increase in kinetic energy is 1.78 times, versus an additional deformation factor of 2.67 times. Again, the proportional change in deformation with respect to additional kinetic energy is similar. Note that the magnitude of deformation is small and any slight variation in results can greatly alter the ratios. However, in the limited amount of data obtained to compare damaged test units, the correlation between the experimental findings and additional available energy is good.

3.3.3 Unit Penetration

With respect to unit penetration, the relationship between increased kinetic energy and penetration depth depends on the type of target. For soil, the increase in penetration was less than the relative addition in kinetic energy. From 44 ft/s to 66 ft/s the unit traveled an additional distance from 19 inches to 25 inches. This represents an increase of 1.32 times compared to the kinetic energy factor of 2.25. The 36 inch travel into the soil after impacting at 88 ft/s is 1.89 times greater than the penetration found from impacting at 44 ft/s. This is less than half of the kinetic energy factor of 4.0. The closest soil correlation came between the 88 ft/s and 66 ft/s impacts. The experimental penetration ratio is 1.44 compared to the increased energy factor of 1.78. In every case the additional available kinetic energy factor was greater than the proportional increase in penetration depth obtained from impacting the soil targets.

For the concrete roadway and runway the increase in penetration was larger than the kinetic energy factor. Close correlation occurred between the 88 ft/s and 44 ft/s impact into the concrete highway. The 19 inch and 4 inch penetration results in a ratio of 4.75 versus the kinetic energy factor of 4.0. Also, the penetration ratio of 8 inches from the 88 ft/s impact and 4 inches from the 44 ft/s impact into the concrete runway obtains a ratio of 2 compared to the 1.78 kinetic energy factor. However a penetration component of 32 between the 88 ft/s and 44 ft/s impact into the concrete runway far exceeds the 2.0 kinetic energy factor. The same occurs between the 66 ft/s and 44 ft/s impact into the runway resulting in the 16 penetration factor versus the 2.25 kinetic energy component . Hence, unlike the soil tests, in every impact into the concrete surfaces a larger target penetration occurred than suggested by the additional amount of available kinetic energy. This can be explained by the fact a specific amount of finite energy is needed to produce the shear plug formed in the concrete targets. Once this shear plug is formed, the remaining kinetic energy is applied to compressing the soil underneath. The soil targets are less involved with formations of shear planes and primarily resist cask motion when the material compresses. This material compression is dependent on a variety of factors characterized by its properties. These factors influence the penetration depth from dynamic loading. This may imply that the energy to produce soil lock-up is less dependent on impact velocity than the energy needed to produce a shear plug in a brittle material such as concrete.

4.0 ANALYSIS

An important part of the program was the analytical evaluation of the problem presented by impacting the cylindrical-shaped object into a variety of targets. As was done with the experimental phase of the program, analytical results and methods were focused toward comparison against the 30-ft drop onto an unyielding target.

Analytical methods varied with respect to both problem definition and analytical codes used. The 30-ft drop onto an unyielding target provided the most consistent results that closely matched the data obtained from experimental testing. In comparison, the analytical process for the concrete and soil targets was complex and time consuming. As the complexity of the problem increased, so did the difficulty of defining it into practical constraints and also establishing analytical codes that produced meaningful results.

The following sections review the analytical process and tools used. Each analysis is given in terms of the respective target impacted.

4.1 Unyielding Target

DYNA2D [13], an explicit two-dimensional finite element code, was used to analyze the 30-ft drop onto an unyielding target. The problem was defined using a preprocessor, PATRAN-G [14], to construct the geometry required for input into the DYNA2D program.

Because the cask geometry and loading is symmetric about its longitudinal centerline the problem was treated as axisymmetric. This allowed for a two-dimensional analysis. The resulting finite element model consisted of 642 nodes and 568 quadrilateral elements (Figure 49). The unit was modeled as a solid monolithic steel mass. The hole at the lower corner represents the gap formed by the inner sleeve, internal plates and bottom cap. Maximum stresses and deformations were expected to be generated at this point. Regular Grade A36 steel material properties were used for the cask's yield and ultimate strengths. Strain hardening effects were also included in the analysis. To simulate the unyielding target, a stonewall option offered by DYNA2D was enacted. This forces all available energy from the impact to be totally absorbed by the projectile. This option provides a conservative analysis since in real life no such surface exists that will transmit 100% of the available energy to the striking object. However, from past tests at SNL with the same unyielding target used for this work, comparable results between analytical calculations and experimental testing have been favorable.

DYNA2D results show that at approximately one millisecond into the impact event the available kinetic energy has been expended and rebound begins to occur (Figure 50). This correlates well with experimental duration of approximately 1 to 2 milliseconds shown in Figure 17. The velocity of the center of mass with respect to time is shown in Figure 51. Taking the slope of the line determines the analytical acceleration giving a value of 1600 g's, Keeping in mind the conservatism of the analysis, this compares well with the 1300 g's obtained from experimental testing. The radial deformation from the analysis at the point approximately 3.5 inches from the bottom of the unit

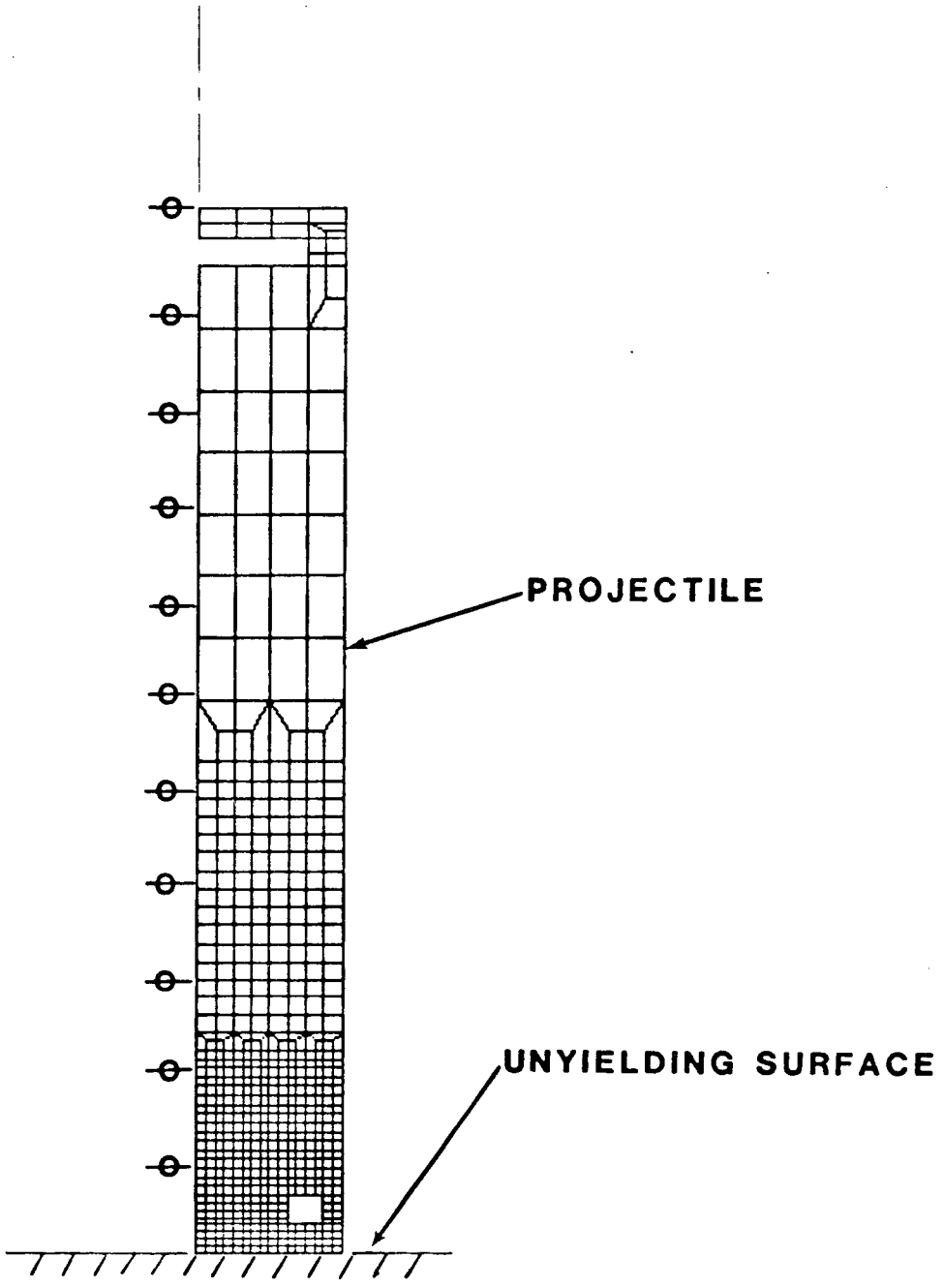

Figure 49 Finite Element Model for Unyielding Target Analysis

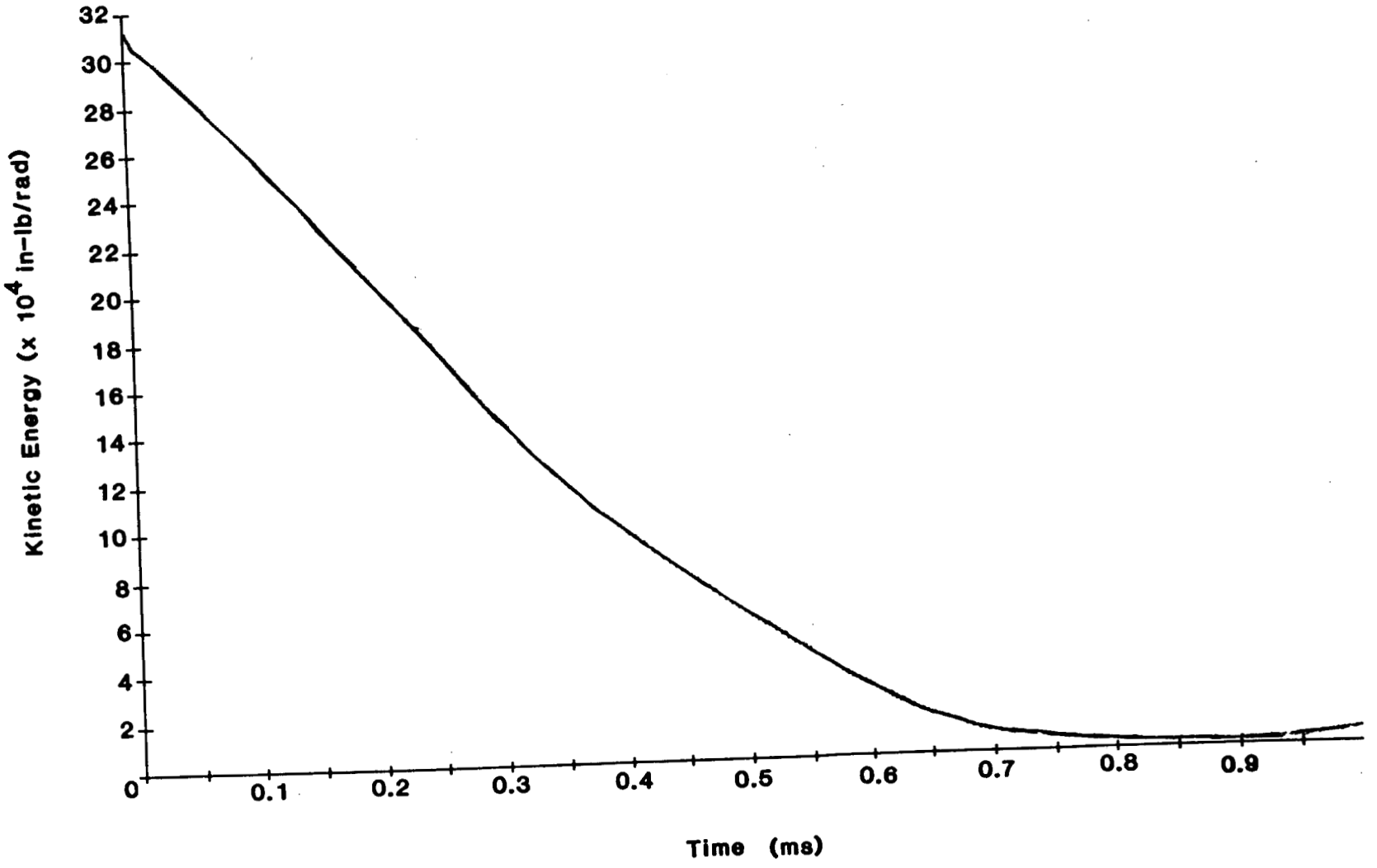

Figure 50 Kinetic Energy vs. Time from Unyielding Target Analysis

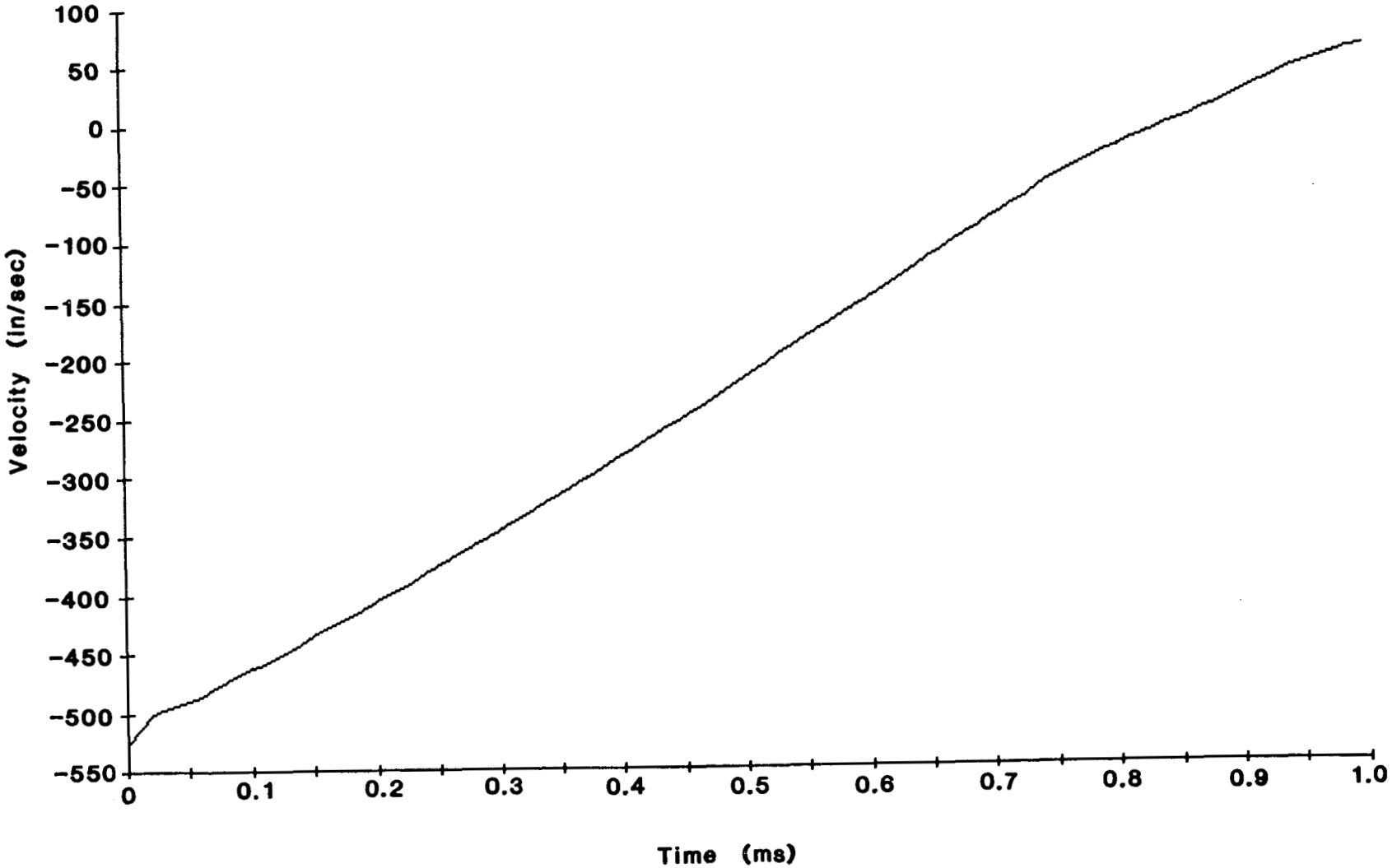

Figure 51 Velocity vs. Time from Unyielding Target Analysis

came to 0.12 inches (Figure 52). This also compares well with the experimentally measured amount of 0.09 inches.

At the point of strain measurement, 12 inches from the bottom, the calculated stress was approximately 38,000 psi (Figure 53). From the experimental strain reading of 3000 μ in./in., this correlates to approximately 37,000 psi stress at the same location.

The analytical results compare favorably with experimental findings. In every case, the conservatism of the analysis produced results that enveloped the data obtained from experimental testing. The analysis was relatively easy to perform and duplicate both in terms of analytical complexity and computer cost.

4.2 Concrete Target

The degree of analytical complexity increases substantially with analyzing the yielding targets. In this program, properly modeling the cask becomes secondary in difficulty to mathematically analyzing the target itself. Two immediate problems arise with respect to this type of analysis. First, determining the material characteristics of concrete and soil under impact loading must be made. Second, and more difficult, is properly accounting for the failure mechanisms associated with each type of material.

In the case of the concrete target, the 45° shear plug formed at impact was taken into account directly in the finite element model (Figure 54). The section below the concrete shear plug is the soil that must be compressed in order to increase resistance and stop the unit. Only the concrete highway targets were evaluated at this time.

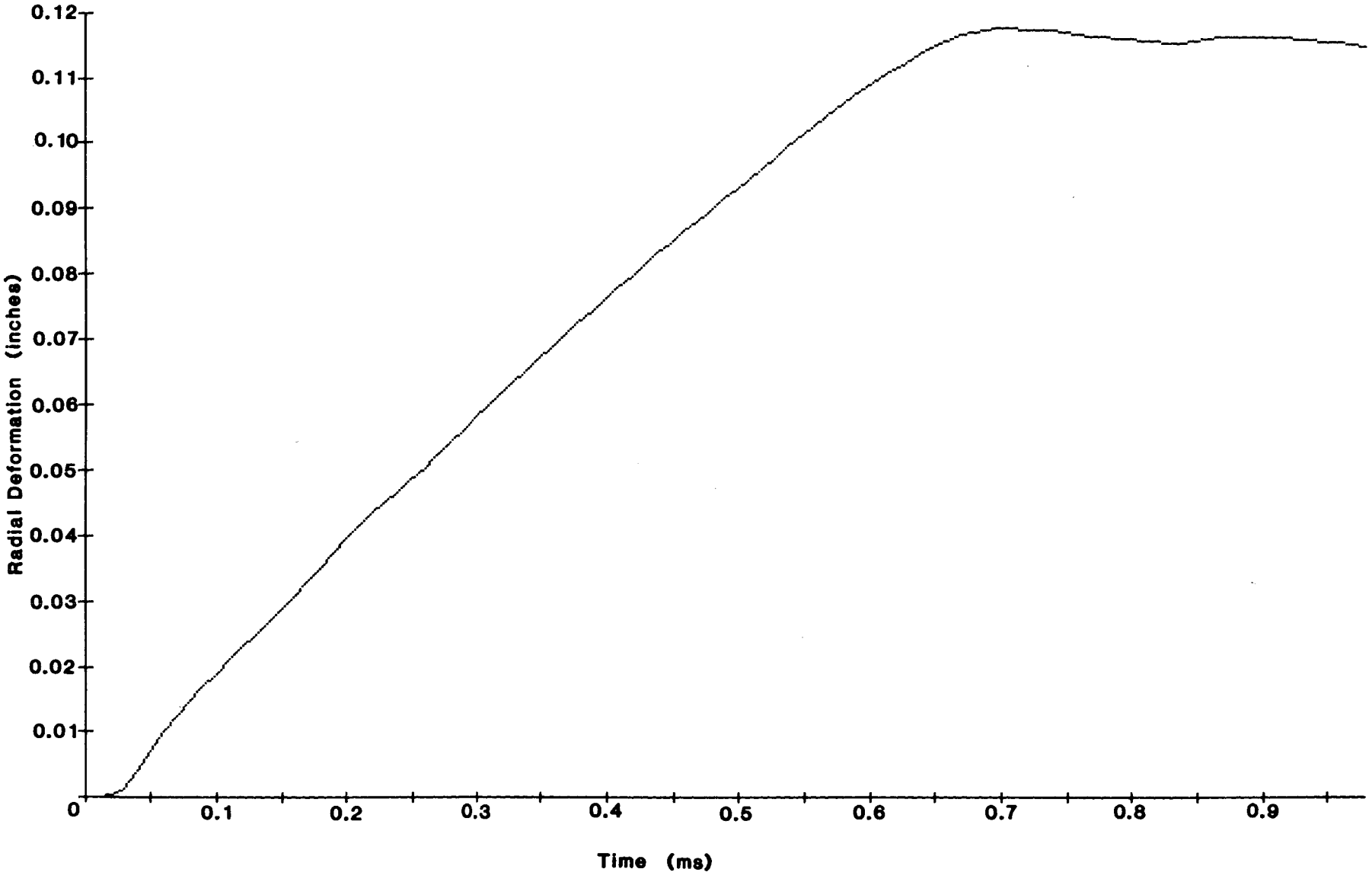

Figure 52 Radial Deformation from Unyielding Target Analysis

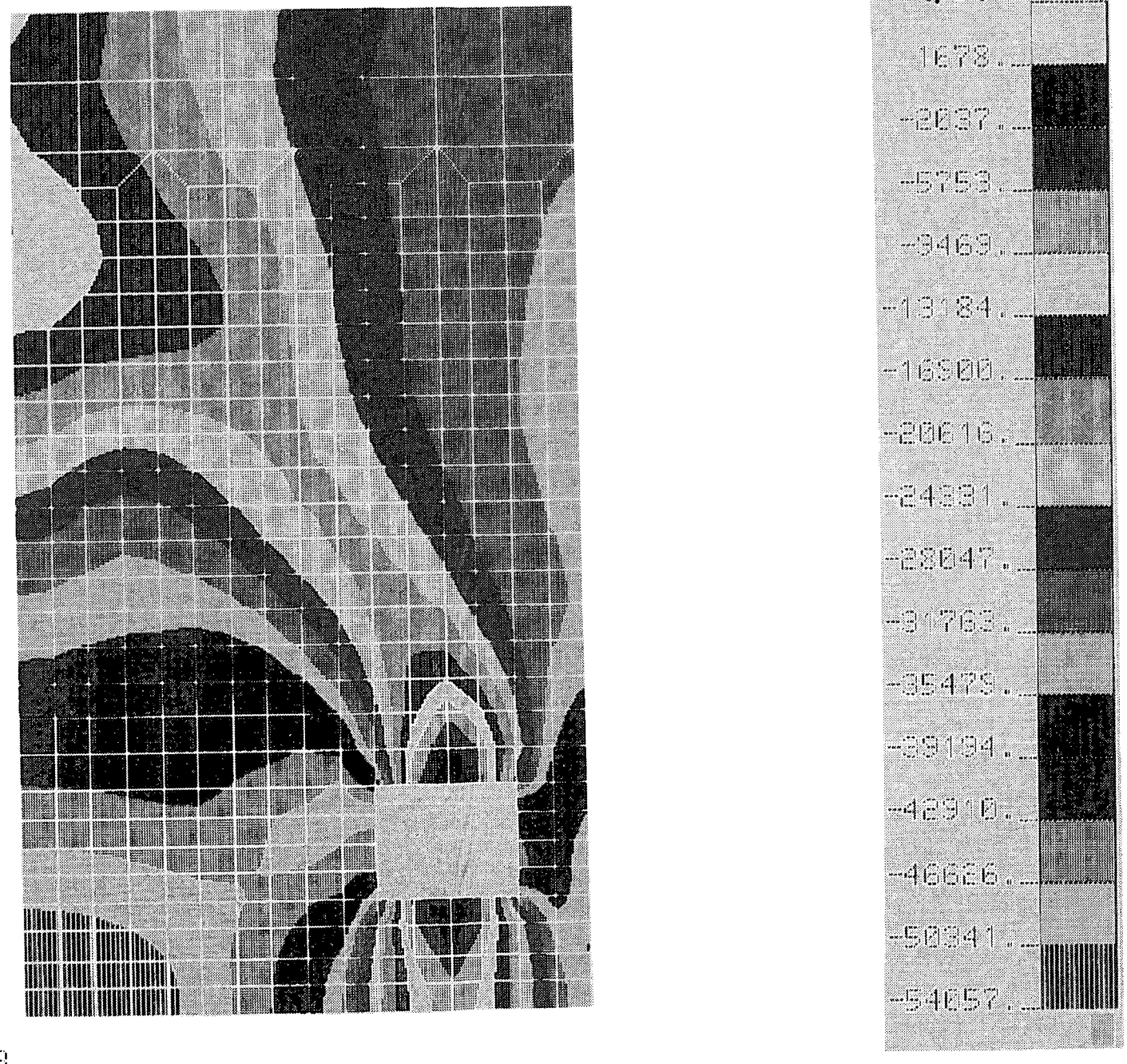

Figure 53 Stresses from Unyielding Target Analysis

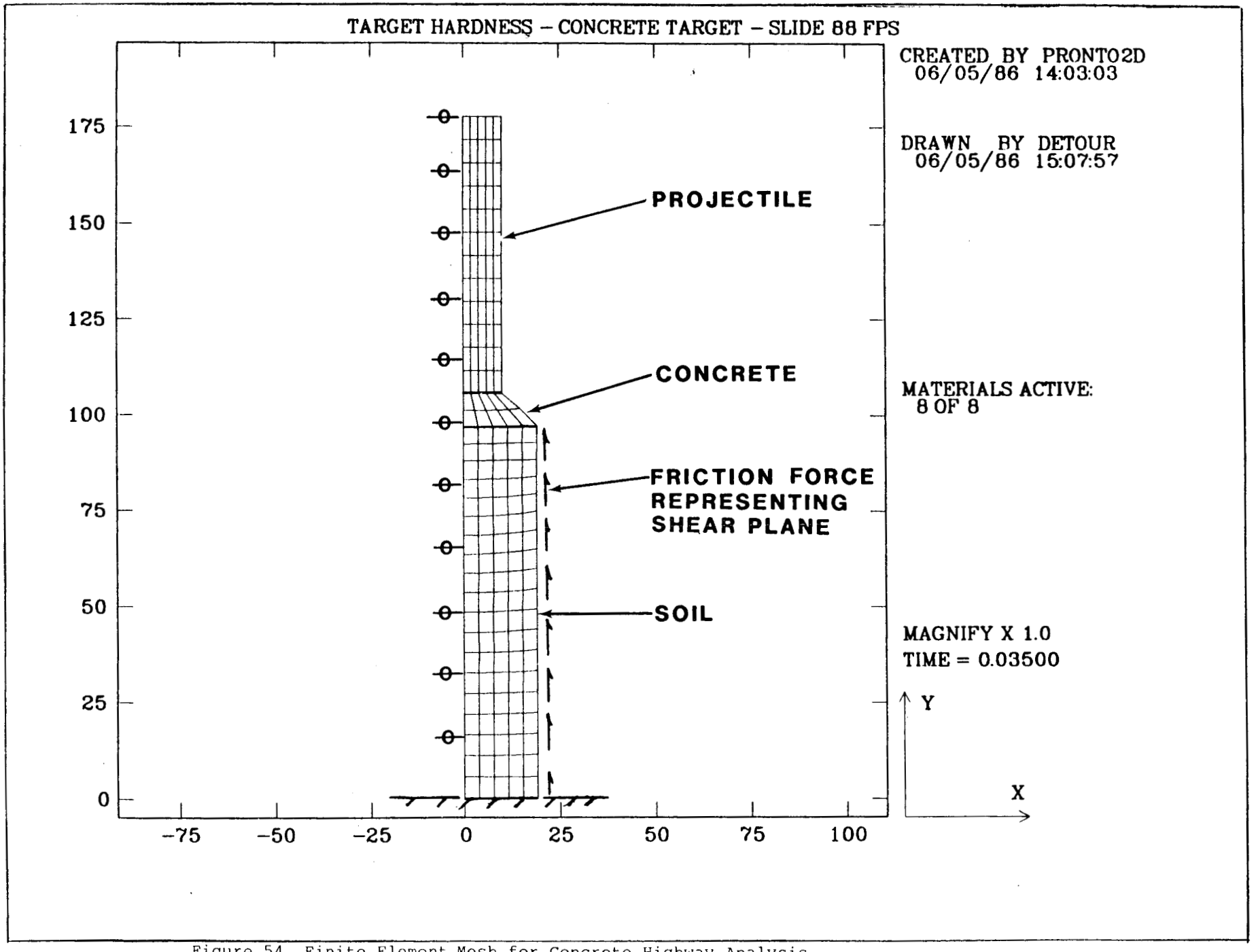

Figure 54 Finite Element Mesh for Concrete Highway Analysis

Because of the geometry of the test unit and the assumption made that the target failure was symmetrical, an axisymmetric two-dimensional analysis was performed using PRONTO [15]. Only the 44 ft/s and 88 ft/s impacts were evaluated. An analytical assumption was made that no significant energy is absorbed by crack generation. The boundary conditions of the target was total vertical constraint at the bottom and a resistance to movement of the outer edge produced by friction.

A plot of velocity vs. time for the 44 ft/s impact reveals an analytical acceleration of approximately 300 g's at the point of impact (Figure 55). This compares well with the 350 g's measured during the experimental test (Figure 33). The maximum calculated penetration of approximately 8.0 inches (Figure 56) is double that produced from impacting experimentally. The particular deviation between predicted and experimental penetration is probably a result of the analytical assumption that no significant energy is absorbed by crack generation.

Reviewing the analytical results of the 88 ft/s impact shows the initial slope of the velocity vs. time curve gives an acceleration of 600 g's (Figure 57). This is quite different than the 7500 g's measured experimentally, which is not surprising considering the lack of confidence in the experimental value. The penetration was calculated to be about 14 inches which is less than the 19 inches the unit actually experienced.(Figure 58). For such a complex failure phenomenon exhibited by the concrete target, these penetration values are comparable.

Reviewing the concrete analysis reveals a complex problem that requires special analytical considerations. Unlike the analysis of impacting an unyielding target where the only concern is modeling the projectile, the

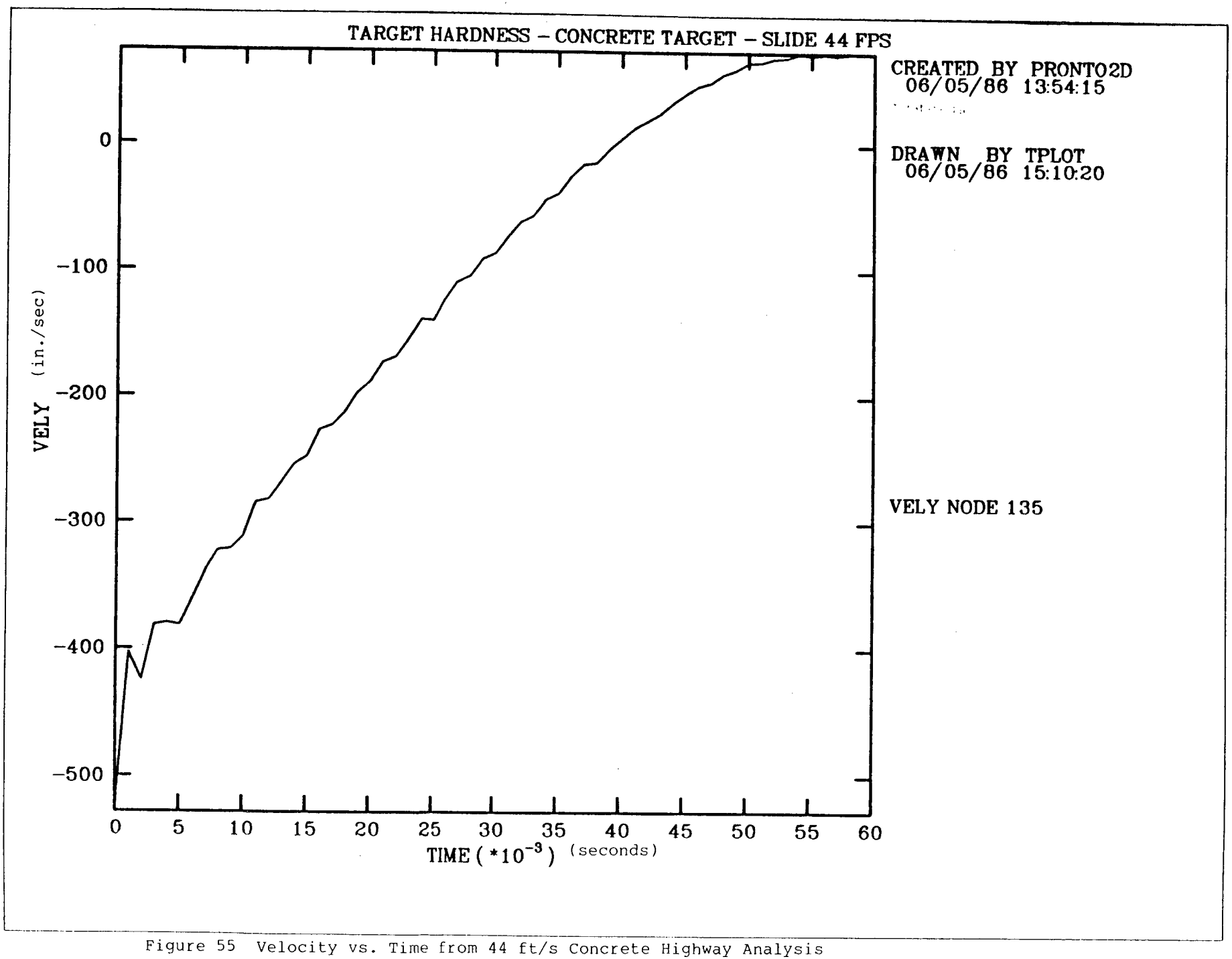

Figure 55 Velocity vs. Time from 44 ft/s Concrete Highway Analysis

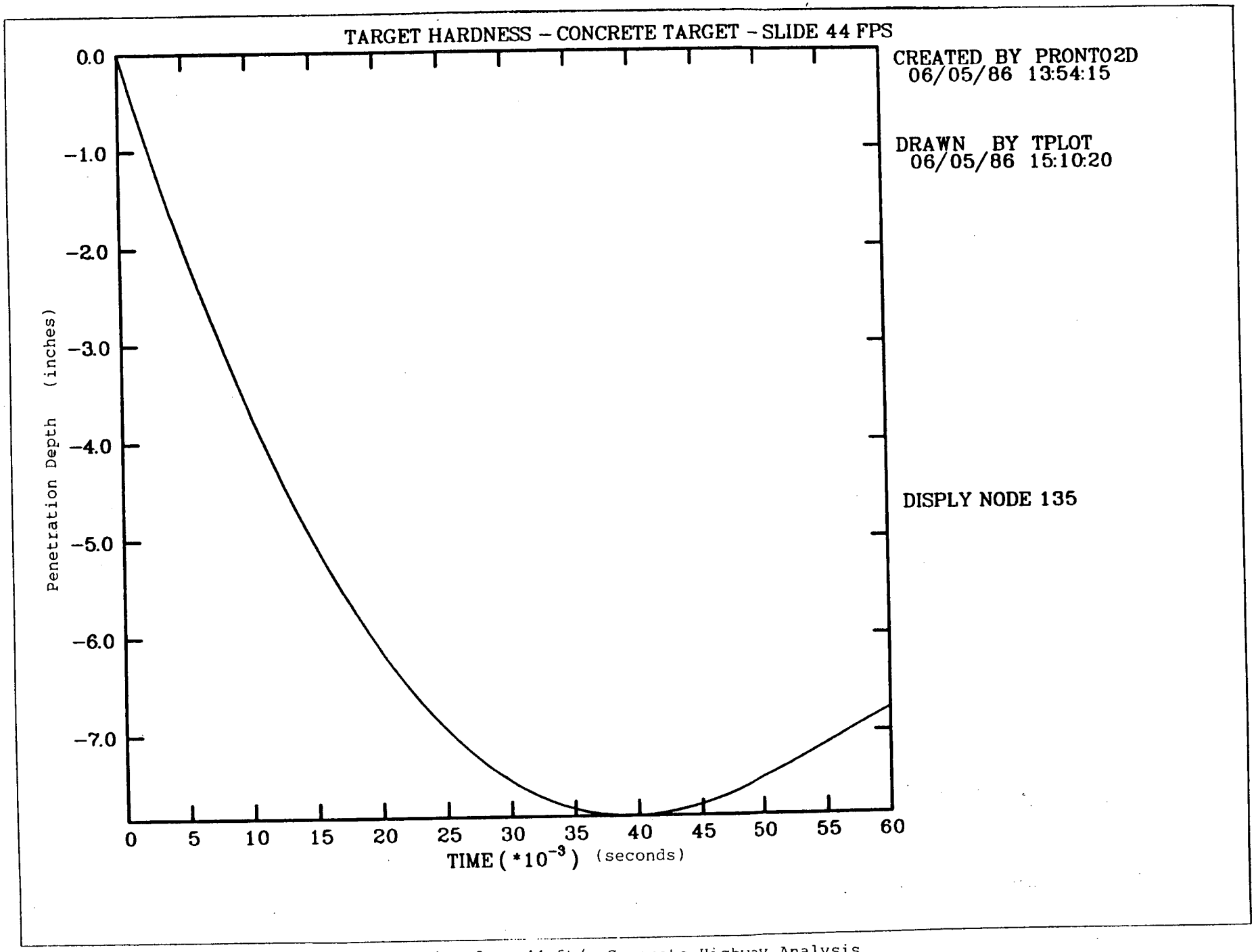

Figure 56 Penetration vs. Time from 44 ft/s Concrete Highway Analysis

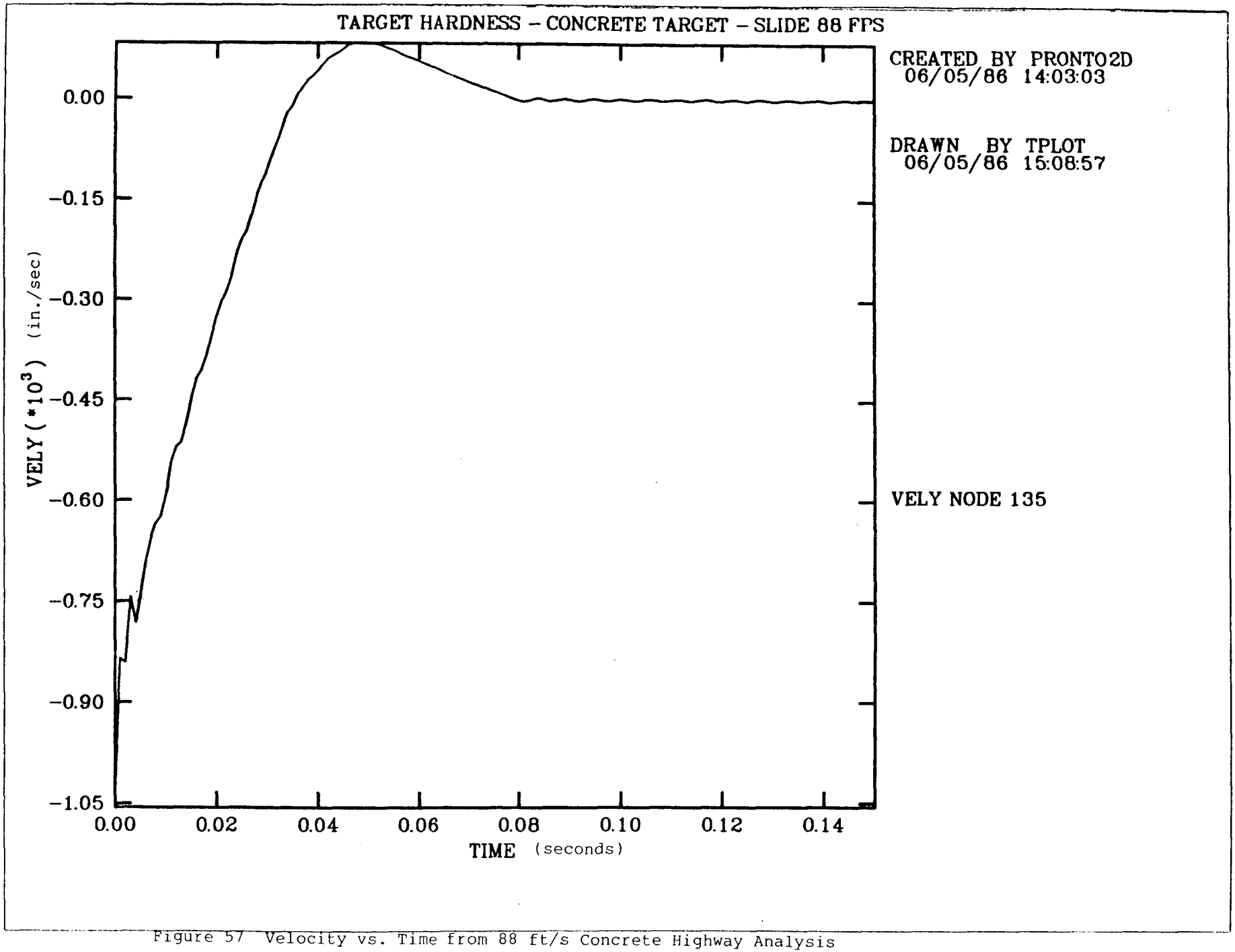

Figure 57 Velocity vs. Time from 88 ft/s Concrete Highway Analysis

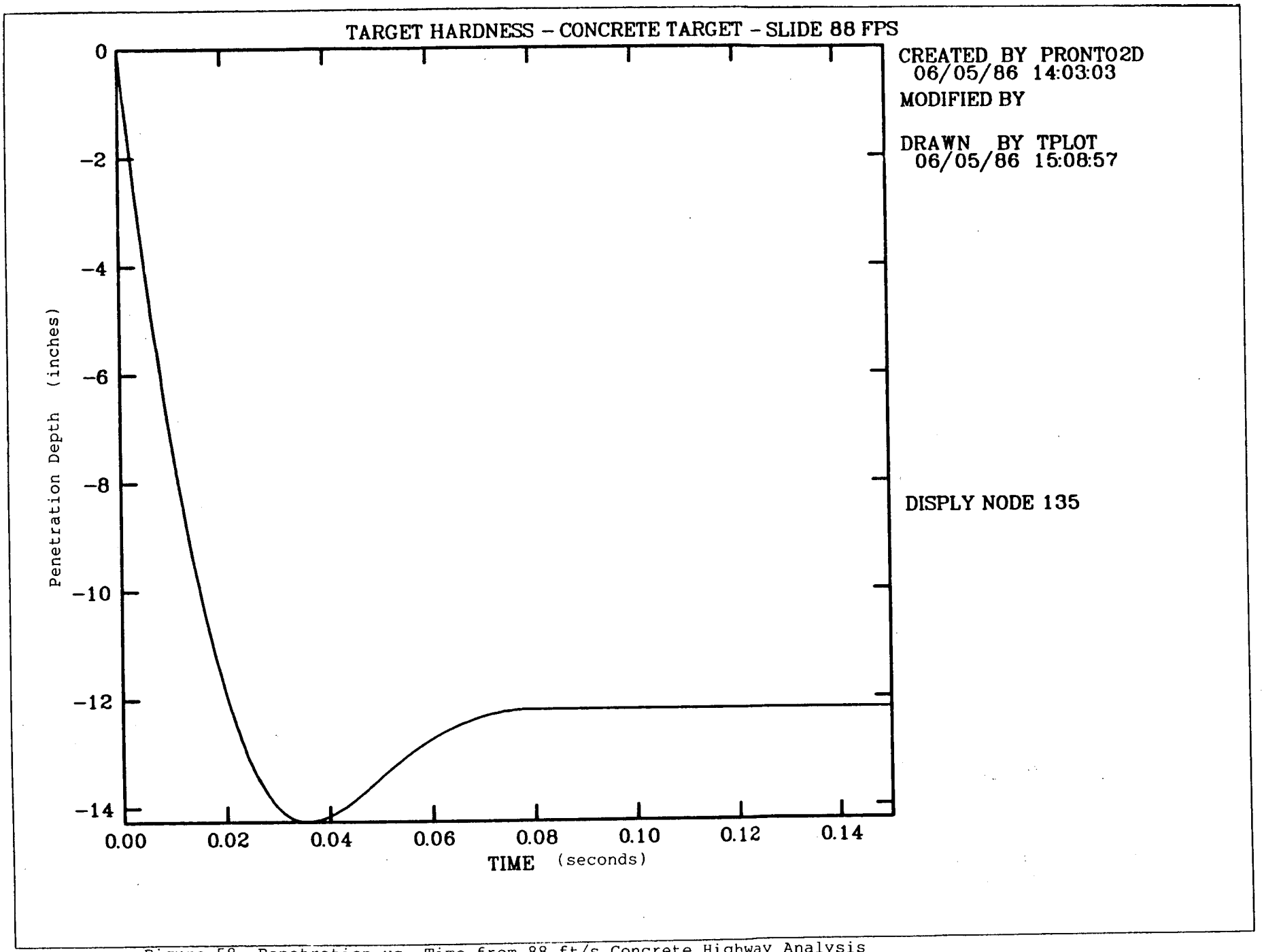

Figure 58 Penetration vs. Time from 88 ft/s Concrete Highway Analysis

concrete analysis had to also include accurately representing the target. This presents inherent problems that must be taken into account. The material properties of both the concrete and soil beneath the concrete had to be determined. In addition, the projectile/impact surface and the concrete/soil interaction had to be formulated. However, the most difficult aspect of modeling the concrete targets is properly accounting for the radial cracking that occurs during impact. In this particular analytical evaluation, radial cracking was ignored. The concrete analysis provided results that were within reasonable proximity to the experimental findings but there were some differences. The relative agreement between experimental and analytical results is particularly encouraging since only the concrete shear plug and soil directly underneath was modeled.

4.3 Soil Target

An initial series of analyses [16] was completed to determine the behavior of a cask dropped onto a soil target. This initial series indicated that penetration depths of 1.0 to 60.0 inches would be expected for drops with an impact velocity of 66 ft/s onto various soil targets. Results from these analyses indicated detailed mechanical properties for the soil would be needed to generate accurate predictions of penetration depths for tests at the cable drop site.

An additional series of analyses has been completed using results from the New Mexico Engineering Research Institute (NMERI) soil tests [6]. Results from the NMERI soil classification tests indicated the material present at the cable drop site at depths greater than 12 inches was a sand-clay mixture (SC).

The top 12 inches of material contained large amounts of gravel (3-inch maximum diameter) and could not be sampled with a Shelby tube. Engineering properties for the soil at depths greater than 12 inches were determined from a series of uniaxial and triaxial compression tests (Table 4).

For these tests, the soil samples were first loaded hydrostatically to a prescribed confining pressure. A confining pressure of 0 psi was used for the uniaxial tests. Next, additional stress was applied to the soil sample in only one direction. Plots of principal stress difference versus axial strain from the triaxial compression tests were used to determine a value for Young's modulus for this soil. For the triaxial compression tests, principal stress difference is equal in magnitude to the additional stress that is applied in only one direction. Young's modulus for this soil was approximately 3000 psi on initial loading. All of the uniaxial and triaxial tests were performed at very low strain rates; consequently, no information on strain rate effects was obtained. A linear pressure volume strain behavior was used in the finite element analyses.

4.3.1 Soil Finite Element Analysis

A finite element series of analyses was completed using the soil model in DYNA2D [13] and PRONTO-2D [15]. This soil constitutive model [17] combines volumetric plasticity with pressure dependent deviatoric plasticity. The following input parameters are required to use this model:

SOIL PROPERTIES[+]

DEPTH (in)	NATURAL DRY DENSITY (pcf)	UNCONFINED COMPRESSIVE STRENGTH (psi)	COHESION (psi)	INTERNAL FRICTION ANGLE (degree)
12 - 24	89.	12.5	3.0	34
24 - 36	100.	17.2	6.0	28
36 - 48	103.	14.0	4.5	28
48 - 60	103.	13.5	4.0	27

[+] Since soil properties were not uniformly available for a depth of 0 - 12 inches, the propeties between 12 - 24 inches were used in calculations

Table 4

- shear modulus, G
- bulk unloading modulus, B
- deviatoric yield function constants
- pressure-volumetric strain data.

The shear and bulk moduli were derived using the experimentally measured Young's modulus and an estimated Poisson's ratio of 0.25. The deviatoric yield function constants were derived from the experimentally measured cohesion and internal friction angle values. The pressure volumetric strain data was generated using the bulk modulus and the following equation

$$\gamma = -\ell n(1 - P/B),$$

where

γ = volumetric strain

P = pressure

B = bulk modulus.

The bulk modulus is not expected to remain constant during each drop test but since the experimental pressure-volumetric strain behavior was not reported, there was no way to determine how it would vary as a function of pressure; therefore, a constant bulk modulus was used for each drop test.

Different values were used for the bulk modulus for some of the analyses to determine what effect this change would have on the results. Material properties used in this series of analyses are given in Table 5. Since

MATERIAL PROPERTIES USED IN FINITE ELEMENT ANALYSES

CASK: YOUNG'S MODULUS = 29.0E+6 psi
POISSON'S RATIO = 0.30
DENSITY = 6.74E-4 lbs/in.

SOIL: BULK MODULUS = 2000. psi
SHEAR MODULUS = 1200. psi

COEFFICIENT OF FRICTION AND DEVIATORIC YIELD FUNCTION CONSTANTS

DEPTH (In)	FRICTION COEFF.	DYNA-2D a0	DYNA-2D a1	DYNA-2D a2	PRONTO-2D a0	PRONTO-2D a1	PRONTO-2D a2
0 - 24	0.675	15.3	6.21	0.630	6.77	1.38	0.00
24 - 36	0.532	39.0	8.03	0.413	10.82	1.11	0.00
36 - 48	0.532	25.8	6.53	0.413	8.81	1.11	0.00
48 - 60	0.509	25.1	6.20	0.381	8.69	1.07	0.00
60+	0.488	24.3	5.85	0.351	8.55	1.03	0.00

Table 5

material properties for the top 12 inches of soil were not available, properties for the 12- to 24-inch layer were used for the top 12-inch layer. The deviatoric yield function constants for PRONTO-2D are different than those for DYNA2D because the deviatoric yield function in the soil constitutive model in PRONTO-2D uses effective stress in place of the second invariant of deviatoric stress used in DYNA2D. The deviatoric yield function constants in Table 5 actually represent the same deviatoric yield surface.

Since both the loading and the geometry were axisymmetric, two-dimensional axisymmetric finite element models were used in this series of calculations (Figure 59). Model A was used with the DYNA2D finite element code and Model B was used with the PRONTO-2D finite element code. These two different models were used to take advantage of special features found in each code. The series of analyses completed with DYNA2D and Model A used the mesh rezoning capability for large strains. Since a rezoning capability was not available in PRONTO-2D a different model was required. The series of analyses completed with PRONTO-2D and Model B used slide lines with friction on the right edge to represent the effects of the rest of the soil on the model.

In the second series of analyses with PRONTO-2D and Model B, sliding was expected along the right edge when the magnitude of the shear stress along this edge (τ) exceeded the magnitude of the soil cohesion (C) plus the product of the internal friction coefficient (μ) and the normal stress (σ_n). In equation form, sliding is expected if

$$\tau > C + \mu\sigma_n$$

The internal friction coefficient, μ, is given by the following equation

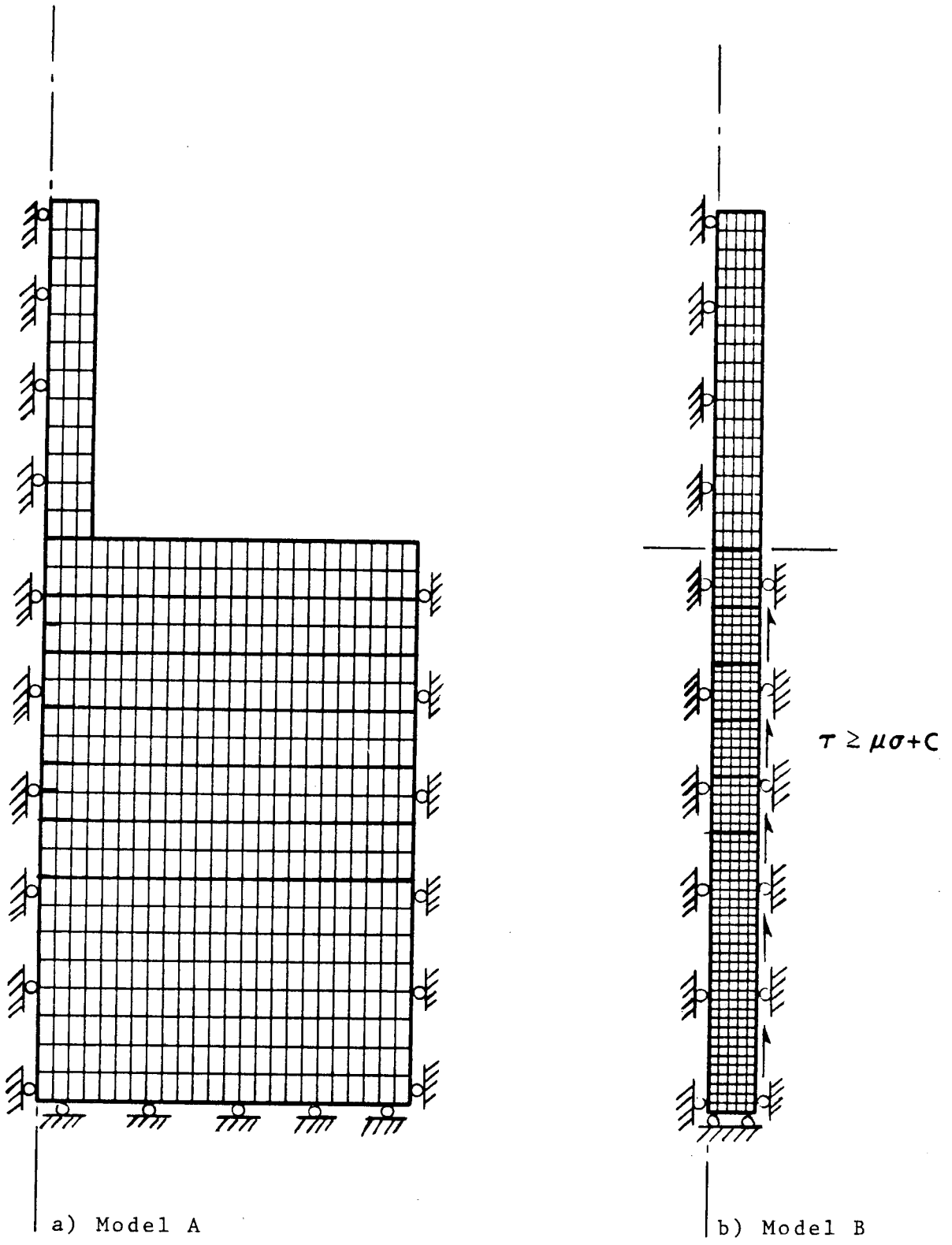

Figure 59 Finite Element Model for Soil Analysis

$$\mu = \tan \phi$$

where ϕ is the experimentally measured internal friction angle. Internal friction coefficient values used in this analysis are given in Table 5. For this series of analyses, the small cohesion values were neglected and sliding was allowed along the right edge when the magnitude of the shear stress along this edge exceeded the product of the internal friction coefficient and the normal stress.

4.3.2 Soil Finite Element Results

Plots of the deformed finite element meshes are shown in Figures 60 and 61. The top soil layer in the DYNA2D series of calculations was rezoned at several time steps during these analyses. Effects of the slide line friction in the PRONTO-2D series of analyses can be seen in Figure 61. The models in both series of analyses predicted the soil behavior very well. Plots of cask penetration as a function of time are shown in Figure 62. For the series of analyses completed with DYNA2D, estimates of cask acceleration were obtained by dividing the change in cask velocity during a time step by the time step magnitude. For the series of analyses completed with PRONTO-2D, estimates of cask acceleration as a function of time are shown in Figure 63. For the drop with an initial velocity of 88 ft/s, a peak acceleration of 38 g's was predicted by the series of analyses with DYNA2D and a peak acceleration of 50 g's was predicted with PRONTO-2D. A computer analysis was not performed for the 110 ft/s impact into the uncompacted soil.

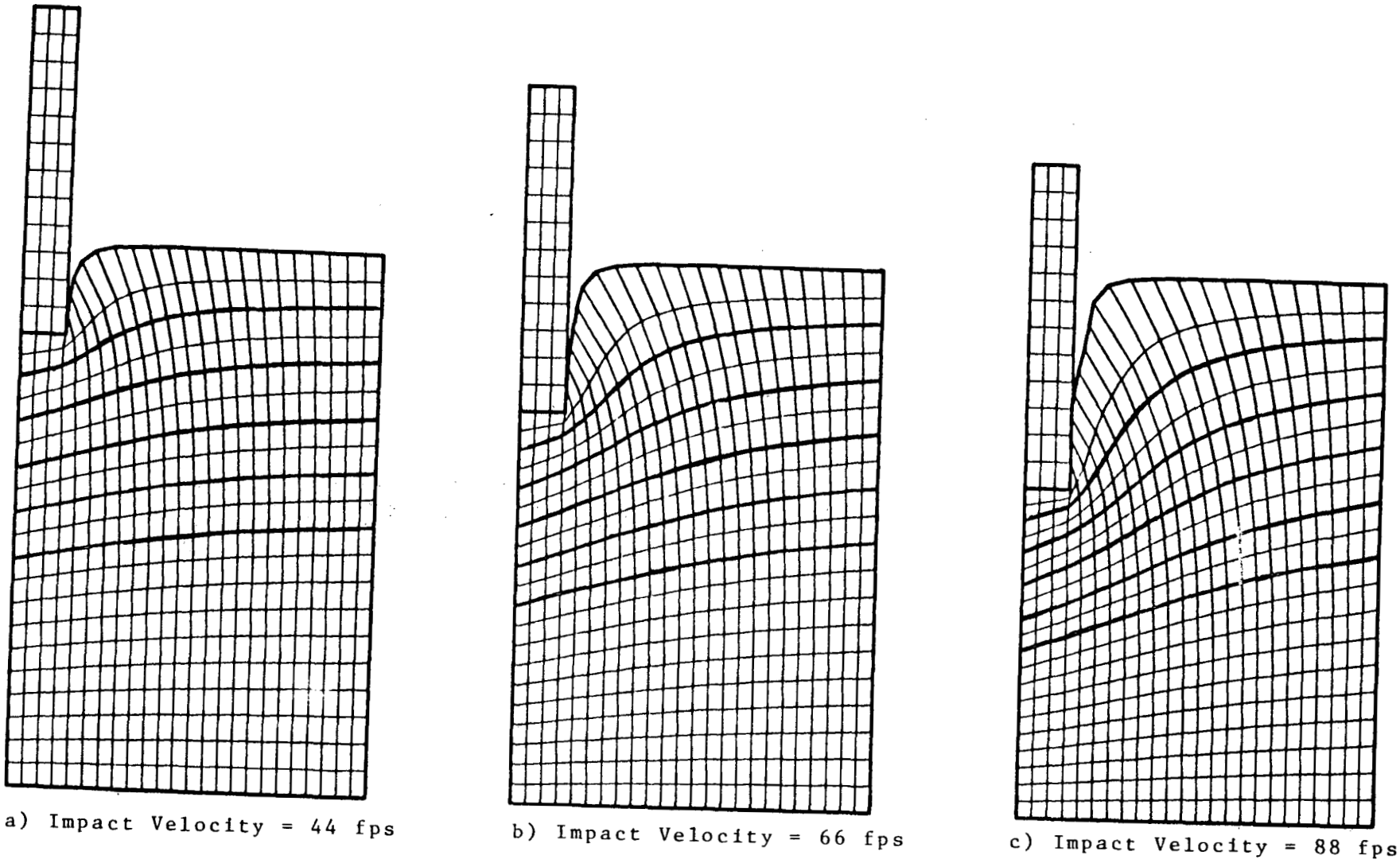

a) Impact Velocity = 44 fps

b) Impact Velocity = 66 fps

c) Impact Velocity = 88 fps

Figure 60 Deformed Shape of Finite Element Model 'A' at Maximum Cask Penetration

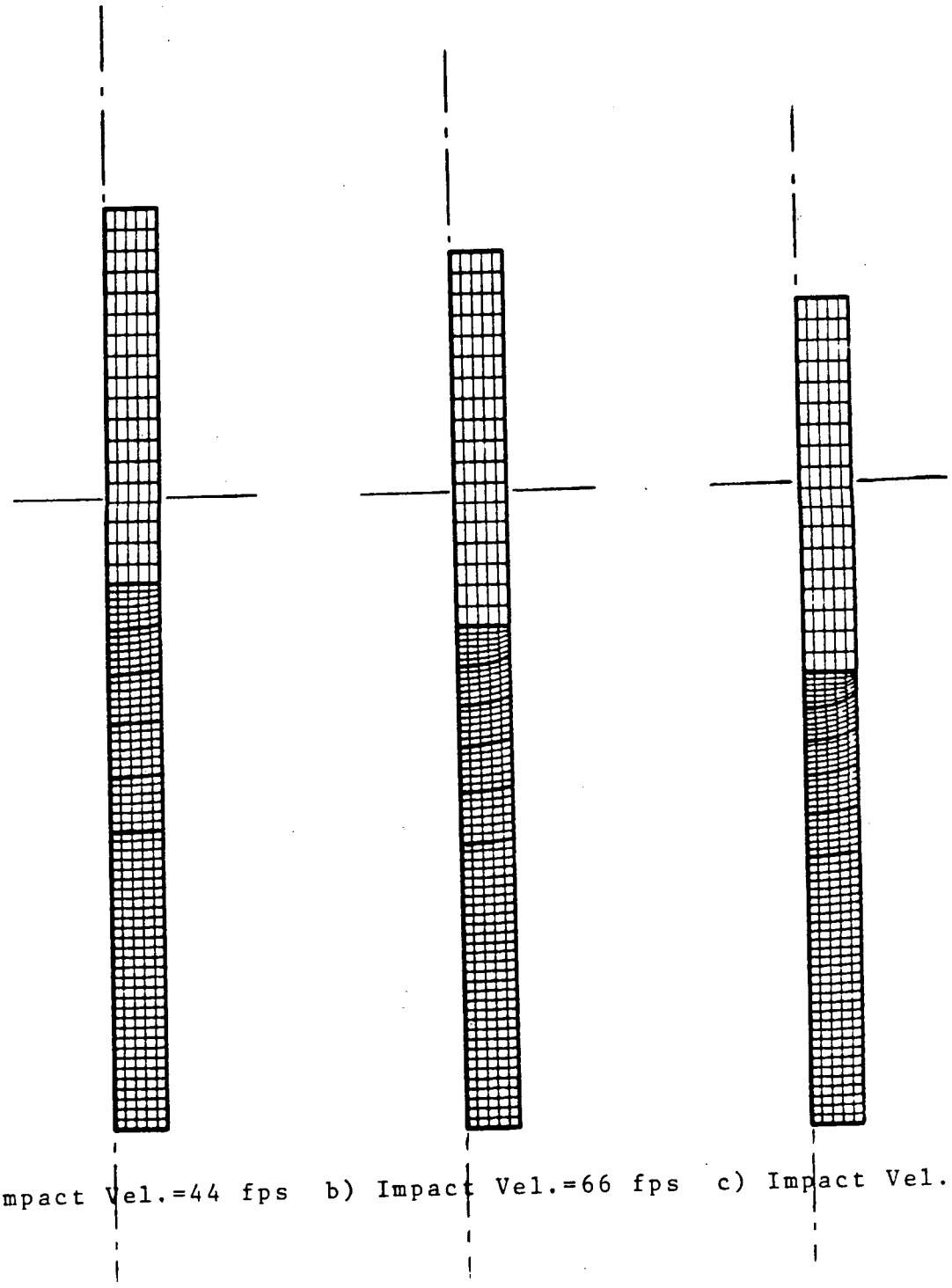

a) Impact Vel.=44 fps b) Impact Vel.=66 fps c) Impact Vel.=88 fps

Figure 61 Deformed Shape of Finite Element Model 'B' at Maximum Cask Penetration

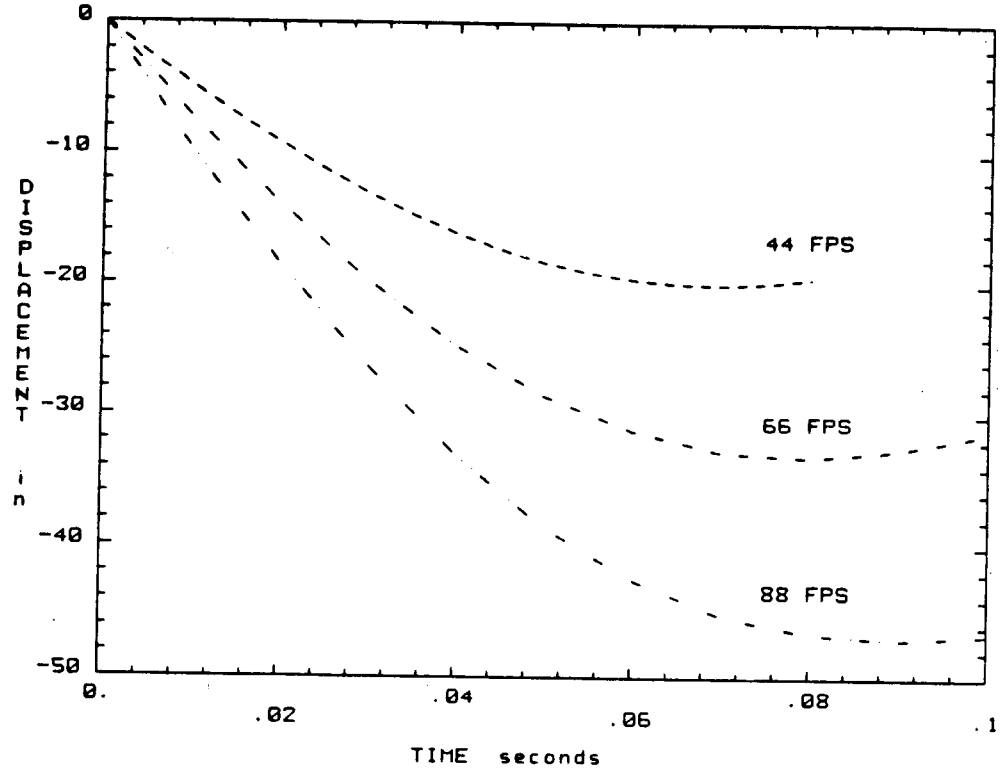

a) Model A and DYNA-2D

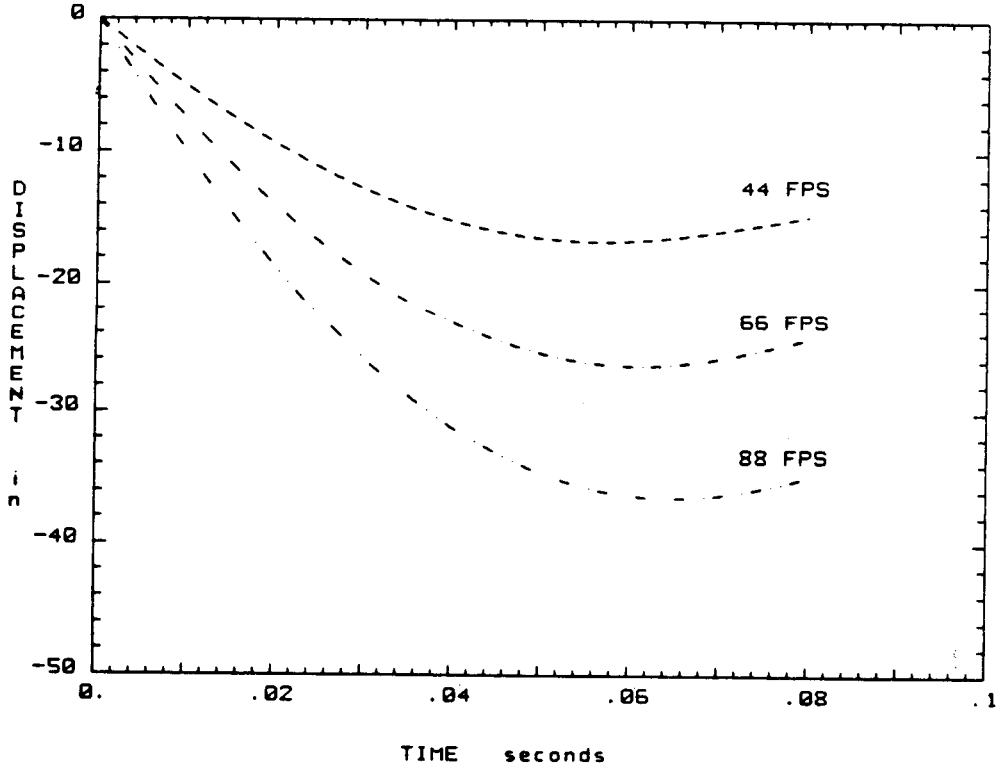

b) Model B and PRONTO-2D

Figure 62 Penetration vs. Time from Soil Analysis

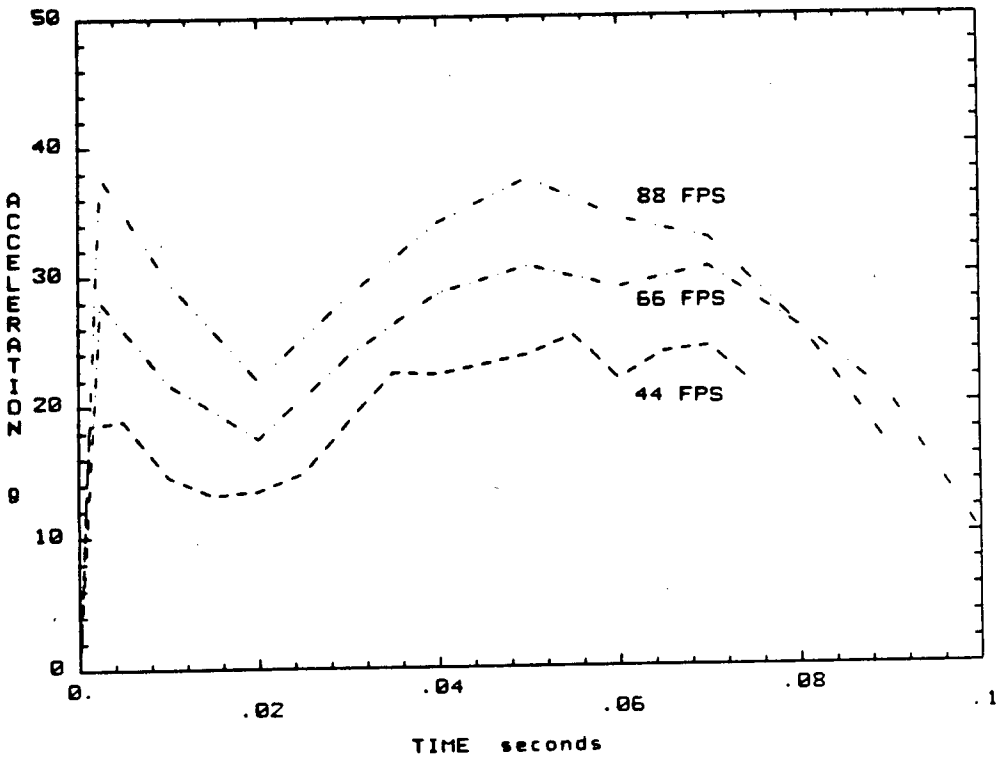

a) Model A and DYNA-2D

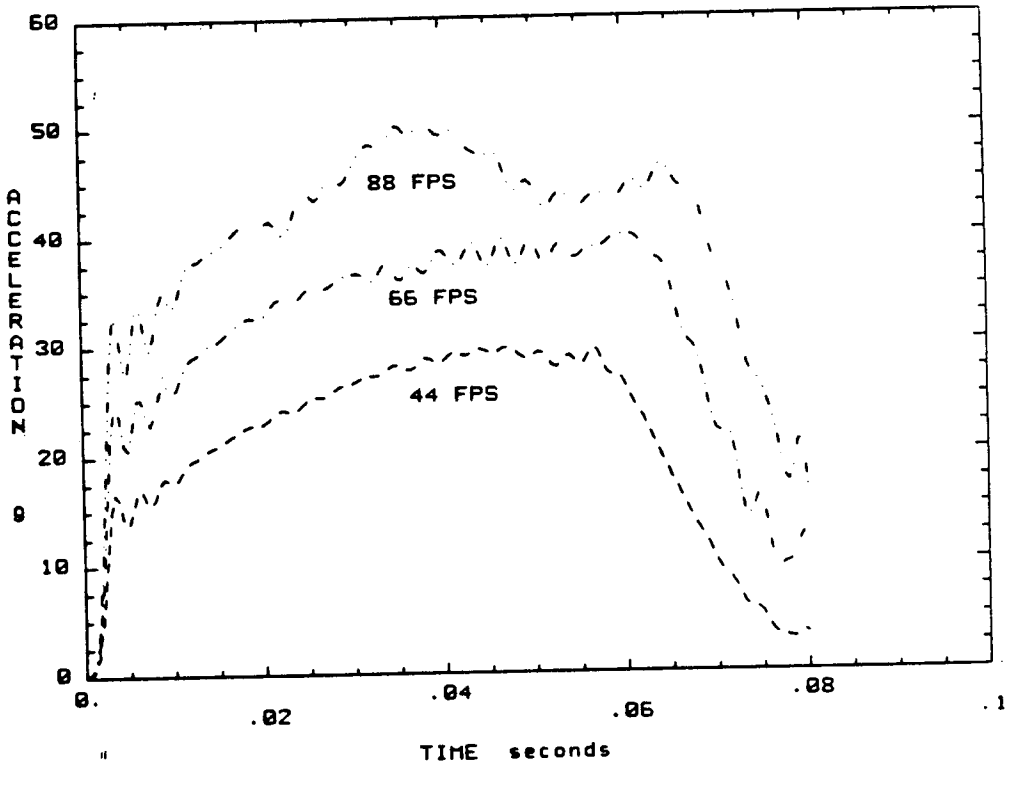

b) Model B and PRONTO-2D

Figure 63 Acceleration vs. Time from Soil Analysis

The next series of analyses was completed to determine what effects variations in the volumetric behavior of the soil would give on the results. This series of analyses was completed using PRONTO-2D and Model B, and an impact velocity of 66 ft/s. Results from this series of analyses indicate that when the bulk modulus was increased from 2000 to 4000 psi, the expected penetration depth decreased from 26 to 18 inches (Figure 64). When the bulk modulus was decreased from 2000 to 1000 psi, the expected penetration depth increased from 26 to 38 inches. The results were sensitive to variation in bulk modulus.

A final series of analyses was completed to determine how sensitive the results were to friction coefficient variations. This series of analyses was also completed using PRONTO-2D and Model B and an impact velocity of 66 ft/s. For this analyses, all soil layers were given the same friction coefficient. Results from this series of analyses indicated that selection of friction coefficients of 0.25 and 0.75 would generate penetration depth estimates of 36 and 24 inches, respectively (Figure 65).

4.3.3 Comparison of Experimental and Analytical Results

Penetration depths predicted by the finite element analyses were compared with experimental results in Table 6. This comparison indicated that the finite element analyses completed with PRONTO-2D generated the most accurate estimates of penetration depth. A graphical comparison of penetration depths is shown in Figure 66.

Included in Figure 66 is a curve obtained from an empirical equation used to predict the penetration depth of various penetrators. The relationship was

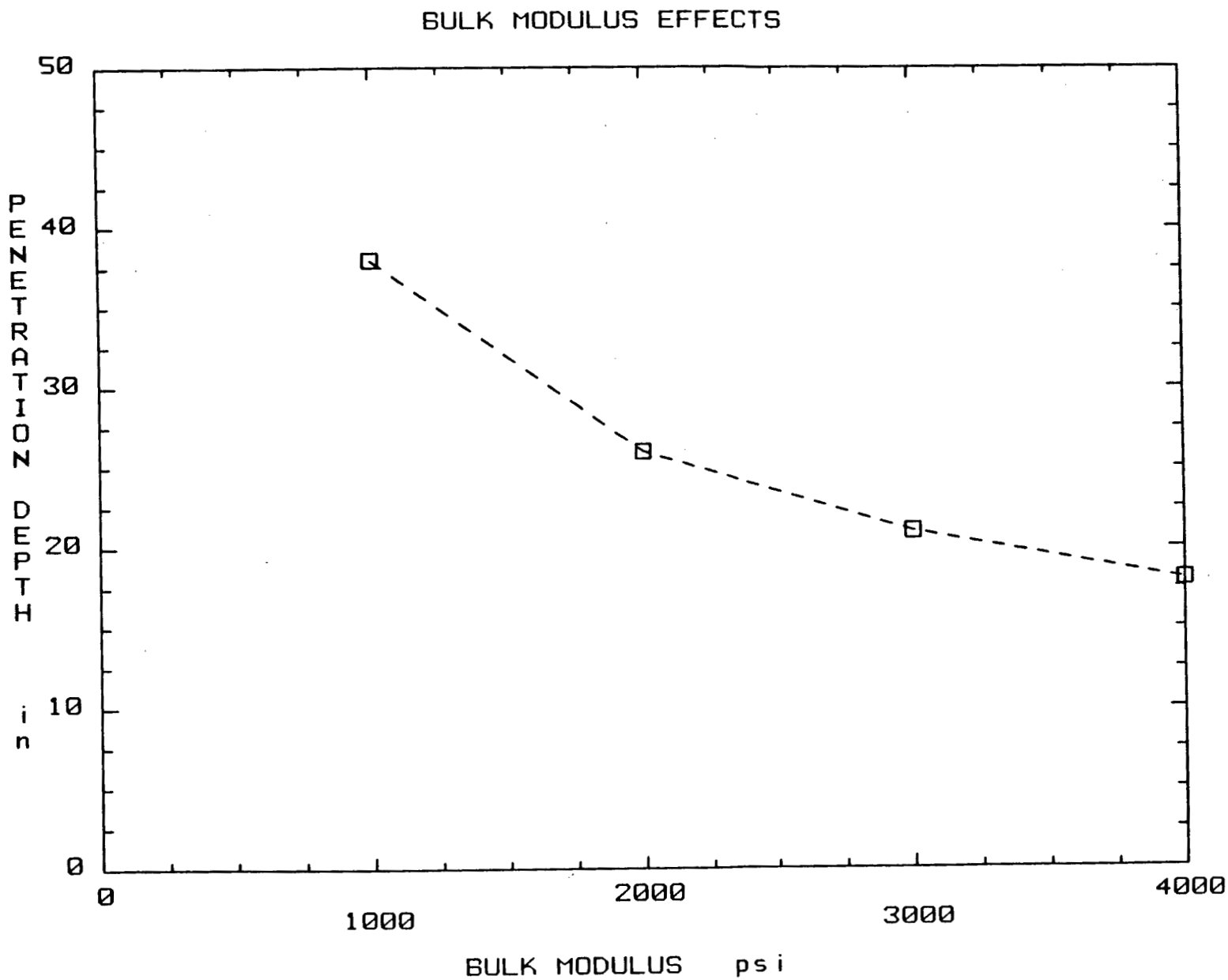

Figure 64 Effect of Variations in Soil Volumetric Behavior - Model B and PRONTO-2D, Impact Velocity at 66 ft/s

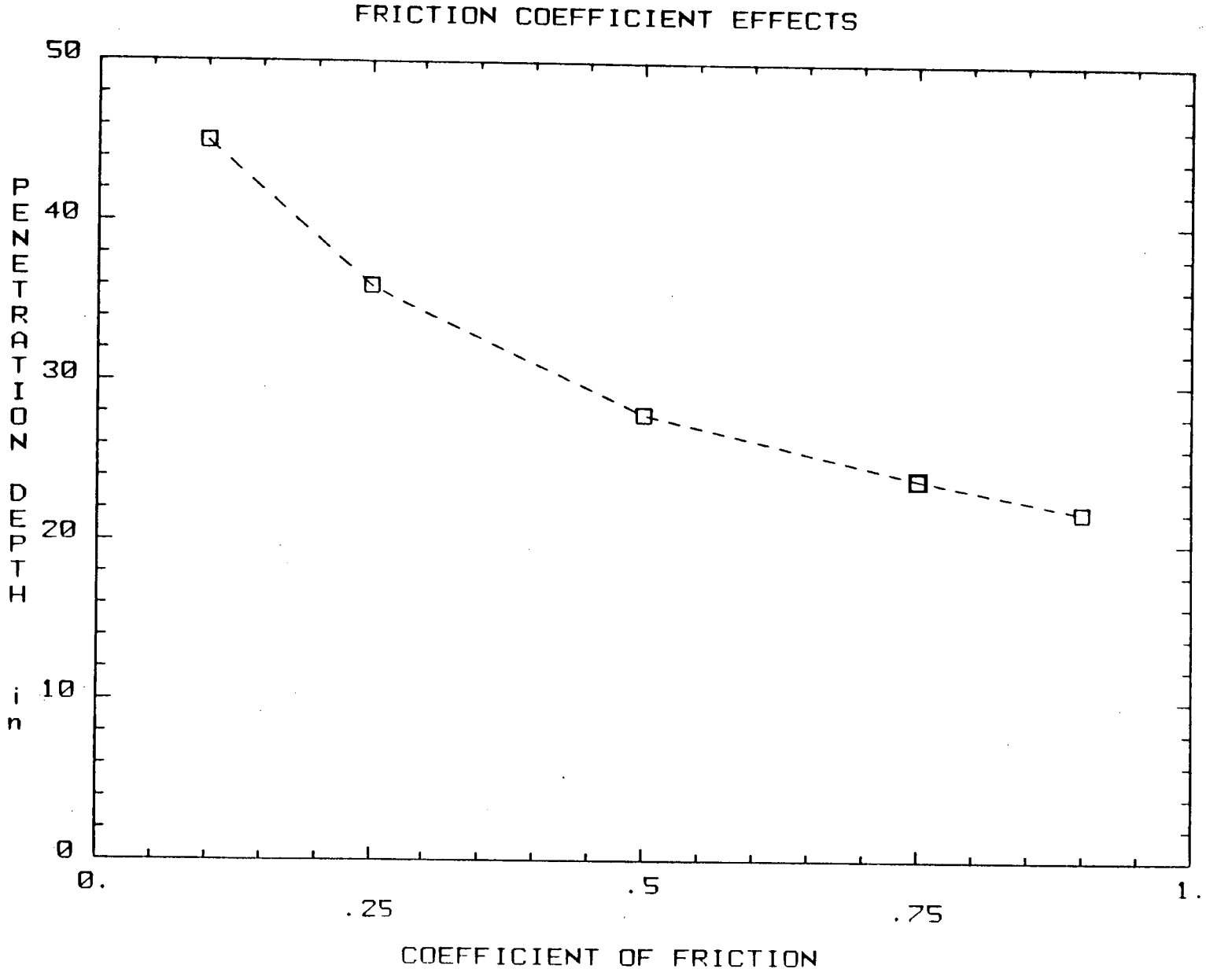

Figure 65 Effect of Variations in Friction Coefficient - Model B and PRONTO-2D, Impact Velocity of 66 ft/s

SOIL PENETRATION DEPTH (inches)			
IMPACT VELOCITY (ft/s)	44	66	88
EXPERIMENTAL	19	25	36
DYNA2D AND MODEL A	20	33	47
PRONTO-2D AND MODEL B	17	26	36

Table 6

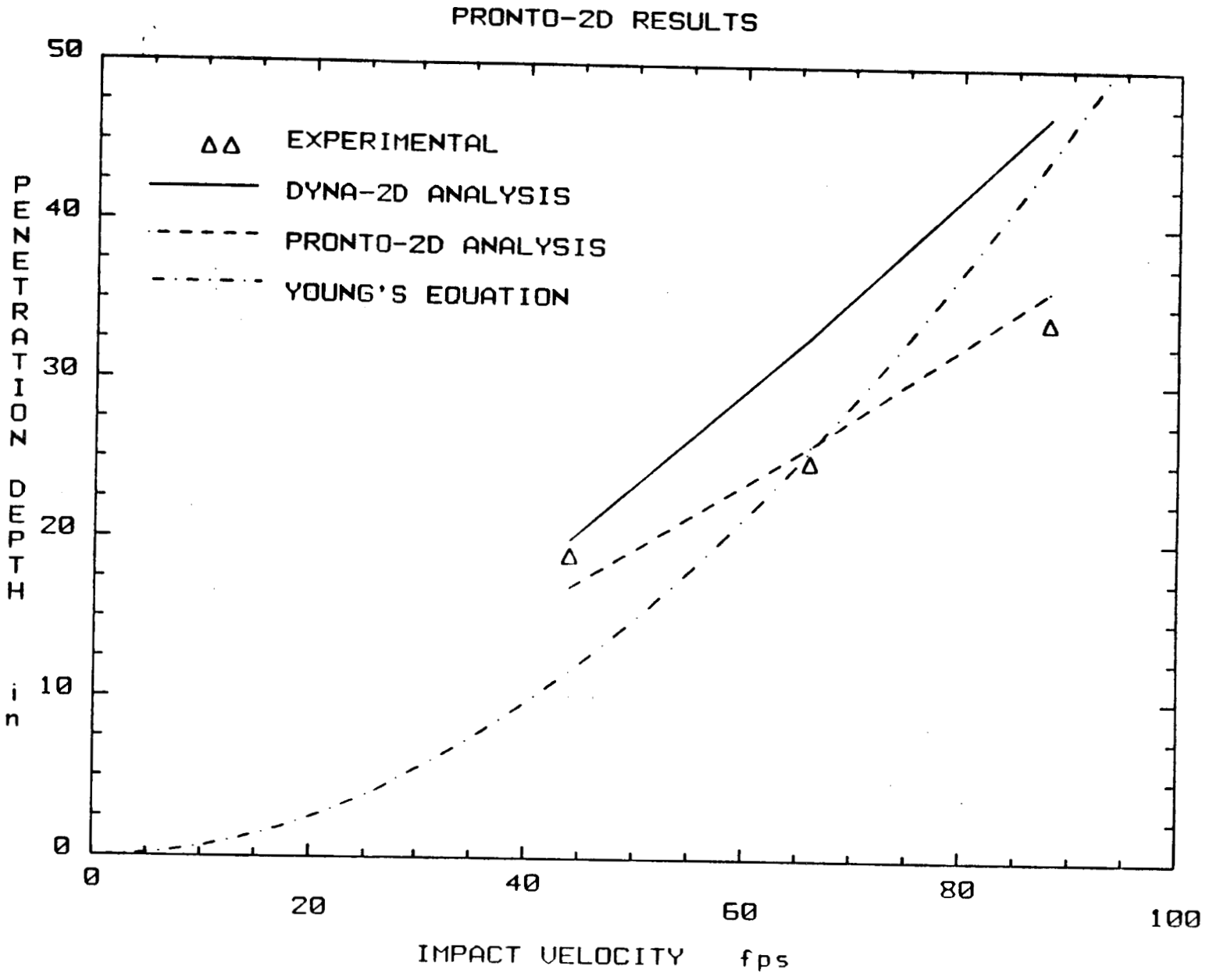

Figure 66 Comparison of Experimental and Analytical Soil Results of Penetration Depth at 44 ft/s

developed and published by C. W. Young in 1969 [18] and based on experimental results from a series of drop tests completed during the 1960s. For a penetrator with an impact velocity of less than 200 ft/s the equation developed is:

$$D = 0.535N\ (W/A)^{1/2}\ \ln\ (1 + 2 \times 10^{-5}\ V^2)$$

where

D = depth of penetration, ft

S = soil constant (Table 7)

N = nose performance constant (Table 7)

W = penetration weight, lbs

A = penetration sectional area, in^2

V = impact velocity, ft/s

The major difficulty encountered using this equation is the selection of an appropriate soil constant (S). For this analysis, a soil constant of 19.4 generated the best fit of Young's equation to the experimental data (Figure 66). In Table 7 a soil constant between 9 and 14 is suggested for topsoil. Penetration depths would have been seriously underestimated if these values were used.

Cask accelerations predicted by the finite element analyses were compared with the experimental results in Figures 67 to 69. These plots were filtered with a low pass filter with a cut-off frequency of 500 Hz. Both finite element analyses predicted the cask acceleration would remain nearly constant

COEFICIENTS FOR YOUNG'S EMPIRICAL EQUATION

SOIL TYPE	S	NOSE TYPE	N
Rock	1.0 - 1.1	Flat	0.56
Loose Sand	6.0 - 8.0	Cone (l/d = 0.3)	1.32
Topsoil	9.0 - 14.0		
Saturated Clay	33.0 - 60.0		

Table 7

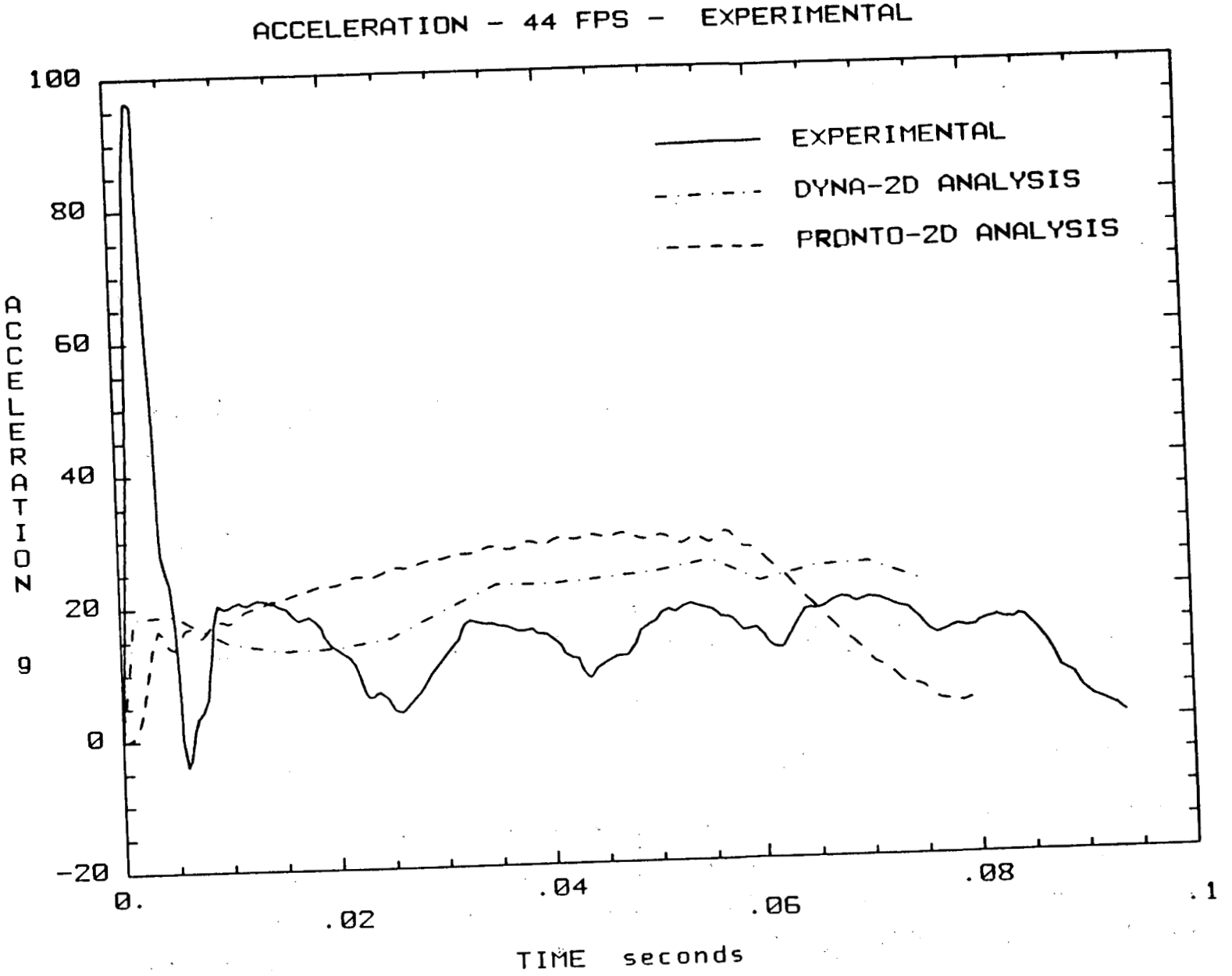

Figure 67 Comparison of Experimental and Analytical Soil Results - Cask Acceleration - 44 ft/s

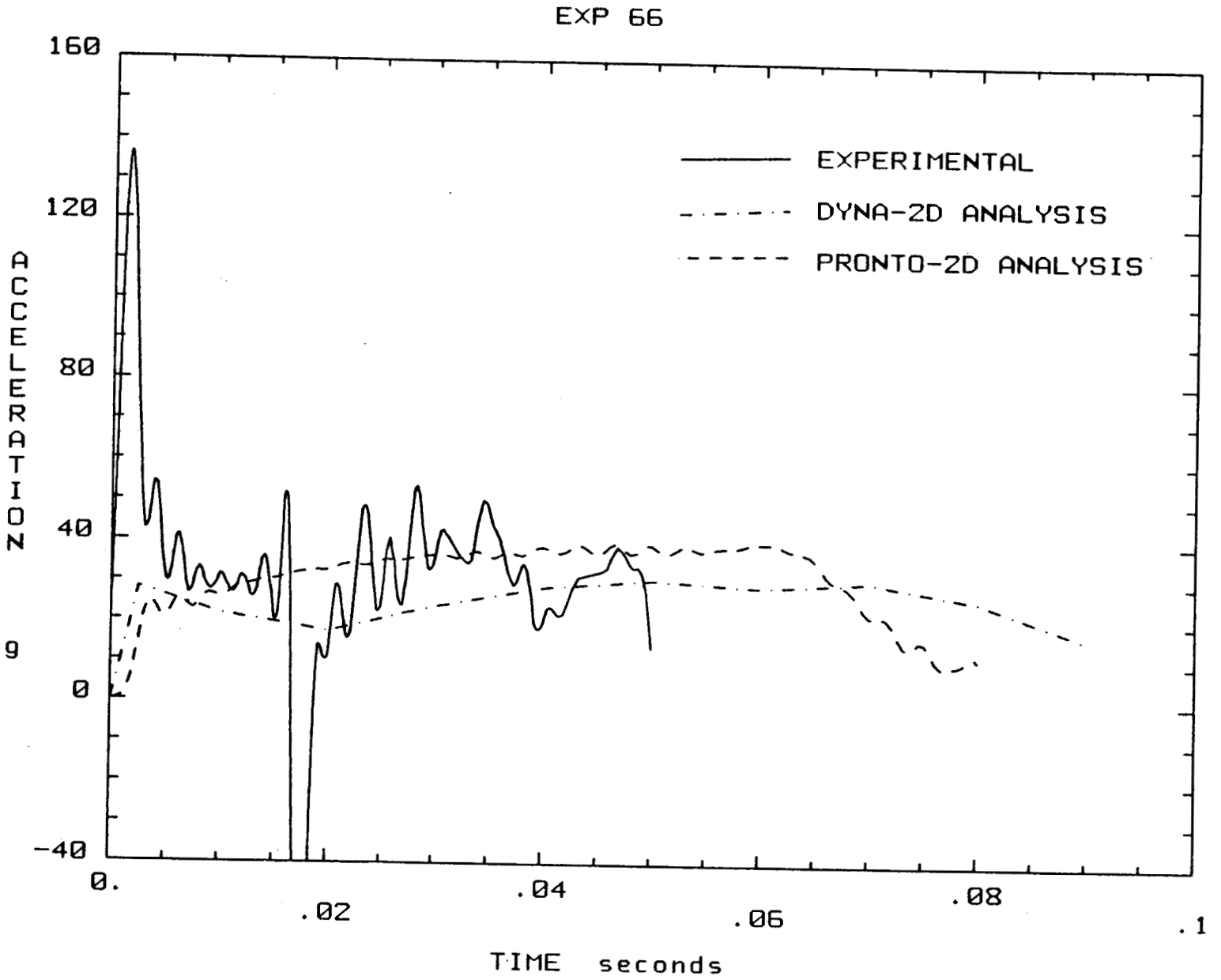

Figure 68 Comparison of Experimental and Analytical Soil Results of Cask Acceleration at 66 ft/s

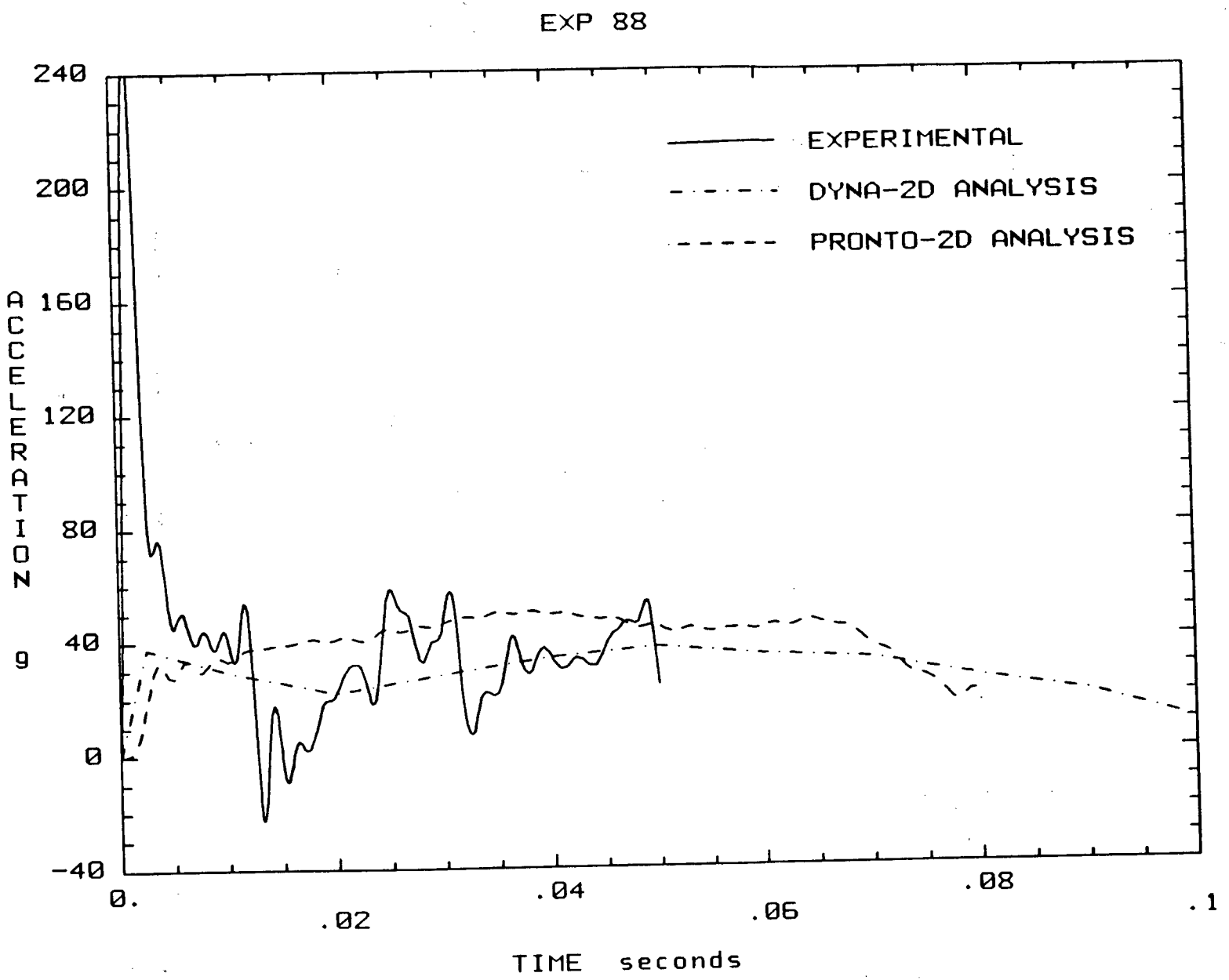

Figure 69 Comparison of Experimental and Analytical Soil Results of Cask Acceleration at 88 ft/s

during the impact event which correlates with experimental findings. Experimental results indicated the cask acceleration would be significantly higher during the first few milliseconds of the impact event. Both analyses failed to predict the relatively large acceleration that was generated during the first few milliseconds of the impact event. One possible reason for this discrepancy between analytical and experimental results is that the top 12 inches of soil material was not accurately modeled because mechanical properties for this top soil layer were not measured. Also, the acceleration spike from rebound was not reproduced in the analysis. Experimental soil classification tests indicated that the top 12 inches of soil material contained a large amount of gravel and was significantly different than the rest of the soil.

5.0 CONCLUSIONS

Impacting a blunt-end cylindrical object into a series of various targets at a range of velocities produced results ranging from both anticipated to unexpected. The most severe damage to the test unit was from impacting the unyielding target at 44 ft/s. Only the 88 ft/s impact into the concrete runway produced unit responses on the same order of magnitude. However, several observations are made from this testing and analytical program.

The analytical calculations concerning the concrete and soil targets were difficult and cumbersome despite the fact several experimental findings were reproduced. A more detailed analysis may result in a mathematical process and procedure that more accurately predicts projectile and target response, but,

the complexity associated with this type of analysis is far more difficult than the problem of a projectile striking an unyielding target.

In analyzing the effects of impacting an object into an unyielding target, only the actual projectile needs to be modeled. Computer codes mathematically represent an impenetrable surface enabling all of the available energy to be applied to the striking projectile. Analyzing a yielding target entails representing the geometry, materials and boundary conditions of the impacted surface itself. In addition, the complex failure mechanisms of each type of target must also be taken into account.

Overall, the correlation between experimental results and analytical calculations were encouraging (Table 8). The unyielding target results obtained analytically were well matched with those found experimentally. The penetration values with respect to the soil targets were reproduced between experimental and analytical results, however, acceleration levels did not match. This discrepancy in acceleration levels was common in all the yielding targets.

With regard to a yielding target's response upon impact, the phenomenon of a double spike was evident. At the instant of impact the projectile experiences a response producing measurable accelerations and strains. This first spike is evidence of the shear planes that are forming in the concrete and soil targets. Depending on the impact velocity and nature of the target, a second response representing the unit rebounding is likely to occur after the unit comes to a complete stop. However, note that this phenomenon is representative of a blunt-end object without impact limiters. If impact limiters were employed, the phenomenon of the double spike would most likely disappear. Depending on the impact limiters, the softer the material, the

COMPARISON OF EXPERIMENTAL VS ANALYTICAL RESULTS

TEST		ACCELERATIONS (g's)		PENETRATION (inches)	
		Experimental	Analytical	Experimental	Analytical
UNYIELDING TARGET	44 ft/s	1300	1600	0	0
CONCRETE HIGHWAY	44 ft/s	350	300	4	8
	88 ft/s	7500	600	8	14
NATIVE DESERT SOIL	44 ft/s	100	20	19	17
	66 ft/s	130	30	25	26
	88 ft/s	250	40	36	36

Table 8

more closely a yielding target such as concrete would appear to be unyielding. However, that correlation strictly relies on the impact limiters, test unit and target used.

Comparison of the additional available kinetic energy involved by increasing the impact velocity was made with respect to unit damage and penetration depth. A good correlation was obtained between the increased kinetic energy and unit damage. Radial deformation was used to represent the test unit damage. The relationship between damage and increased available energy was within a factor of a half. However, comparison between penetration depth and kinetic energy was not so close. The additional penetration into the soil was less than the ratio of increased available energy. On the other hand, the change in penetration into the concrete targets was greater than the increase kinetic energy ratio. This suggests that a finite amount of energy is required to form the concrete shear plug. Once that has occurred, travel through the concrete target is less restricted. Forming the shear planes in the soil target and then compressing the soil to lock-up becomes more difficult as penetration depth increases. It is quite probable as impact speeds increase far beyond the 88 ft/s impact velocity used in this program, the same phenomenon would occur in the concrete targets.

REFERENCES

1. IAEA, IAEA Safety Standards, Safety Series No. 6, IAEA, Vienna, Austria, Ed. 1985.

2. IAEA, IAEA Safety Standards Safety Series No. 37, IAEA, Vienna, Austria, Ed. 1982.

3. Airport Pavement Design and Evaluation, U. S. Department of Transportation, Federal Aviation Administration, Washington DC, AC 150/5320-6C, 1978.

4. New Mexico State Highway Department, Standard Specifications for Road and Bridge Construction, Ed. 1984.

5. ASTM, Annual Book of ASTM Standards, Part 19, Soil and Rock Building Stone, Ed. 1985.

6. V. Casino, Soils Laboratory Test Results - Sandia Cable Drop Site, RE. Doc. Num. 95-3756, University of New Mexico, February 1986.

7. Measurements Group, Micro-Measurements and Instrumentation Division Product and Technical Information, Raleigh, N.C., 1985.

8. Entran Devices Inc. Catalog, Entran Devices Inc., Fairfield, N.J.

9. Endevco Catalog, Endevco Corp., San Juan Capistrano, CA.

10. P. L. Walter, H. D. Nelson, Limitations and Corrections in Measuring Structural Dynamics, Experimental Mechanics, Vol. 19, No. 9, September 1979, page 309 - 316.

11. P. L. Walter, L. Patrick, R. Rodeman, Characterization of Digital Filters Used in Sandia National Laboratories Test Data Analysis Division, SAND-79-1230, December 1979.

12. D. P. Schafer, Sandia National Laboratories Standard Environmental Test Methods, Sandia National Laboratories, SC-4452E(M), December 1983.

13. J. O. Hallquist, User's Manual for DYNA2D, University of California, LLNL, Report UCID 18756, Rev. 1, March 1978.

14. PDA/PATRAN-G User Guide, Santa Ana, CA: PDA Engineering, 1980.

15. L. M. Taylor and D. P. Flanagan, PRONTO - A Two Dimensional Transient Solid Dynamic Program, SAND86-0594, Sandia National Laboratories, Albuquerque, NM 1982.

16. M. K. Neilsen, Target Hardness Study, internal memorandum to A. Gonzales, Sandia National Laboratories, May 1985.

17. R. D. Krieg, A Simple Constitutive Description for Soils and Crushable Foams, SC-DR-72-0883, Sandia National Laboratories, Albuquerque, New Mexico, 1972.

18. C. W. Young, Depth Prediction for Earth-Penetrating Projectiles, Journal of the Soil Mechanics and Foundations, May 1969, page 803 - 817.

Distribution:
U.S. Department of Energy
Office of Scientific & Technical Information (226)
Oak Ridge, TN 37830
Attn: DOE/OSTI-4500-R74 UC-71

U.S. Department of Energy
Routing RW-33 (6)
1000 Independence SW
Washington, DC 20585

U.S. Department of Energy
Routing DP-123 (1)
Washington, DC 20545
Attn: J. Lytle
L. Harmon
F. Falci

Office of Security Evaluations
Defense Programs - DP-4, GTN (1)
Washington, DC 20545
Attn: Dr. Julio L. Torres

U.S. Department of Energy
Albuquerque Operations Office (1)
Albuquerque Headquarters
P.O. Box 5400
Albuquerque, NM 87115
Attn: J. E. Bickel

U.S. Department of Energy
Albuquerque Operations Office (1)
4308 Carlisle N.E.
Albuquerque, NM 87107
Attn: J. McGough
K. Golliher

U.S. Department of Energy
Chicago Operations Office (1)
9800 S. Cass Avenue, Bldg. 350
Argonne, IL 60439
Attn: S. Mann
P. Kearns
C. Boggs-Mayes
J. Holm

U.S. Department of Energy
Idaho Operations Office (1)
550 Second Street
Idaho Falls, ID 83401
Attn: C. P. Gertz
W. W. Bixby

Joint Integration Office (1)
4308 Carlisle, N.E.
Albuquerque, NM 87107
Attn: J. Roll, Westinghouse
K. McKinley, Rockwell
R. M. Jefferson

3141 S. A. Landenberger (5)
3151 W. L. Garner (3)
3154-1 C. K. Dalin (28)
for DOE/OSTI
6000 D. L. Hartley
6300 R. W. Lynch
6320 J. E. Stiegler
Attn: TTC Master File
6320 TTC Library (25)
6321 R. E. Luna
6322 J. M. Freedman
6322 R. G. Eakes
6323 G. C. Allen, Jr.
6323 J. L. Moya
6323 H. R. Yoshimura
6323 A. Gonzales (20)
8024 P. W. Dean

Appendix A

Accelerometer and Stain Gage Specifications

MINIATURE ACCELEROMETER, HI-OVERRANGE PROTECTED, PIEZORESISTIVE
FULL BRIDGE, DAMPED, WITH FLANGE MOUNTING.
ENTRAN DEVICES MODEL NO. EGAXT-23-F-5000/CERTIFIED

Accelerometer range +/- 5000 g

Overrange at approximately +/- 7000 g

Overrange in all three axes

Sensitivity .05 Mv/g

Full scale output 250 Mv

Resonate frequency 8.5 KHz

Nonlinearity +/- 1%

Transverse sensitivity 3% max

Damping .7 critical nominal at 75 Deg F flat to 1/2 db

Useful frequency range 30% to 50% resonate frequency at 75 Deg F

Thermal and mechanical conditioning

Input impedance 1000 ohms

Output impedance 450 ohms

Excitation voltage 15 VDC

Case material 300 series stainless steel

Compensated temperature 0 Deg F to 100 Deg F

Operating temperature -40 Deg F to 250 Deg F

Compensation module at 18 inches

Accelerometer to be supplied with 48 inch lead length

Unit to be flange mounted

Supplier to furnish requester with drawings of mounting configuration and manufactures specification for installation and torque values for mounting

Supplier will furnish accelerometers with unique identification numbers, which will be referenced to the supplier furnished certifications

Units to be supplied with E5 type shielded cable

Units to be supplied calibrated at -20 Deg F and 75 Deg F

Shock test units to 10,000 g prior to final calibration

Vibration testing @ 40 g +/- 20 percent of natural frequency 3 sec/sweep for a total time of 15 minutes

Thermal testing @ 250 Deg F for 30 minutes and -40 Deg F for 30 minutes test to be repeated 8 times.

Unit body length to be .500 inches

Units to be supplied with 0-80 unf mounting holes with a center to center spacing of .270.

MINIATURE ACCELEROMETER, HI-OVERRANGE PROTECTED, PIEZORESISTIVE
FULL BRIDGE, DAMPED, WITH FLANGE MOUNTING.
ENTRAN DEVICES MODEL NO. EGAXT-48-F-10000/CERTIFIED

Accelerometer range +/- 10000 g

Overrange at approximately +/- 15000 g

Overrange in all three axes

Sensitivity .025 Mv/g nominal

Full scale output 250 Mv +/- 20 percent

Resonate frequency 12 KHz nominal

Nonlinearity +/- 1% of full scale

Transverse sensitivity +/- 3% max

Response at 75 Deg F flat to +/- .5 db from 20 Hz to 4.5 KHz minimal

Total unit response at 75 Deg F not to exceed +/- .5 db

Thermal and mechanical conditioning

Input impedance 1000 ohms nominal

Output impedance 450 ohms nominal

Excitation voltage 15 VDC

Case material 300 series stainless steel

Compensated temperature -20 Deg F to 100 Deg F

Operating temperature -40 Deg F to 250 Deg F

Compensation module located at 48 inches

Accelerometer to be supplied with 120 inch lead length

Unit to be flange mounted

Supplier to furnish requester with drawings of mounting configuration and manufactures specification for installation and torque values for mounting

Supplier will furnish accelerometers with unique identification numbers, which will be referenced to the supplier furnished calibrations

Units to be supplied with E5 type shielded cable

Units to be supplied calibrated at -20 Deg F and 74 Deg F

Shock test units to 10,000 g prior to final calibration

Vibration testing @ 40 g +/- 20 percent of natural frequency 3 sec/ sweep for a total time of 15 minutes

Thermal testing @ 250 Deg F for 30 minutes and -40 Deg F for 30 minutes test to be repeated 8 times

Unit body length to be .500 inches

Units to be supplied with 0-80 unf mounting holes with a center to center spacing of .270

ENDEVCO PRODUCT DATA

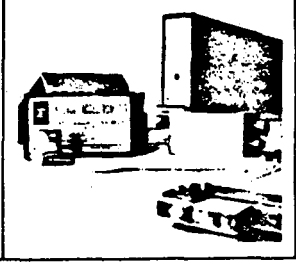

MODELS 2262-1000 2262C-1000

±1000 g Damped

PIEZORESISTIVE ACCELEROMETERS

The Models 2262-1000 and 2262C-1000 are rugged and damped accelerometers that measure static and dynamic acceleration. Endevco Piezite® Type P-9 piezoresistive elements are employed in a full bridge circuit to obtain a high level, low impedance output at ±1000 g full scale. The Model 2262C is a 6-wire device with a pair of fixed precision resistors in half the bridge, designed especially for shunt calibration.

The units will withstand up to 2.5 times their rated range without damage or calibration shift. The use of subcritical viscous damping extends their useful frequency range and reduces the effect of spurious, high frequency vibrations.

The broad frequency response from steady state to 2000 Hz makes these transducers ideal for measurement of transient type phenomena such as encountered in rocket engine ignitions, package testing, transportation shock, and automotive crash studies.

Sandia Stk 758710

SPECIFICATIONS FOR THE MODEL 2262-1000 AND 2262C-1000 ACCELEROMETERS

(According to ANSI and ISA Standards)

DYNAMIC

	Model 2262-1000	Model 2262C-1000
RANGE	± 1000 g	± 1000 g
SENSITIVITY	0.5 mV/g, nominal	0.25 mV/g, nominal
MOUNTED NATURAL FREQUENCY (at 75°F)	6000 Hz, nominal	6000 Hz, nominal
FREQUENCY RESPONSE[1]	± 5%, 0 to 2000 Hz, at 75°F; —35%/+ 10%, nominal, at 0°F/200°F and 2000 Hz, reference 75°F.	
DAMPING RATIO	0.7 nominal, at 75°F	
TRANSVERSE SENSITIVITY[2]	3% maximum	
THERMAL SENSITIVITY SHIFT	—2%/0/—4% nominal at 0°F/75°F/200°F	
LINEARITY AND HYSTERESIS	± 1% of reading, maximum, to ± 1000 g	

ELECTRICAL

EXCITATION[3]	10.0 Vdc	10.0 Vdc
INPUT RESISTANCE (at 75°F)	560Ω nominal	1000Ω nominal
OUTPUT RESISTANCE (at 75°F)	350Ω nominal	1000Ω nominal
INSULATION RESISTANCE[4]	100 MΩ minimum	100 MΩ minimum
ZERO MEASURAND OUTPUT	± 10 mV, maximum, at 10.0 Vdc and 75°F.	
THERMAL ZERO SHIFT	± 10 mV, maximum, at 0°F and 200°F, reference 75°F (24°C).	

NOTES

[1] Response is ±5%, 0 Hz to 250 Hz, over the temperature range of 0°F to 200°F.

[2] Worst case error in any axis perpendicular to sensitive axis. Selection of 1% is available on special order.

[3] Unit is calibrated at 10.0 Vdc. Lower excitation voltages may be employed, but should be specified at time of order to obtain best thermal compensation. Warmup time to meet all specifications is 1 minute. Endevco® Model 4470 Signal Conditioner is recommended as the excitation source.

[4] Measured with 100 Vdc, maximum, all leads to case. Cable shield common to case.

TYPICAL TEMPERATURE RESPONSE

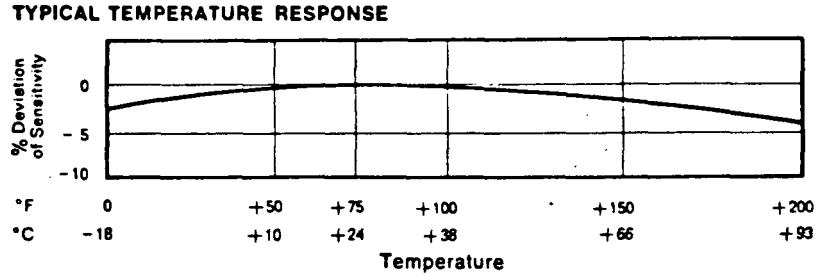

The curve shows the typical deviation of sensitivity with temperature.

SPECIFICATIONS FOR THE MODEL 2262-1000 AND 2262C-1000

WIRING DIAGRAM

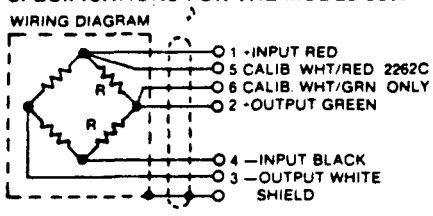

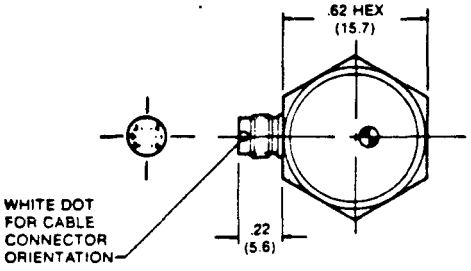

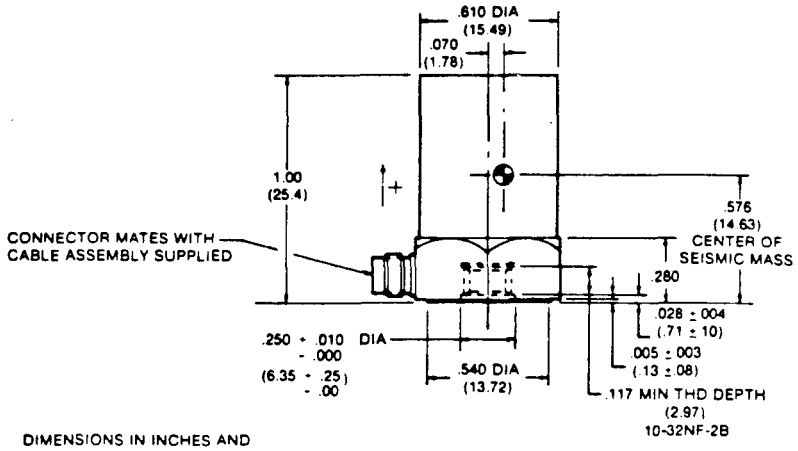

DIMENSIONS IN INCHES AND (MILLIMETERS)

TOLERANCES: .XX = ±0.03 (.8) .XXX = ± 0.010 (.25)

IN MODEL 2262C, R = 1000 Ω ±1%

PHYSICAL

WEIGHT	1 oz. (28 grams) nominal
CASE MATERIAL	Stainless Steel
SENSING ELEMENTS	Piezite® Type P-9
MOUNTING	Tapped hole for 10-32 x ⅛ in. stud. Recommended mounting torque: 18 lbf-in (2Nm)
ELECTRICAL CONNECTIONS	Integral six-pin connector
ACCESSORIES INCLUDED	Model 2981-3 (10-32) or 2981-4 (M5 metric) Mounting Stud.
	2262: Model 3022B-30 Cable Assembly, 30 inch, four conductor, shielded, with accelerometer mating connector.
	2262C: Model 3023B-30 Cable Assembly, 30 inch, six conductor, shielded, with accelerometer mating connector.

ENVIRONMENTAL

ACCELERATION LIMITS (in any direction)	Static:	2500 g
	Vibration:	1000 g pk sinusoidal
	Shock:	2500 g pk half sine pulse
TEMPERATURE	Compensated:	0°F to 200°F (-18°C to 93°C)
	Non-Operating:	-20°F to 220°F (-29°C to 104°C)
HUMIDITY		Hermetically sealed
BASE STRAIN SENSITIVITY		0.0002 equivalent g, nominal, per μ strain.

Continued product improvement necessitates that Endevco reserve the right to modify these specifications without notice.

RELIABILITY: Endevco maintains a program of constant surveillance over all products to ensure a high level of reliability. This program includes attention to reliability factors during product design, the support of stringent Quality Control requirements, and compulsory corrective action procedures. These measures, together with conservative specifications, have made the name Endevco synonymous with reliability.

CALIBRATION: Each unit is calibrated at room temperature for sensitivity, input resistance, output resistance, maximum transverse sensitivity, mounted natural frequency, and zero measurand output. Temperature response data taken during initial calibration is available on request. Shock and other calibrations are available on special order. See Calibration Bulletin No. 301.

Estimated calibration errors: 5-1000 Hz, ±1.5%; 1000-10 000 Hz, ±2.5%.

U.S. Patent No. 3,351,880 applies to this transducer.

ENDEVCO

RANCHO VIEJO ROAD · SAN JUAN CAPISTRANO, CA 92675 · TELEPHONE (714) 493-8181

ATLANTA GA • BALTIMORE MD • CHICAGO IL • DAYTON OH • E BRUNSWICK NJ • HOUSTON TX • LOS ANGELES CA • NASHUA NH • PALO ALTO CA • FRANCE • SWEDEN • UNITED KINGDOM
W GERMANY • AUSTRALIA • CANADA • FINLAND • INDIA • ITALY • JAPAN • MALAYSIA • MEXICO • NETHERLANDS • NORWAY • S AFRICA • SPAIN • SWITZERLAND • U S S R

TWX 910 596 1415 TELEX 68 5608 DIVISION OF BECTON DICKINSON AND COMPANY PRINTED IN USA 1/78

Appendix B

Analytical Input
for Finite Element Calculations

Finite Element Input
for Unyielding Target Analysis
into DYNA2D Code

```
 UNYIEELDING TARGET - REFINED MESH
ND  1  642  568    0    0    0    0                        0
    0    0    0    0    0    1    1    0    0    0    0    0
     0.001      1E-05      1E-05      1E-05    0 9000    0
    1    3  6.42E-04
 STAINLESS STEEL
 29E+06
 0.3
 30000.0
 300000.0
 0.5

    1    1 0.000E+00 0.000E+00    0
    2    1 0.000E+00 5.000E-01    0
    3    1 0.000E+00 1.000E+00    0
    4    1 0.000E+00 1.500E+00    0
    5    1 0.000E+00 2.000E+00    0
    6    0 6.250E-01 0.000E+00    0
    7    0 6.250E-01 5.000E-01    0
    8    0 6.250E-01 1.000E+00    0
    9    0 6.250E-01 1.500E+00    0
   10    0 6.250E-01 2.000E+00    0
   11    0 1.250E+00 0.000E+00    0
   12    0 1.250E+00 5.000E-01    0
   13    0 1.250E+00 1.000E+00    0
   14    0 1.250E+00 1.500E+00    0
   15    0 1.250E+00 2.000E+00    0
   16    0 1.875E+00 0.000E+00    0
   17    0 1.875E+00 5.000E-01    0
   18    0 1.875E+00 1.000E+00    0
   19    0 1.875E+00 1.500E+00    0
   20    0 1.875E+00 2.000E+00    0
   21    0 2.500E+00 0.000E+00    0
   22    0 2.500E+00 5.000E-01    0
   23    0 2.500E+00 1.000E+00    0
   24    0 2.500E+00 1.500E+00    0
   25    0 2.500E+00 2.000E+00    0
   26    0 3.125E+00 0.000E+00    0
   27    0 3.125E+00 5.000E-01    0
   28    0 3.125E+00 1.000E+00    0
   29    0 3.125E+00 1.500E+00    0
   30    0 3.125E+00 2.000E+00    0
   31    0 3.750E+00 0.000E+00    0
   32    0 3.750E+00 5.000E-01    0
```

```
33    0 3.750E+00 1.000E+00    0
34    0 3.750E+00 1.500E+00    0
35    0 3.750E+00 2.000E+00    0
36    0 4.375E+00 0.000E+00    0
37    0 4.375E+00 5.000E-01    0
38    0 4.375E+00 1.000E+00    0
39    0 4.375E+00 1.500E+00    0
40    0 4.375E+00 2.000E+00    0
41    0 5.000E+00 0.000E+00    0
42    0 5.000E+00 5.000E-01    0
43    0 5.000E+00 1.000E+00    0
44    0 5.000E+00 1.500E+00    0
45    0 5.000E+00 2.000E+00    0
46    0 5.625E+00 0.000E+00    0
47    0 5.625E+00 5.000E-01    0
48    0 5.625E+00 1.000E+00    0
49    0 5.625E+00 1.500E+00    0
50    0 5.625E+00 2.000E+00    0
51    0 6.250E+00 0.000E+00    0
52    0 6.250E+00 5.000E-01    0
53    0 6.250E+00 1.000E+00    0
54    0 6.250E+00 1.500E+00    0
55    0 6.250E+00 2.000E+00    0
56    0 6.875E+00 0.000E+00    0
57    0 6.875E+00 5.000E-01    0
58    0 6.875E+00 1.000E+00    0
59    0 6.875E+00 1.500E+00    0
60    0 6.875E+00 2.000E+00    0
61    0 7.500E+00 0.000E+00    0
62    0 7.500E+00 5.000E-01    0
63    0 7.500E+00 1.000E+00    0
64    0 7.500E+00 1.500E+00    0
65    0 7.500E+00 2.000E+00    0
66    0 8.125E+00 0.000E+00    0
67    0 8.125E+00 5.000E-01    0
68    0 8.125E+00 1.000E+00    0
69    0 8.125E+00 1.500E+00    0
70    0 8.125E+00 2.000E+00    0
71    0 8.750E+00 0.000E+00    0
72    0 8.750E+00 5.000E-01    0
73    0 8.750E+00 1.000E+00    0
74    0 8.750E+00 1.500E+00    0
75    0 8.750E+00 2.000E+00    0
76    0 9.375E+00 0.000E+00    0
```

77	0	9.375E+00	5.000E-01	0
78	0	9.375E+00	1.000E+00	0
79	0	9.375E+00	1.500E+00	0
80	0	9.375E+00	2.000E+00	0
81	0	1.000E+01	0.000E+00	0
82	0	1.000E+01	5.000E-01	0
83	0	1.000E+01	1.000E+00	0
84	0	1.000E+01	1.500E+00	0
85	0	1.000E+01	2.000E+00	0
86	1	0.000E+00	2.500E+00	0
87	1	0.000E+00	3.000E+00	0
88	1	0.000E+00	3.500E+00	0
89	1	0.000E+00	4.000E+00	0
90	0	6.250E-01	2.500E+00	0
91	0	6.250E-01	3.000E+00	0
92	0	6.250E-01	3.500E+00	0
93	0	6.250E-01	4.000E+00	0
94	0	1.250E+00	2.500E+00	0
95	0	1.250E+00	3.000E+00	0
96	0	1.250E+00	3.500E+00	0
97	0	1.250E+00	4.000E+00	0
98	0	1.875E+00	2.500E+00	0
99	0	1.875E+00	3.000E+00	0
100	0	1.875E+00	3.500E+00	0
101	0	1.875E+00	4.000E+00	0
102	0	2.500E+00	2.500E+00	0
103	0	2.500E+00	3.000E+00	0
104	0	2.500E+00	3.500E+00	0
105	0	2.500E+00	4.000E+00	0
106	0	3.125E+00	2.500E+00	0
107	0	3.125E+00	3.000E+00	0
108	0	3.125E+00	3.500E+00	0
109	0	3.125E+00	4.000E+00	0
110	0	3.750E+00	2.500E+00	0
111	0	3.750E+00	3.000E+00	0
112	0	3.750E+00	3.500E+00	0
113	0	3.750E+00	4.000E+00	0
114	0	4.375E+00	2.500E+00	0
115	0	4.375E+00	3.000E+00	0
116	0	4.375E+00	3.500E+00	0
117	0	4.375E+00	4.000E+00	0
118	0	5.000E+00	2.500E+00	0
119	0	5.000E+00	3.000E+00	0
120	0	5.000E+00	3.500E+00	0

121	0	5.000E+00	4.000E+00	0
122	0	5.625E+00	2.500E+00	0
123	0	5.625E+00	3.000E+00	0
124	0	5.625E+00	3.500E+00	0
125	0	5.625E+00	4.000E+00	0
126	0	6.250E+00	2.500E+00	0
127	0	6.250E+00	3.000E+00	0
128	0	6.250E+00	3.500E+00	0
129	0	6.250E+00	4.000E+00	0
130	0	8.750E+00	2.500E+00	0
131	0	9.375E+00	2.500E+00	0
132	0	1.000E+01	2.500E+00	0
133	0	8.750E+00	3.000E+00	0
134	0	9.375E+00	3.000E+00	0
135	0	1.000E+01	3.000E+00	0
136	0	8.750E+00	3.500E+00	0
137	0	9.375E+00	3.500E+00	0
138	0	1.000E+01	3.500E+00	0
139	0	8.750E+00	4.000E+00	0
140	0	9.375E+00	4.000E+00	0
141	0	1.000E+01	4.000E+00	0
142	0	6.875E+00	4.000E+00	0
143	0	7.500E+00	4.000E+00	0
144	0	8.125E+00	4.000E+00	0
145	1	0.000E+00	4.625E+00	0
146	0	6.250E-01	4.625E+00	0
147	0	1.250E+00	4.625E+00	0
148	0	1.875E+00	4.625E+00	0
149	0	2.500E+00	4.625E+00	0
150	0	3.125E+00	4.625E+00	0
151	0	3.750E+00	4.625E+00	0
152	0	4.375E+00	4.625E+00	0
153	0	5.000E+00	4.625E+00	0
154	0	5.625E+00	4.625E+00	0
155	0	6.250E+00	4.625E+00	0
156	0	6.875E+00	4.625E+00	0
157	0	7.500E+00	4.625E+00	0
158	0	8.125E+00	4.625E+00	0
159	0	8.750E+00	4.625E+00	0
160	0	9.375E+00	4.625E+00	0
161	0	1.000E+01	4.625E+00	0
162	1	0.000E+00	5.250E+00	0
163	0	6.250E-01	5.250E+00	0
164	0	1.250E+00	5.250E+00	0

165	0	1.875E+00	5.250E+00	0
166	0	2.500E+00	5.250E+00	0
167	0	3.125E+00	5.250E+00	0
168	0	3.750E+00	5.250E+00	0
169	0	4.375E+00	5.250E+00	0
170	0	5.000E+00	5.250E+00	0
171	0	5.625E+00	5.250E+00	0
172	0	6.250E+00	5.250E+00	0
173	0	6.875E+00	5.250E+00	0
174	0	7.500E+00	5.250E+00	0
175	0	8.125E+00	5.250E+00	0
176	0	8.750E+00	5.250E+00	0
177	0	9.375E+00	5.250E+00	0
178	0	1.000E+01	5.250E+00	0
179	1	0.000E+00	5.875E+00	0
180	0	6.250E-01	5.875E+00	0
181	0	1.250E+00	5.875E+00	0
182	0	1.875E+00	5.875E+00	0
183	0	2.500E+00	5.875E+00	0
184	0	3.125E+00	5.875E+00	0
185	0	3.750E+00	5.875E+00	0
186	0	4.375E+00	5.875E+00	0
187	0	5.000E+00	5.875E+00	0
188	0	5.625E+00	5.875E+00	0
189	0	6.250E+00	5.875E+00	0
190	0	6.875E+00	5.875E+00	0
191	0	7.500E+00	5.875E+00	0
192	0	8.125E+00	5.875E+00	0
193	0	8.750E+00	5.875E+00	0
194	0	9.375E+00	5.875E+00	0
195	0	1.000E+01	5.875E+00	0
196	1	0.000E+00	6.500E+00	0
197	0	6.250E-01	6.500E+00	0
198	0	1.250E+00	6.500E+00	0
199	0	1.875E+00	6.500E+00	0
200	0	2.500E+00	6.500E+00	0
201	0	3.125E+00	6.500E+00	0
202	0	3.750E+00	6.500E+00	0
203	0	4.375E+00	6.500E+00	0
204	0	5.000E+00	6.500E+00	0
205	0	5.625E+00	6.500E+00	0
206	0	6.250E+00	6.500E+00	0
207	0	6.875E+00	6.500E+00	0
208	0	7.500E+00	6.500E+00	0

209	0	8.125E+00	6.500E+00	0
210	0	8.750E+00	6.500E+00	0
211	0	9.375E+00	6.500E+00	0
212	0	1.000E+01	6.500E+00	0
213	1	0.000E+00	7.125E+00	0
214	0	6.250E-01	7.125E+00	0
215	0	1.250E+00	7.125E+00	0
216	0	1.875E+00	7.125E+00	0
217	0	2.500E+00	7.125E+00	0
218	0	3.125E+00	7.125E+00	0
219	0	3.750E+00	7.125E+00	0
220	0	4.375E+00	7.125E+00	0
221	0	5.000E+00	7.125E+00	0
222	0	5.625E+00	7.125E+00	0
223	0	6.250E+00	7.125E+00	0
224	0	6.875E+00	7.125E+00	0
225	0	7.500E+00	7.125E+00	0
226	0	8.125E+00	7.125E+00	0
227	0	8.750E+00	7.125E+00	0
228	0	9.375E+00	7.125E+00	0
229	0	1.000E+01	7.125E+00	0
230	1	0.000E+00	7.750E+00	0
231	0	6.250E-01	7.750E+00	0
232	0	1.250E+00	7.750E+00	0
233	0	1.875E+00	7.750E+00	0
234	0	2.500E+00	7.750E+00	0
235	0	3.125E+00	7.750E+00	0
236	0	3.750E+00	7.750E+00	0
237	0	4.375E+00	7.750E+00	0
238	0	5.000E+00	7.750E+00	0
239	0	5.625E+00	7.750E+00	0
240	0	6.250E+00	7.750E+00	0
241	0	6.875E+00	7.750E+00	0
242	0	7.500E+00	7.750E+00	0
243	0	8.125E+00	7.750E+00	0
244	0	8.750E+00	7.750E+00	0
245	0	9.375E+00	7.750E+00	0
246	0	1.000E+01	7.750E+00	0
247	1	0.000E+00	8.375E+00	0
248	0	6.250E-01	8.375E+00	0
249	0	1.250E+00	8.375E+00	0
250	0	1.875E+00	8.375E+00	0
251	0	2.500E+00	8.375E+00	0
252	0	3.125E+00	8.375E+00	0

253	0	3.750E+00	8.375E+00	0
254	0	4.375E+00	8.375E+00	0
255	0	5.000E+00	8.375E+00	0
256	0	5.625E+00	8.375E+00	0
257	0	6.250E+00	8.375E+00	0
258	0	6.875E+00	8.375E+00	0
259	0	7.500E+00	8.375E+00	0
260	0	8.125E+00	8.375E+00	0
261	0	8.750E+00	8.375E+00	0
262	0	9.375E+00	8.375E+00	0
263	0	1.000E+01	8.375E+00	0
264	1	0.000E+00	9.000E+00	0
265	0	6.250E-01	9.000E+00	0
266	0	1.250E+00	9.000E+00	0
267	0	1.875E+00	9.000E+00	0
268	0	2.500E+00	9.000E+00	0
269	0	3.125E+00	9.000E+00	0
270	0	3.750E+00	9.000E+00	0
271	0	4.375E+00	9.000E+00	0
272	0	5.000E+00	9.000E+00	0
273	0	5.625E+00	9.000E+00	0
274	0	6.250E+00	9.000E+00	0
275	0	6.875E+00	9.000E+00	0
276	0	7.500E+00	9.000E+00	0
277	0	8.125E+00	9.000E+00	0
278	0	8.750E+00	9.000E+00	0
279	0	9.375E+00	9.000E+00	0
280	0	1.000E+01	9.000E+00	0
281	1	0.000E+00	9.625E+00	0
282	0	6.250E-01	9.625E+00	0
283	0	1.250E+00	9.625E+00	0
284	0	1.875E+00	9.625E+00	0
285	0	2.500E+00	9.625E+00	0
286	0	3.125E+00	9.625E+00	0
287	0	3.750E+00	9.625E+00	0
288	0	4.375E+00	9.625E+00	0
289	0	5.000E+00	9.625E+00	0
290	0	5.625E+00	9.625E+00	0
291	0	6.250E+00	9.625E+00	0
292	0	6.875E+00	9.625E+00	0
293	0	7.500E+00	9.625E+00	0
294	0	8.125E+00	9.625E+00	0
295	0	8.750E+00	9.625E+00	0
296	0	9.375E+00	9.625E+00	0

297	0	1.000E+01	9.625E+00	0
298	1	0.000E+00	1.025E+01	0
299	0	6.250E-01	1.025E+01	0
300	0	1.250E+00	1.025E+01	0
301	0	1.875E+00	1.025E+01	0
302	0	2.500E+00	1.025E+01	0
303	0	3.125E+00	1.025E+01	0
304	0	3.750E+00	1.025E+01	0
305	0	4.375E+00	1.025E+01	0
306	0	5.000E+00	1.025E+01	0
307	0	5.625E+00	1.025E+01	0
308	0	6.250E+00	1.025E+01	0
309	0	6.875E+00	1.025E+01	0
310	0	7.500E+00	1.025E+01	0
311	0	8.125E+00	1.025E+01	0
312	0	8.750E+00	1.025E+01	0
313	0	9.375E+00	1.025E+01	0
314	0	1.000E+01	1.025E+01	0
315	1	0.000E+00	1.088E+01	0
316	0	6.250E-01	1.088E+01	0
317	0	1.250E+00	1.088E+01	0
318	0	1.875E+00	1.088E+01	0
319	0	2.500E+00	1.088E+01	0
320	0	3.125E+00	1.088E+01	0
321	0	3.750E+00	1.088E+01	0
322	0	4.375E+00	1.088E+01	0
323	0	5.000E+00	1.088E+01	0
324	0	5.625E+00	1.088E+01	0
325	0	6.250E+00	1.088E+01	0
326	0	6.875E+00	1.088E+01	0
327	0	7.500E+00	1.088E+01	0
328	0	8.125E+00	1.088E+01	0
329	0	8.750E+00	1.088E+01	0
330	0	9.375E+00	1.088E+01	0
331	0	1.000E+01	1.088E+01	0
332	1	0.000E+00	1.150E+01	0
333	0	6.250E-01	1.150E+01	0
334	0	1.250E+00	1.150E+01	0
335	0	1.875E+00	1.150E+01	0
336	0	2.500E+00	1.150E+01	0
337	0	3.125E+00	1.150E+01	0
338	0	3.750E+00	1.150E+01	0
339	0	4.375E+00	1.150E+01	0
340	0	5.000E+00	1.150E+01	0

341	0	5.625E+00	1.150E+01	0
342	0	6.250E+00	1.150E+01	0
343	0	6.875E+00	1.150E+01	0
344	0	7.500E+00	1.150E+01	0
345	0	8.125E+00	1.150E+01	0
346	0	8.750E+00	1.150E+01	0
347	0	9.375E+00	1.150E+01	0
348	0	1.000E+01	1.150E+01	0
349	1	0.000E+00	1.213E+01	0
350	0	6.250E-01	1.213E+01	0
351	0	1.250E+00	1.213E+01	0
352	0	1.875E+00	1.213E+01	0
353	0	2.500E+00	1.213E+01	0
354	0	3.125E+00	1.213E+01	0
355	0	3.750E+00	1.213E+01	0
356	0	4.375E+00	1.213E+01	0
357	0	5.000E+00	1.213E+01	0
358	0	5.625E+00	1.213E+01	0
359	0	6.250E+00	1.213E+01	0
360	0	6.875E+00	1.213E+01	0
361	0	7.500E+00	1.213E+01	0
362	0	8.125E+00	1.213E+01	0
363	0	8.750E+00	1.213E+01	0
364	0	9.375E+00	1.213E+01	0
365	0	1.000E+01	1.213E+01	0
366	1	0.000E+00	1.275E+01	0
367	0	6.250E-01	1.275E+01	0
368	0	1.250E+00	1.275E+01	0
369	0	1.875E+00	1.275E+01	0
370	0	2.500E+00	1.275E+01	0
371	0	3.125E+00	1.275E+01	0
372	0	3.750E+00	1.275E+01	0
373	0	4.375E+00	1.275E+01	0
374	0	5.000E+00	1.275E+01	0
375	0	5.625E+00	1.275E+01	0
376	0	6.250E+00	1.275E+01	0
377	0	6.875E+00	1.275E+01	0
378	0	7.500E+00	1.275E+01	0
379	0	8.125E+00	1.275E+01	0
380	0	8.750E+00	1.275E+01	0
381	0	9.375E+00	1.275E+01	0
382	0	1.000E+01	1.275E+01	0
383	1	0.000E+00	1.338E+01	0
384	0	6.250E-01	1.338E+01	0

385	0	1.250E+00	1.338E+01	0
386	0	1.875E+00	1.338E+01	0
387	0	2.500E+00	1.338E+01	0
388	0	3.125E+00	1.338E+01	0
389	0	3.750E+00	1.338E+01	0
390	0	4.375E+00	1.338E+01	0
391	0	5.000E+00	1.338E+01	0
392	0	5.625E+00	1.338E+01	0
393	0	6.250E+00	1.338E+01	0
394	0	6.875E+00	1.338E+01	0
395	0	7.500E+00	1.338E+01	0
396	0	8.125E+00	1.338E+01	0
397	0	8.750E+00	1.338E+01	0
398	0	9.375E+00	1.338E+01	0
399	0	1.000E+01	1.338E+01	0
400	1	0.000E+00	1.400E+01	0
401	0	6.250E-01	1.400E+01	0
402	0	1.250E+00	1.400E+01	0
403	0	1.875E+00	1.400E+01	0
404	0	2.500E+00	1.400E+01	0
405	0	3.125E+00	1.400E+01	0
406	0	3.750E+00	1.400E+01	0
407	0	4.375E+00	1.400E+01	0
408	0	5.000E+00	1.400E+01	0
409	0	5.625E+00	1.400E+01	0
410	0	6.250E+00	1.400E+01	0
411	0	6.875E+00	1.400E+01	0
412	0	7.500E+00	1.400E+01	0
413	0	8.125E+00	1.400E+01	0
414	0	8.750E+00	1.400E+01	0
415	0	9.375E+00	1.400E+01	0
416	0	1.000E+01	1.400E+01	0
417	0	6.250E-01	1.463E+01	0
418	0	1.250E+00	1.463E+01	0
419	0	1.875E+00	1.463E+01	0
420	0	3.125E+00	1.463E+01	0
421	0	3.750E+00	1.463E+01	0
422	0	4.375E+00	1.463E+01	0
423	0	5.625E+00	1.463E+01	0
424	0	6.250E+00	1.463E+01	0
425	0	6.875E+00	1.463E+01	0
426	0	8.125E+00	1.463E+01	0
427	0	8.750E+00	1.463E+01	0
428	0	9.375E+00	1.463E+01	0

```
429     1 0.000E+00 1.525E+01     0
430     0 1.250E+00 1.525E+01     0
431     0 2.500E+00 1.525E+01     0
432     0 3.750E+00 1.525E+01     0
433     0 5.000E+00 1.525E+01     0
434     0 6.250E+00 1.525E+01     0
435     0 7.500E+00 1.525E+01     0
436     0 8.750E+00 1.525E+01     0
437     0 1.000E+01 1.525E+01     0
438     1 0.000E+00 1.650E+01     0
439     0 1.250E+00 1.650E+01     0
440     0 2.500E+00 1.650E+01     0
441     0 3.750E+00 1.650E+01     0
442     0 5.000E+00 1.650E+01     0
443     0 6.250E+00 1.650E+01     0
444     0 7.500E+00 1.650E+01     0
445     0 8.750E+00 1.650E+01     0
446     0 1.000E+01 1.650E+01     0
447     1 0.000E+00 1.775E+01     0
448     0 1.250E+00 1.775E+01     0
449     0 2.500E+00 1.775E+01     0
450     0 3.750E+00 1.775E+01     0
451     0 5.000E+00 1.775E+01     0
452     0 6.250E+00 1.775E+01     0
453     0 7.500E+00 1.775E+01     0
454     0 8.750E+00 1.775E+01     0
455     0 1.000E+01 1.775E+01     0
456     1 0.000E+00 1.900E+01     0
457     0 1.250E+00 1.900E+01     0
458     0 2.500E+00 1.900E+01     0
459     0 3.750E+00 1.900E+01     0
460     0 5.000E+00 1.900E+01     0
461     0 6.250E+00 1.900E+01     0
462     0 7.500E+00 1.900E+01     0
463     0 8.750E+00 1.900E+01     0
464     0 1.000E+01 1.900E+01     0
465     1 0.000E+00 2.025E+01     0
466     0 1.250E+00 2.025E+01     0
467     0 2.500E+00 2.025E+01     0
468     0 3.750E+00 2.025E+01     0
469     0 5.000E+00 2.025E+01     0
470     0 6.250E+00 2.025E+01     0
471     0 7.500E+00 2.025E+01     0
472     0 8.750E+00 2.025E+01     0
```

473	0	1.000E+01	2.025E+01	0
474	1	0.000E+00	2.150E+01	0
475	0	1.250E+00	2.150E+01	0
476	0	2.500E+00	2.150E+01	0
477	0	3.750E+00	2.150E+01	0
478	0	5.000E+00	2.150E+01	0
479	0	6.250E+00	2.150E+01	0
480	0	7.500E+00	2.150E+01	0
481	0	8.750E+00	2.150E+01	0
482	0	1.000E+01	2.150E+01	0
483	1	0.000E+00	2.275E+01	0
484	0	1.250E+00	2.275E+01	0
485	0	2.500E+00	2.275E+01	0
486	0	3.750E+00	2.275E+01	0
487	0	5.000E+00	2.275E+01	0
488	0	6.250E+00	2.275E+01	0
489	0	7.500E+00	2.275E+01	0
490	0	8.750E+00	2.275E+01	0
491	0	1.000E+01	2.275E+01	0
492	1	0.000E+00	2.400E+01	0
493	0	1.250E+00	2.400E+01	0
494	0	2.500E+00	2.400E+01	0
495	0	3.750E+00	2.400E+01	0
496	0	5.000E+00	2.400E+01	0
497	0	6.250E+00	2.400E+01	0
498	0	7.500E+00	2.400E+01	0
499	0	8.750E+00	2.400E+01	0
500	0	1.000E+01	2.400E+01	0
501	1	0.000E+00	2.525E+01	0
502	0	1.250E+00	2.525E+01	0
503	0	2.500E+00	2.525E+01	0
504	0	3.750E+00	2.525E+01	0
505	0	5.000E+00	2.525E+01	0
506	0	6.250E+00	2.525E+01	0
507	0	7.500E+00	2.525E+01	0
508	0	8.750E+00	2.525E+01	0
509	0	1.000E+01	2.525E+01	0
510	1	0.000E+00	2.650E+01	0
511	0	1.250E+00	2.650E+01	0
512	0	2.500E+00	2.650E+01	0
513	0	3.750E+00	2.650E+01	0
514	0	5.000E+00	2.650E+01	0
515	0	6.250E+00	2.650E+01	0
516	0	7.500E+00	2.650E+01	0

517	0	8.750E+00	2.650E+01	0
518	0	1.000E+01	2.650E+01	0
519	1	0.000E+00	2.775E+01	0
520	0	1.250E+00	2.775E+01	0
521	0	2.500E+00	2.775E+01	0
522	0	3.750E+00	2.775E+01	0
523	0	5.000E+00	2.775E+01	0
524	0	6.250E+00	2.775E+01	0
525	0	7.500E+00	2.775E+01	0
526	0	8.750E+00	2.775E+01	0
527	0	1.000E+01	2.775E+01	0
528	1	0.000E+00	2.900E+01	0
529	0	1.250E+00	2.900E+01	0
530	0	2.500E+00	2.900E+01	0
531	0	3.750E+00	2.900E+01	0
532	0	5.000E+00	2.900E+01	0
533	0	6.250E+00	2.900E+01	0
534	0	7.500E+00	2.900E+01	0
535	0	8.750E+00	2.900E+01	0
536	0	1.000E+01	2.900E+01	0
537	1	0.000E+00	3.025E+01	0
538	0	1.250E+00	3.025E+01	0
539	0	2.500E+00	3.025E+01	0
540	0	3.750E+00	3.025E+01	0
541	0	5.000E+00	3.025E+01	0
542	0	6.250E+00	3.025E+01	0
543	0	7.500E+00	3.025E+01	0
544	0	8.750E+00	3.025E+01	0
545	0	1.000E+01	3.025E+01	0
546	1	0.000E+00	3.150E+01	0
547	0	1.250E+00	3.150E+01	0
548	0	2.500E+00	3.150E+01	0
549	0	3.750E+00	3.150E+01	0
550	0	5.000E+00	3.150E+01	0
551	0	6.250E+00	3.150E+01	0
552	0	7.500E+00	3.150E+01	0
553	0	8.750E+00	3.150E+01	0
554	0	1.000E+01	3.150E+01	0
555	1	0.000E+00	3.275E+01	0
556	0	1.250E+00	3.275E+01	0
557	0	2.500E+00	3.275E+01	0
558	0	3.750E+00	3.275E+01	0
559	0	5.000E+00	3.275E+01	0
560	0	6.250E+00	3.275E+01	0

561	0	7.500E+00	3.275E+01	0
562	0	8.750E+00	3.275E+01	0
563	0	1.000E+01	3.275E+01	0
564	1	0.000E+00	3.400E+01	0
565	0	1.250E+00	3.400E+01	0
566	0	2.500E+00	3.400E+01	0
567	0	3.750E+00	3.400E+01	0
568	0	5.000E+00	3.400E+01	0
569	0	6.250E+00	3.400E+01	0
570	0	7.500E+00	3.400E+01	0
571	0	8.750E+00	3.400E+01	0
572	0	1.000E+01	3.400E+01	0
573	0	1.250E+00	3.613E+01	0
574	0	2.500E+00	3.613E+01	0
575	0	3.750E+00	3.613E+01	0
576	0	6.250E+00	3.613E+01	0
577	0	7.500E+00	3.613E+01	0
578	0	8.750E+00	3.613E+01	0
579	1	0.000E+00	3.825E+01	0
580	0	2.500E+00	3.825E+01	0
581	0	5.000E+00	3.825E+01	0
582	0	7.500E+00	3.825E+01	0
583	0	1.000E+01	3.825E+01	0
584	1	0.000E+00	4.250E+01	0
585	0	2.500E+00	4.250E+01	0
586	0	5.000E+00	4.250E+01	0
587	0	7.500E+00	4.250E+01	0
588	0	1.000E+01	4.250E+01	0
589	1	0.000E+00	4.675E+01	0
590	0	2.500E+00	4.675E+01	0
591	0	5.000E+00	4.675E+01	0
592	0	7.500E+00	4.675E+01	0
593	0	1.000E+01	4.675E+01	0
594	1	0.000E+00	5.100E+01	0
595	0	2.500E+00	5.100E+01	0
596	0	5.000E+00	5.100E+01	0
597	0	7.500E+00	5.100E+01	0
598	0	1.000E+01	5.100E+01	0
599	1	0.000E+00	5.525E+01	0
600	0	2.500E+00	5.525E+01	0
601	0	5.000E+00	5.525E+01	0
602	0	7.500E+00	5.525E+01	0
603	0	1.000E+01	5.525E+01	0
604	1	0.000E+00	5.950E+01	0

561	0	7.500E+00	3.275E+01	0
562	0	8.750E+00	3.275E+01	0
563	0	1.000E+01	3.275E+01	0
564	1	0.000E+00	3.400E+01	0
565	0	1.250E+00	3.400E+01	0
566	0	2.500E+00	3.400E+01	0
567	0	3.750E+00	3.400E+01	0
568	0	5.000E+00	3.400E+01	0
569	0	6.250E+00	3.400E+01	0
570	0	7.500E+00	3.400E+01	0
571	0	8.750E+00	3.400E+01	0
572	0	1.000E+01	3.400E+01	0
573	0	1.250E+00	3.613E+01	0
574	0	2.500E+00	3.613E+01	0
575	0	3.750E+00	3.613E+01	0
576	0	6.250E+00	3.613E+01	0
577	0	7.500E+00	3.613E+01	0
578	0	8.750E+00	3.613E+01	0
579	1	0.000E+00	3.825E+01	0
580	0	2.500E+00	3.825E+01	0
581	0	5.000E+00	3.825E+01	0
582	0	7.500E+00	3.825E+01	0
583	0	1.000E+01	3.825E+01	0
584	1	0.000E+00	4.250E+01	0
585	0	2.500E+00	4.250E+01	0
586	0	5.000E+00	4.250E+01	0
587	0	7.500E+00	4.250E+01	0
588	0	1.000E+01	4.250E+01	0
589	1	0.000E+00	4.675E+01	0
590	0	2.500E+00	4.675E+01	0
591	0	5.000E+00	4.675E+01	0
592	0	7.500E+00	4.675E+01	0
593	0	1.000E+01	4.675E+01	0
594	1	0.000E+00	5.100E+01	0
595	0	2.500E+00	5.100E+01	0
596	0	5.000E+00	5.100E+01	0
597	0	7.500E+00	5.100E+01	0
598	0	1.000E+01	5.100E+01	0
599	1	0.000E+00	5.525E+01	0
600	0	2.500E+00	5.525E+01	0
601	0	5.000E+00	5.525E+01	0
602	0	7.500E+00	5.525E+01	0
603	0	1.000E+01	5.525E+01	0
604	1	0.000E+00	5.950E+01	0

```
605     0 2.500E+00 5.950E+01     0
606     0 5.000E+00 5.950E+01     0
607     0 7.500E+00 5.950E+01     0
608     0 1.000E+01 5.950E+01     0
609     1 0.000E+00 6.375E+01     0
610     0 2.500E+00 6.375E+01     0
611     0 5.000E+00 6.375E+01     0
612     0 7.500E+00 6.375E+01     0
613     0 1.000E+01 6.375E+01     0
614     1 0.000E+00 6.800E+01     0
615     0 2.500E+00 6.800E+01     0
616     0 5.000E+00 6.800E+01     0
617     0 7.500E+00 6.800E+01     0
618     0 1.000E+01 6.800E+01     0
619     0 8.750E+00 6.588E+01     0
620     0 1.000E+01 6.588E+01     0
621     0 8.750E+00 6.800E+01     0
622     0 7.500E+00 6.900E+01     0
623     0 8.750E+00 6.900E+01     0
624     0 1.000E+01 6.900E+01     0
625     0 7.500E+00 7.000E+01     0
626     0 8.750E+00 7.000E+01     0
627     0 1.000E+01 7.000E+01     0
628     1 0.000E+00 7.000E+01     0
629     1 0.000E+00 7.100E+01     0
630     1 0.000E+00 7.200E+01     0
631     0 2.500E+00 7.000E+01     0
632     0 2.500E+00 7.100E+01     0
633     0 2.500E+00 7.200E+01     0
634     0 5.000E+00 7.000E+01     0
635     0 5.000E+00 7.100E+01     0
636     0 5.000E+00 7.200E+01     0
637     0 7.500E+00 7.100E+01     0
638     0 7.500E+00 7.200E+01     0
639     0 8.750E+00 7.050E+01     0
640     0 1.000E+01 7.050E+01     0
641     0 1.000E+01 7.100E+01     0
642     0 1.000E+01 7.200E+01     0
  1     1     6     7     2     1
  2     6    11    12     7     1
  3    11    16    17    12     1
  4    16    21    22    17     1
  5    21    26    27    22     1
  6    26    31    32    27     1
```

7	31	36	37	32	1
8	36	41	42	37	1
9	41	46	47	42	1
10	46	51	52	47	1
11	51	56	57	52	1
12	56	61	62	57	1
13	61	66	67	62	1
14	66	71	72	67	1
15	71	76	77	72	1
16	76	81	82	77	1
17	2	7	8	3	1
18	7	12	13	8	1
19	12	17	18	13	1
20	17	22	23	18	1
21	22	27	28	23	1
22	27	32	33	28	1
23	32	37	38	33	1
24	37	42	43	38	1
25	42	47	48	43	1
26	47	52	53	48	1
27	52	57	58	53	1
28	57	62	63	58	1
29	62	67	68	63	1
30	67	72	73	68	1
31	72	77	78	73	1
32	77	82	83	78	1
33	3	8	9	4	1
34	8	13	14	9	1
35	13	18	19	14	1
36	18	23	24	19	1
37	23	28	29	24	1
38	28	33	34	29	1
39	33	38	39	34	1
40	38	43	44	39	1
41	43	48	49	44	1
42	48	53	54	49	1
43	53	58	59	54	1
44	58	63	64	59	1
45	63	68	69	64	1
46	68	73	74	69	1
47	73	78	79	74	1
48	78	83	84	79	1
49	4	9	10	5	1
50	9	14	15	10	1

51	14	19	20	15	1
52	19	24	25	20	1
53	24	29	30	25	1
54	29	34	35	30	1
55	34	39	40	35	1
56	39	44	45	40	1
57	44	49	50	45	1
58	49	54	55	50	1
59	54	59	60	55	1
60	59	64	65	60	1
61	64	69	70	65	1
62	69	74	75	70	1
63	74	79	80	75	1
64	79	84	85	80	1
65	5	10	90	86	1
66	10	15	94	90	1
67	15	20	98	94	1
68	20	25	102	98	1
69	25	30	106	102	1
70	30	35	110	106	1
71	35	40	114	110	1
72	40	45	118	114	1
73	45	50	122	118	1
74	50	55	126	122	1
75	86	90	91	87	1
76	90	94	95	91	1
77	94	98	99	95	1
78	98	102	103	99	1
79	102	106	107	103	1
80	106	110	111	107	1
81	110	114	115	111	1
82	114	118	119	115	1
83	118	122	123	119	1
84	122	126	127	123	1
85	87	91	92	88	1
86	91	95	96	92	1
87	95	99	100	96	1
88	99	103	104	100	1
89	103	107	108	104	1
90	107	111	112	108	1
91	111	115	116	112	1
92	115	119	120	116	1
93	119	123	124	120	1
94	123	127	128	124	1

95	88	92	93	89	1
96	92	96	97	93	1
97	96	100	101	97	1
98	100	104	105	101	1
99	104	108	109	105	1
100	108	112	113	109	1
101	112	116	117	113	1
102	116	120	121	117	1
103	120	124	125	121	1
104	124	128	129	125	1
105	75	80	131	130	1
106	80	85	132	131	1
107	130	131	134	133	1
108	131	132	135	134	1
109	133	134	137	136	1
110	134	135	138	137	1
111	136	137	140	139	1
112	137	138	141	140	1
113	89	93	146	145	1
114	93	97	147	146	1
115	97	101	148	147	1
116	101	105	149	148	1
117	105	109	150	149	1
118	109	113	151	150	1
119	113	117	152	151	1
120	117	121	153	152	1
121	121	125	154	153	1
122	125	129	155	154	1
123	129	142	156	155	1
124	142	143	157	156	1
125	143	144	158	157	1
126	144	139	159	158	1
127	139	140	160	159	1
128	140	141	161	160	1
129	145	146	163	162	1
130	146	147	164	163	1
131	147	148	165	164	1
132	148	149	166	165	1
133	149	150	167	166	1
134	150	151	168	167	1
135	151	152	169	168	1
136	152	153	170	169	1
137	153	154	171	170	1
138	154	155	172	171	1

139	155	156	173	172	1
140	156	157	174	173	1
141	157	158	175	174	1
142	158	159	176	175	1
143	159	160	177	176	1
144	160	161	178	177	1
145	162	163	180	179	1
146	163	164	181	180	1
147	164	165	182	181	1
148	165	166	183	182	1
149	166	167	184	183	1
150	167	168	185	184	1
151	168	169	186	185	1
152	169	170	187	186	1
153	170	171	188	187	1
154	171	172	189	188	1
155	172	173	190	189	1
156	173	174	191	190	1
157	174	175	192	191	1
158	175	176	193	192	1
159	176	177	194	193	1
160	177	178	195	194	1
161	179	180	197	196	1
162	180	181	198	197	1
163	181	182	199	198	1
164	182	183	200	199	1
165	183	184	201	200	1
166	184	185	202	201	1
167	185	186	203	202	1
168	186	187	204	203	1
169	187	188	205	204	1
170	188	189	206	205	1
171	189	190	207	206	1
172	190	191	208	207	1
173	191	192	209	208	1
174	192	193	210	209	1
175	193	194	211	210	1
176	194	195	212	211	1
177	196	197	214	213	1
178	197	198	215	214	1
179	198	199	216	215	1
180	199	200	217	216	1
181	200	201	218	217	1
182	201	202	219	218	1

183	202	203	220	219	1
184	203	204	221	220	1
185	204	205	222	221	1
186	205	206	223	222	1
187	206	207	224	223	1
188	207	208	225	224	1
189	208	209	226	225	1
190	209	210	227	226	1
191	210	211	228	227	1
192	211	212	229	228	1
193	213	214	231	230	1
194	214	215	232	231	1
195	215	216	233	232	1
196	216	217	234	233	1
197	217	218	235	234	1
198	218	219	236	235	1
199	219	220	237	236	1
200	220	221	238	237	1
201	221	222	239	238	1
202	222	223	240	239	1
203	223	224	241	240	1
204	224	225	242	241	1
205	225	226	243	242	1
206	226	227	244	243	1
207	227	228	245	244	1
208	228	229	246	245	1
209	230	231	248	247	1
210	231	232	249	248	1
211	232	233	250	249	1
212	233	234	251	250	1
213	234	235	252	251	1
214	235	236	253	252	1
215	236	237	254	253	1
216	237	238	255	254	1
217	238	239	256	255	1
218	239	240	257	256	1
219	240	241	258	257	1
220	241	242	259	258	1
221	242	243	260	259	1
222	243	244	261	260	1
223	244	245	262	261	1
224	245	246	263	262	1
225	247	248	265	264	1
226	248	249	266	265	1

227	249	250	267	266	1
228	250	251	268	267	1
229	251	252	269	268	1
230	252	253	270	269	1
231	253	254	271	270	1
232	254	255	272	271	1
233	255	256	273	272	1
234	256	257	274	273	1
235	257	258	275	274	1
236	258	259	276	275	1
237	259	260	277	276	1
238	260	261	278	277	1
239	261	262	279	278	1
240	262	263	280	279	1
241	264	265	282	281	1
242	265	266	283	282	1
243	266	267	284	283	1
244	267	268	285	284	1
245	268	269	286	285	1
246	269	270	287	286	1
247	270	271	288	287	1
248	271	272	289	288	1
249	272	273	290	289	1
250	273	274	291	290	1
251	274	275	292	291	1
252	275	276	293	292	1
253	276	277	294	293	1
254	277	278	295	294	1
255	278	279	296	295	1
256	279	280	297	296	1
257	281	282	299	298	1
258	282	283	300	299	1
259	283	284	301	300	1
260	284	285	302	301	1
261	285	286	303	302	1
262	286	287	304	303	1
263	287	288	305	304	1
264	288	289	306	305	1
265	289	290	307	306	1
266	290	291	308	307	1
267	291	292	309	308	1
268	292	293	310	309	1
269	293	294	311	310	1
270	294	295	312	311	1

271	295	296	313	312	1
272	296	297	314	313	1
273	298	299	316	315	1
274	299	300	317	316	1
275	300	301	318	317	1
276	301	302	319	318	1
277	302	303	320	319	1
278	303	304	321	320	1
279	304	305	322	321	1
280	305	306	323	322	1
281	306	307	324	323	1
282	307	308	325	324	1
283	308	309	326	325	1
284	309	310	327	326	1
285	310	311	328	327	1
286	311	312	329	328	1
287	312	313	330	329	1
288	313	314	331	330	1
289	315	316	333	332	1
290	316	317	334	333	1
291	317	318	335	334	1
292	318	319	336	335	1
293	319	320	337	336	1
294	320	321	338	337	1
295	321	322	339	338	1
296	322	323	340	339	1
297	323	324	341	340	1
298	324	325	342	341	1
299	325	326	343	342	1
300	326	327	344	343	1
301	327	328	345	344	1
302	328	329	346	345	1
303	329	330	347	346	1
304	330	331	348	347	1
305	332	333	350	349	1
306	333	334	351	350	1
307	334	335	352	351	1
308	335	336	353	352	1
309	336	337	354	353	1
310	337	338	355	354	1
311	338	339	356	355	1
312	339	340	357	356	1
313	340	341	358	357	1
314	341	342	359	358	1

315	342	343	360	359	1
316	343	344	361	360	1
317	344	345	362	361	1
318	345	346	363	362	1
319	346	347	364	363	1
320	347	348	365	364	1
321	349	350	367	366	1
322	350	351	368	367	1
323	351	352	369	368	1
324	352	353	370	369	1
325	353	354	371	370	1
326	354	355	372	371	1
327	355	356	373	372	1
328	356	357	374	373	1
329	357	358	375	374	1
330	358	359	376	375	1
331	359	360	377	376	1
332	360	361	378	377	1
333	361	362	379	378	1
334	362	363	380	379	1
335	363	364	381	380	1
336	364	365	382	381	1
337	366	367	384	383	1
338	367	368	385	384	1
339	368	369	386	385	1
340	369	370	387	386	1
341	370	371	388	387	1
342	371	372	389	388	1
343	372	373	390	389	1
344	373	374	391	390	1
345	374	375	392	391	1
346	375	376	393	392	1
347	376	377	394	393	1
348	377	378	395	394	1
349	378	379	396	395	1
350	379	380	397	396	1
351	380	381	398	397	1
352	381	382	399	398	1
353	383	384	401	400	1
354	384	385	402	401	1
355	385	386	403	402	1
356	386	387	404	403	1
357	387	388	405	404	1
358	388	389	406	405	1

359	389	390	407	406	1
360	390	391	408	407	1
361	391	392	409	408	1
362	392	393	410	409	1
363	393	394	411	410	1
364	394	395	412	411	1
365	395	396	413	412	1
366	396	397	414	413	1
367	397	398	415	414	1
368	398	399	416	415	1
369	402	418	417	401	1
370	401	417	429	400	1
371	418	430	429	417	1
372	402	403	419	418	1
373	418	419	431	430	1
374	403	404	431	419	1
375	406	421	420	405	1
376	405	420	431	404	1
377	421	432	431	420	1
378	406	407	422	421	1
379	421	422	433	432	1
380	407	408	433	422	1
381	410	424	423	409	1
382	409	423	433	408	1
383	424	434	433	423	1
384	410	411	425	424	1
385	424	425	435	434	1
386	411	412	435	425	1
387	414	427	426	413	1
388	413	426	435	412	1
389	427	436	435	426	1
390	414	415	428	427	1
391	427	428	437	436	1
392	415	416	437	428	1
393	429	430	439	438	1
394	430	431	440	439	1
395	431	432	441	440	1
396	432	433	442	441	1
397	433	434	443	442	1
398	434	435	444	443	1
399	435	436	445	444	1
400	436	437	446	445	1
401	438	439	448	447	1
402	439	440	449	448	1

403	440	441	450	449	1
404	441	442	451	450	1
405	442	443	452	451	1
406	443	444	453	452	1
407	444	445	454	453	1
408	445	446	455	454	1
409	447	448	457	456	1
410	448	449	458	457	1
411	449	450	459	458	1
412	450	451	460	459	1
413	451	452	461	460	1
414	452	453	462	461	1
415	453	454	463	462	1
416	454	455	464	463	1
417	456	457	466	465	1
418	457	458	467	466	1
419	458	459	468	467	1
420	459	460	469	468	1
421	460	461	470	469	1
422	461	462	471	470	1
423	462	463	472	471	1
424	463	464	473	472	1
425	465	466	475	474	1
426	466	467	476	475	1
427	467	468	477	476	1
428	468	469	478	477	1
429	469	470	479	478	1
430	470	471	480	479	1
431	471	472	481	480	1
432	472	473	482	481	1
433	474	475	484	483	1
434	475	476	485	484	1
435	476	477	486	485	1
436	477	478	487	486	1
437	478	479	488	487	1
438	479	480	489	488	1
439	480	481	490	489	1
440	481	482	491	490	1
441	483	484	493	492	1
442	484	485	494	493	1
443	485	486	495	494	1
444	486	487	496	495	1
445	487	488	497	496	1
446	488	489	498	497	1

447	489	490	499	498	1
448	490	491	500	499	1
449	492	493	502	501	1
450	493	494	503	502	1
451	494	495	504	503	1
452	495	496	505	504	1
453	496	497	506	505	1
454	497	498	507	506	1
455	498	499	508	507	1
456	499	500	509	508	1
457	501	502	511	510	1
458	502	503	512	511	1
459	503	504	513	512	1
460	504	505	514	513	1
461	505	506	515	514	1
462	506	507	516	515	1
463	507	508	517	516	1
464	508	509	518	517	1
465	510	511	520	519	1
466	511	512	521	520	1
467	512	513	522	521	1
468	513	514	523	522	1
469	514	515	524	523	1
470	515	516	525	524	1
471	516	517	526	525	1
472	517	518	527	526	1
473	519	520	529	528	1
474	520	521	530	529	1
475	521	522	531	530	1
476	522	523	532	531	1
477	523	524	533	532	1
478	524	525	534	533	1
479	525	526	535	534	1
480	526	527	536	535	1
481	528	529	538	537	1
482	529	530	539	538	1
483	530	531	540	539	1
484	531	532	541	540	1
485	532	533	542	541	1
486	533	534	543	542	1
487	534	535	544	543	1
488	535	536	545	544	1
489	537	538	547	546	1
490	538	539	548	547	1

491	539	540	549	548	1
492	540	541	550	549	1
493	541	542	551	550	1
494	542	543	552	551	1
495	543	544	553	552	1
496	544	545	554	553	1
497	546	547	556	555	1
498	547	548	557	556	1
499	548	549	558	557	1
500	549	550	559	558	1
501	550	551	560	559	1
502	551	552	561	560	1
503	552	553	562	561	1
504	553	554	563	562	1
505	555	556	565	564	1
506	556	557	566	565	1
507	557	558	567	566	1
508	558	559	568	567	1
509	559	560	569	568	1
510	560	561	570	569	1
511	561	562	571	570	1
512	562	563	572	571	1
513	566	574	573	565	1
514	565	573	579	564	1
515	574	580	579	573	1
516	566	567	575	574	1
517	574	575	581	580	1
518	567	568	581	575	1
519	570	577	576	569	1
520	569	576	581	568	1
521	577	582	581	576	1
522	570	571	578	577	1
523	577	578	583	582	1
524	571	572	583	578	1
525	579	580	585	584	1
526	580	581	586	585	1
527	581	582	587	586	1
528	582	583	588	587	1
529	584	585	590	589	1
530	585	586	591	590	1
531	586	587	592	591	1
532	587	588	593	592	1
533	589	590	595	594	1
534	590	591	596	595	1

```
535  591  592  597  596    1
536  592  593  598  597    1
537  594  595  600  599    1
538  595  596  601  600    1
539  596  597  602  601    1
540  597  598  603  602    1
541  599  600  605  604    1
542  600  601  606  605    1
543  601  602  607  606    1
544  602  603  608  607    1
545  604  605  610  609    1
546  605  606  611  610    1
547  606  607  612  611    1
548  607  608  613  612    1
549  609  610  615  614    1
550  610  611  616  615    1
551  611  612  617  616    1
552  618  621  619  620    1
553  620  619  612  613    1
554  621  617  612  619    1
555  617  621  623  622    1
556  621  618  624  623    1
557  622  623  626  625    1
558  623  624  627  626    1
559  628  631  632  629    1
560  631  634  635  632    1
561  634  625  637  635    1
562  627  640  639  626    1
563  626  639  637  625    1
564  640  641  637  639    1
565  629  632  633  630    1
566  632  635  636  633    1
567  635  637  638  636    1
568  637  641  642  638    1
  1        0.0    -528.0          1
642        0.0    -528.0
 17        0.0       0.0      0.0        1.0
  1    1
  2    6
  3   11
  4   16
  5   21
  6   26
  7   31
```

```
  568   637   641   642   638     1
    1         0.0     -528.0           1
  642         0.0     -528.0
   17         0.0        0.0         0.0         1.0
    1     1
    2     6
    3    11
    4    16
    5    21
    6    26
    7    31
    8    36
    9    41
   10    46
   11    51
   12    56
   13    61
   14    66
   15    71
   16    76
   17    81
[EOB]
```

Finite Element Input
for Concrete Highway Target
Analysis into PRONTO-2D Code

ASSUME:

- NO SIGNIFICANT ENERGY IS ABSORBED BY CRACK GENERATION
- CRACK PROPAGATES AT 45° ANGLE
- $\mu_{rock} \approx \mu_{soil}$

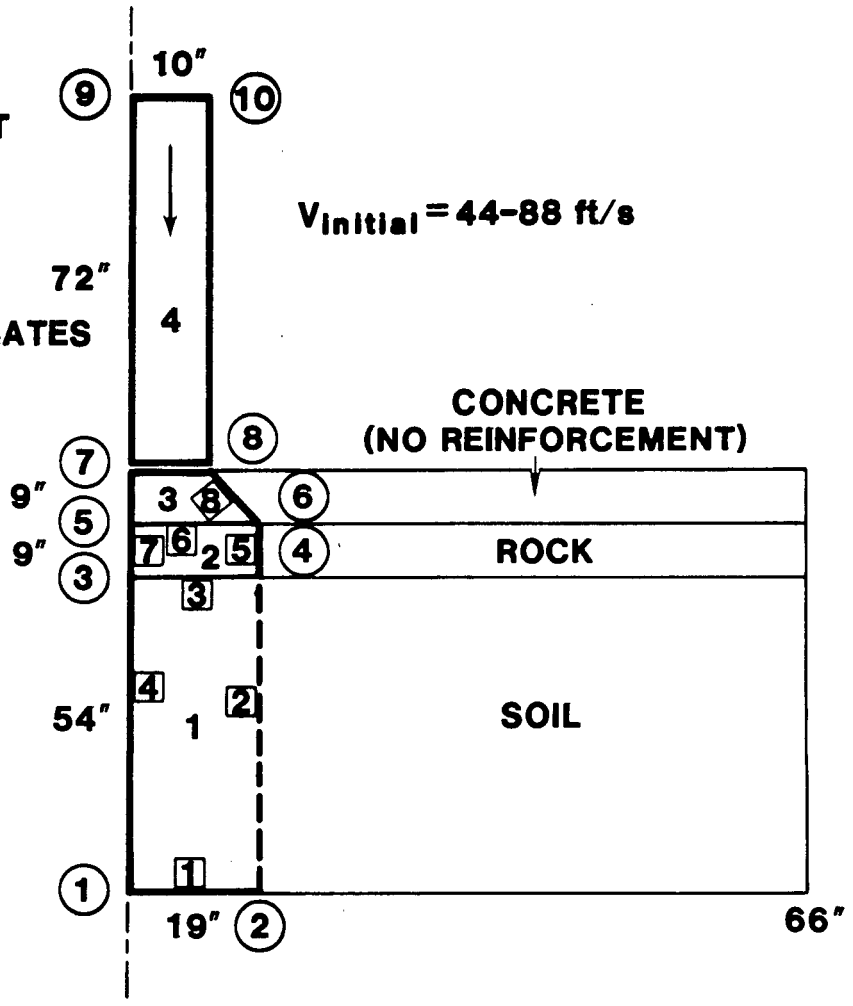

INITIAL VELOCITY ft/s	44 ft/s	66 ft/s	88 ft/s
MAXIMUM DISPLACEMENT (inches)	16.4	25.2	34.8
MAXIMUM ACCELERATION (g's)	37.2	55.0	71.8
AVERAGE ACCELERATION (g's)	22.0	32.2	41.5
$\frac{\text{MAXIMUM}}{\text{AVERAGE}}$ ACCELERATION	1.69	1.71	1.73

CONCRETE PROPERTIES

E (psi)	2.50×10^6
G (psi)	1.06×10^6 ($2.12 \times 10^6 = 2\mu$)
B (psi)	1.30×10^6
σ_t (psi)	250
σ_c (psi)	3500 (C_o)
ν	0.18
α	20°
μ (tan α)	0.364

$f(\sigma_{eff})$: $2600\ a_0$

$0.772\ a_1$

p_m	$\ell n\ (1-p_m/B)$
0	0
5000	0.00385
10000	0.00772
20000	0.01550

$$S_o = \frac{C_o}{2\ [\mu^2 + 1)^{1/2} + \mu]} = \frac{3500}{2\ [1.418]} = 1225 \text{ psi cohesion}$$

$\sigma_1 = 3500,\ \sigma_2 = \sigma_3 = 0$

$$J_2 = \frac{1}{6}[(\sigma_1 - \sigma_2)^2 + (\sigma_2 - \sigma_3)^2 + (\sigma_3 - \sigma_1)^2] = \frac{1}{3}\sigma_y = 4.083 \times 10^6$$

$\sigma_y = 3500$ Pm = 1166.7

for $\sigma_2 = \sigma_3 = \sigma_{max} = 5000$ psi

$$\sigma_1 = \frac{\sigma_{max}[\mu^2 + 1)^{1/2} + \mu] - 2So}{[(\mu^2 + 1)^{1/2} - \mu]} = \frac{-5000(1.428) - 2450}{(0.7002)}$$

$$\sigma_1 = -13{,}696 \text{ psi}$$

$$J_2 = \frac{1}{6}[8696^2 + 8696^2] = 25.2 \times 10^6$$

$$\sigma_y = 8696 \text{ psi} \qquad pm = 7898.7$$

$$\begin{bmatrix} 1 & 1166.7 \\ 1 & 7898.7 \end{bmatrix} \begin{Bmatrix} a_0 \\ a_1 \end{Bmatrix} = \begin{matrix} 3500 \\ 8696 \end{matrix}$$

$$a_0 = 2500$$

$$a_1 = 0.772$$

$$G = \frac{E}{2(1 + \nu)} = 1.06 \times 10^6 \text{ psi}$$

$$B = \frac{E}{3(1 - 2\nu)} = 1.30 \times 10^6 \text{ psi}$$

Finite Element Input
for Soil Analysis
into PRONTO-2D Code

PRONTO-20

```
MRN,JEXL,P12C.
USER,MKNEILS,}PASSWORD{.
CHARGE(8950433)
ACCESS,DN=$PROC,PDN=PROCS,ID=ACCLIB
ACCESS,DN=XPROC,PDN=PROCS,ID=DPFLANA.
ASSIGN,DN=TAPE11,A=FT11
LIBRARY,DN=*XPROC.
FASTQ.
PRONTO2.
SAVE,DN=TAPE11,PDN=PRO66.
EXIT
BFTOV1,FILE=TAPE11.
```

```
TITLE
      TARGET HARDNESS MODEL 1
POINT      1        0.000E+00        0.000E+00
POINT      2        1.000E+01        0.000E+00
POINT      3        0.000E+01        6.000E+01
POINT      4        1.000E+01        6.000E+01
POINT      5        0.000E+01        7.200E+01
POINT      6        1.000E+01        7.200E+01
POINT      7        0.000E+01        8.400E+01
POINT      8        1.000E+01        8.400E+01
POINT      9        0.000E+01        9.600E+01
POINT     10        1.000E+01        9.600E+01
POINT     11        0.000E+00        1.080E+02
POINT     12        1.000E+01        1.080E+02
POINT     13        0.000E+01        1.200E+02
POINT     14        1.000E+01        1.200E+02
POINT     15        0.000E+01        1.920E+02
POINT     16        1.000E+01        1.920E+02
LINE       1   STR      1      2      0      5   1.0000
LINE       2   STR      2      4      0     30   1.0000
LINE       3   STR      4      3      0      5   1.0000
LINE       4   STR      3      1      0     30   1.0000
LINE       5   STR      4      6      0      6   1.0000
LINE       6   STR      6      5      0      5   1.0000
LINE       7   STR      5      3      0      6   1.0000
LINE       8   STR      6      8      0      6   1.0000
LINE       9   STR      8      7      0      5   1.0000
LINE      10   STR      7      5      0      6   1.0000
LINE      11   STR      8     10      0      6   1.0000
LINE      12   STR     10      9      0      5   1.0000
LINE      13   STR      9      7      0      6   1.0000
LINE      14   STR     10     12      0      6   1.0000
LINE      15   STR     12     11      0      5   1.0000
LINE      16   STR     11      9      0      6   1.0000
LINE      17   STR     12     14      0      6   1.0000
LINE      18   STR     14     13      0      5   1.0000
LINE      19   STR     13     11      0      6   1.0000
LINE      20   STR     14     16      0     18   1.0000
LINE      21   STR     16     15      0      5   1.0000
LINE      22   STR     15     13      0     18   1.0000
REGION     1      1     -1     -2     -3     -4
REGION     2      2     -3     -5     -6     -7
REGION     3      3     -6     -8     -9    -10
REGION     4      4     -9    -11    -12    -13
REGION     5      5    -12    -14    -15    -16
REGION     6      6    -15    -17    -18    -19
REGION     7      7    -18    -20    -21    -22
SCHEME     1 M
SCHEME     2 M
SCHEME     3 M
SCHEME     4 M
SCHEME     5 M
SCHEME     6 M
SCHEME     7 M
BODY       1      2      3      4      5      6      7
LINEBC     1      4      7     10     13     16     19     22
LINEBC     2      1
SIDEBC     3      2
SIDEBC     4      5
SIDEBC     5      8
```

```
SIDEBC    6    11
SIDEBC    7    14
SIDEBC    8    17
EXIT
```

PRINTO INPUT

```
TITLE
 TARGET HARDNESS - SLIDE 66 FPS - B = 2000 psi
AXISYMMETRIC
TERM TIME,0.040
OUTPUT TIME,0.0002
PLOT TIME,0.0002
PLOT ELEMENT,STRESS,ENERGY,PRESSURE
NO DISPL,X,1
NO DISPL,Y,2
INITIAL VEL MAT,7,0.0,-792.0
RIGID SURFACE,3,10.,0,-1.,0,0.488
RIGID SURFACE,4,10.,0,-1.,0,0.509
RIGID SURFACE,5,10.,0,-1.,0,0.532
RIGID SURFACE,6,10.,0,-1.,0,0.532
RIGID SURFACE,7,10.,0,-1.,0,0.675
RIGID SURFACE,8,10.,0,-1.,0,0.675
FUNCTION,10
 0,0
 0.0513,100.
 0.1054,200.
 0.1625,300.
 0.2231,400.
 0.2877,500.
 0.3567,600.
END
MATERIAL,1,SOIL N FOAMS,1.5-4
TWO MU,2400.
BULK MODULUS,2000.
A0,8.551
A1,1.027
A2,0
FUNCTION ID,10
END
MATERIAL,2,SOIL N FOAMS,1.5-4
TWO MU,2400.
BULK MODULUS,2000.
A0,8.686
A1,1.070
A2,0
FUNCTION ID,10
END
MATERIAL,3,SOIL N FOAMS,1.5-4
TWO MU,2400.
BULK MODULUS,2000.
A0,8.805
A1,1.113
A2,0
FUNCTION ID,10
END
MATERIAL,4,SOIL N FOAMS,1.5-4
TWO MU,2400.
BULK MODULUS,2000.
A0,10.818
A1,1.113
A2,0
FUNCTION ID,10
END
MATERIAL,5,SOIL N FOAMS,1.33-4
TWO MU,2400.
BULK MODULUS,2000.
```

```
A0,6.772
A1,1.375
A2,0
FUNCTION ID,10
END
MATERIAL,6,SOIL N FOAMS,1.33-4
TWO MU,2400.
BULK MODULUS,2000.
A0,6.772
A1,1.375
A2,0
FUNCTION ID,10
END
MATERIAL,7,ELASTIC,6.74-4
YOUNGS MODULUS,29.+6
POISSONS RATIO,0.300
END
EXIT
```

```
TITLE
 TARGET HARDNESS - SLIDE 66 FPS - M = 0 500
AXISYMMETRIC
TERM TIME,0.040
OUTPUT TIME,0.0002
PLOT TIME,0.0002
PLOT ELEMENT,STRESS,ENERGY,PRESSURE
NO DISPL,X,1
NO DISPL,Y,2
INITIAL VEL MAT,7,0.0,-792.0
RIGID SURFACE,3,10.,0,-1.,0,0.500
RIGID SURFACE,4,10.,0,-1.,0,0.500
RIGID SURFACE,5,10.,0,-1.,0,0.500
RIGID SURFACE,6,10.,0,-1.,0,0.500
RIGID SURFACE,7,10.,0,-1.,0,0.500
RIGID SURFACE,8,10.,0,-1.,0,0.500
FUNCTION,10
 0,0
 0.0513,100.
 0.1054,200.
 0.1625,300.
 0.2231,400.
 0.2877,500.
 0.3567,600.
END
MATERIAL,1,SOIL N FOAMS,1.5-4
TWO MU,2400.
BULK MODULUS,2000.
A0,8.551
A1,1 027
A2,0
FUNCTION ID,10
END
MATERIAL,2,SOIL N FOAMS,1.5-4
TWO MU,2400.
BULK MODULUS,2000.
A0,8.686
A1,1.070
A2,0
FUNCTION ID,10
END
MATERIAL,3,SOIL N FOAMS,1.5-4
TWO MU,2400.
BULK MODULUS,2000.
A0,8.805
A1,1.113
A2,0
FUNCTION ID,10
END
MATERIAL,4,SOIL N FOAMS,1.5-4
TWO MU,2400.
BULK MODULUS,2000.
A0,10.818
A1,1.113
A2,0
FUNCTION ID,10
END
MATERIAL,5,SOIL N FOAMS,1.33-4
TWO MU,2400.
BULK MODULUS,2000.
```

```
A0,6.772
A1,1.375
A2,0
FUNCTION ID,10
END
MATERIAL,6,SOIL N FOAMS,1.33-4
TWO MU,2400.
BULK MODULUS,2000.
A0,6.772
A1,1.375
A2,0
FUNCTION ID,10
END
MATERIAL,7,ELASTIC,6.74-4
YOUNGS MODULUS,29.+6
POISSONS RATIO,0.300
END
EXIT
```

Finite Element Input
for Soil Analysis
into DYNA2D Code

DYNA-2D
CCL

```
MKNEILS.T600.STSCZ.                    MKNEILS. BOX 440
USER.MKNEILS,{PASSWORD}.
CHARGE.8950433.
ACCESS DN=$PROC PDN=PROCS.ID=ACCLIB.
ASSIGN.DN=TAPE10.A=FT10.
QMESH.
RENUM
* QPLOT.DEV=HC1.SITE=R0
*.
ACCESS,DN=RSCALE,PDN=RSCALE.
*.
DYNA2D.C=RSCALE.
*.DYNA2D.
REWIND,DN=TAPE10.
SAVE,DN=TAPE10,PDN=PEN66,RT=21.
*.SAVE,DN=DUMPFL,PDN=PRST66,RT=21.
*.
AUDIT,ID=MKNEILS.
*.
EXIT.
REWIND,DN=TAPE10.
SAVE.DN=TAPE10,PDN=PEN66,RT=5.
*.
AUDIT.ID=MKNEILS.
```

.DAT

```
TARGET HARDNESS - RUN 3 - 66 FPS
ND  6    -2     0     0     0     0            0.00       0.05       0.01
    0     0     0     0     0     1     1      0     0     0
       .050       0010       0010
    1     5  1.50E-04
TARGET MATERIAL  60+
 1.200E+03 2.000E+03 2.430E+01 5.850E+00 3.510E-01
 0.000E+00 0.000E+00 0.513E-01 1.000E+02
 1.625E-01 3.000E+02 3.567E-01 6.000E+02



    2     5  1.50E-04
TARGET MATERIAL  48-60
 1.200E+03 2.000E+03 2.510E+01 6.200E+00 3.810E-01
 0.000E+00 0.000E+00 0.513E-01 1.000E+02
 1.625E-01 3.000E+02 3.567E-01 6.000E+02



    3     5  1.50E-04
TARGET MATERIAL  36-48
 1.200E+03 2.000E+03 2.580E+01 6.530E+00 4.130E-01
 0.000E+00 0.000E+00 0.513E-01 1.000E+02
 1.625E-01 3.000E+02 3.567E-01 6.000E+02



    4     5  1.50E-04
TARGET MATERIAL  24-36
 1.200E+03 2.000E+03 3.900E+01 8.030E+00 4.130E-01
 0.000E+00 0.000E+00 0.513E-01 1.000E+02
 1.625E-01 3.000E+02 3.567E-01 6.000E+02



    5     5  1.33E-04
TARGET MATERIAL  0-24
 1.200E+03 2.000E+03 1.530E+01 6.210E+00 6.300E-01
 0.000E+00 0.000E+00 0.513E-01 1.000E+02
 1.625E-01 3.000E+02 3.567E-01 6.000E+02



    6     1  6.74E-04
STEEL CASK
 2.900E+07
 3.000E-01



BCC      1.          1.
BCC      2.          2.
    1          0.       0.000
  500          0.       0.000
  501          0.       -792.
  504          0.       -792.
  505          0.       0.000
  525          0.       0.000
```

```
526          0.       -792
573          0.       -792.
573          0.          0.          0.          10
  1     1
573   573
```

```
OMMEN     TARGET HARDNESS MODEL 1
OINT          1/   0.0000     0.0000                0
OINT          2/  80.0000     0.0000                0
OINT          3/   0.0000    60.0000                0
OINT          4/  80.0000    60.0000                0
OINT          5/   0.0000    72.0000                0
OINT          6   80.0000    72.0000                0
OINT          7/   0.0000    84.0000                0
OINT          8/  80.0000    84.0000                0
OINT          9/   0.0000    96.0000                0
OINT         10/  80.0000    96.0000                0
OINT         11/   0.0000   120.0000                0
OINT         12/  10.0000   120.0000                0
OINT         13/  80.0000   120.0000                0
OINT         14/   0.0000   192.0000                0
OINT         15/  10.0000   192.0000                0
INE  STR      1/   1    2     0    24     1.0000     2
INE  STR      2/   2    4     0    10     1.0000     1
INE  STR      3/   4    3     0    24     1.0000     0
INE  STR      4/   3    1     0    10     1.0000     1
INE  STR      5/   4    6     0     2     1.0000     1
INE  STR      6/   6    5     0    24     1.0000     0
INE  STR      7/   5    3     0     2     1.0000     1
INE  STR      8/   6    8     0     2     1.0000     1
INE  STR      9/   8    7     0    24     1.0000     0
INE  STR     10/   7    5     0     2     1.0000     1
INE  STR     11/   8   10     0     2     1.0000     1
INE  STR     12/  10    9     0    24     1.0000     0
INE  STR     13/   9    7     0     2     1.0000     1
INE  STR     14/  10   13     0     4     1.0000     1
INE  STR     15/  13   12     0    21     1.0000     0
INE  STR     16/  12   11     0     3     1.0000     0
INE  STR     17/  11    9     0     4     1.0000     1
INE  STR     18/  12   15     0    12     1.0000     0
INE  STR     19/  15   14     0     3     1.0000     0
INE  STR     20/  14   11     0    12     1.0000     1
IDE           1/  15   16
EGION   1     1/  -1   -2    -3    -4
EGION   2     2/  -3   -5    -6    -7
EGION   3     3/  -6   -8    -9   -10
EGION   4     4/  -9  -11   -12   -13
EGION   5     5/ -12  -14     1   -17
EGION   6     6/ -16  -18   -19   -20
CHEME         1M
CHEME         2M
CHEME         3M
CHEME         4M
CHEME         5M
CHEME         6M
ODY            /   1    2     3     4     5     6
ND            4
EOR}
-L-           1    1    2
```